Aus dem Helmholtz-Zentrum München
Research Unit Lung Repair and Regeneration,
Comprehensive Pneumology Center München
Vorstand: Prof. Dr. Dr. Melanie Königshoff

Regulation and function of non-canonical WNT signaling in lung fibroblasts in chronic lung diseases

Dissertation
zum Erwerb des Doktorgrades der Medizin
an der Medizinischen Fakultät der
Ludwig-Maximilians-Universität zu München

vorgelegt von

Florian Bernhard Ciolek

aus

München

Jahr

2021

Mit Genehmigung der Medizinischen Fakultät
der Universität München

Berichterstatter:	Prof. Dr. Dr. Melanie Königshoff
Mitberichterstatter:	Prof. Dr. Jürgen Behr PD Dr. Sandra Frank
Mitbetreuung durch den promovierten Mitarbeiter:	Dr. Hoeke Baarsma
Dekan:	Prof. Dr. med. dent. Reinhard Hickel
Tag der mündlichen Prüfung:	15.07.2021

meiner Familie

I Table of Content

II Abbreviations

ANOVA	analysis of variance
APC	adenomatosis polyposis coli
BCA	bicinchoninic acid
BOLD	Burden Of Obstructive Lung Disease
BSA	bovine serum albumin
cDNA	complementary deoxyribonucleic acid
CCND	cyclin D
CK	casein kinase
COL	collagen
COMP	cartilage oligomeric matrix protein
COPD	chronic obstructive pulmonary disease
CPFE	combined pulmonary fibrosis and emphysema
CSE	cigarette smoke extract
Ct	cycle threshold
CTGF	connective tissue growth factor
DAPI	4′,6-Diamidino-2-phenylindole
DKK	dickkopf
DMEM-F12	Dulbecco's Modified Eagle Medium: Nutrient Mixture F-12
DMSO	dimethyl sulfoxide
DNA	deoxyribonucleic acid
DTT	dithiothreitol
DVL	dishevelled
ds	double stranded
ECL	enhanced chemiluminescence
ECM	extracellular matrix
EDTA	ethylenediaminetetraacetic acid
EGTA	ethylene glycol tetraacetic acid
ELN	elastin
FAM13A	family with sequence similarity 13, member A
FCS	fetal calf serum
FEV_1	forced expiratory volume in 1 second
FGF	fibroblast growth factor

FN	fibronectin
FVC	forced vital capacity
FZD	frizzled
GO	gene ontology
GOLD	Global Initiative for Chronic Obstructive Lung Disease
GSK	glycogen synthase kinase
HRCT	high-resolution computed tomography
HRP	horse radish peroxidase
HPRT	hypoxanthine-guanine phosphoribosyltransferase
ICAT	inhibitor of β-catenin and TCF-4
IKK	inhibitor of nuclear factor kappa-B kinase
IL	interleukin
IPF	idiopathic pulmonary fibrosis
JNK	c-jun N-terminal kinase
LPS	lipopolysaccharide
LRP	low density lipoprotein receptor related proteins receptor
MEK	mitogen-activated protein kinase kinase
miR/miRNA	micro-RNA
MMP	matrix metalloproteinase
NF-κB	nuclear factor kappa-light-chain-enhancer of activated B cells
NNK	nicotine-derived nitrosamine ketone
P/S	penicillin/streptomycin
PAI-1	plasminogen activator inhibitor-1
PBMC	peripheral blood mononuclear cells
PBS	phosphate-buffered saline
PFA	paraformaldehyde
PI3K	phosphatidylinositol-3-kinase
qRT-PCR	quantitative real-time polymerase chain reaction
RIPA	radioimmunoprecipitation assay
RNA	ribonucleic acid
rpm	rotations per minute
SBE	SMAD-binding element
scr	scrambled
SDS-PAGE	sodium dodecyl sulfate-polyacrylamide gel electrophoresis

SMA	smooth muscle actin
SMAD	small mothers against decapentaplegic
SNP	single nucleotide polymorphism
stdev	standard deviation
TAK	TGF-β activated kinase
TBST	triphosphate buffered saline supplemented with 0.05% Tween-20
TCF/LEF	T-cell factor/lymphoid enhancer factor-1
TEMED	tetramethylethylenediamine
TGF-β	transforming growth factor β_1
TNC	tenascin C
TNF	tumor necrosis factor
TNS	tensin
Tris	trishydroxymethylaminomethane
TSPAN	tetraspanin
UIP	usual interstitial pneumonia
WNT	wingless-related integration site
WISP-1	WNT1-inducible signaling protein–1

1 Introduction

1.1 Chronic lung diseases

Chronic lung pathologies, such as chronic obstructive pulmonary disease (COPD) or idiopathic pulmonary fibrosis (IPF), account for a significant health and economic burden worldwide.

COPD is a widespread disease. A meta-analysis conducted in 2006 estimated a global prevalence of around 10 %, while the Burden of Obstructive Lung Disease (BOLD) study collected spirometry data from 12 sites all over the world and assumed an even higher prevalence (1, 2). Although COPD is a slowly progressing disease, its mortality and morbidity is striking. A projection of Mathers et al. estimated COPD to be the fourth leading cause of death worldwide by 2030 and in another study assessing years lived with disability in 2010, COPD was on rank 5 among all diseases (3, 4).

IPF is less common with a global incidence of 3-9 in 100,000 which is still on the rise owing to improved diagnostic tools and raised awareness among physicians (5, 6). What makes IPF a topic of increasing public interest is the clinical course of the disease with a very poor median survival of 2.5 to 3.5 years after diagnosis making it deadlier than many types of cancer (7).

Strikingly, the decline in lung function in both COPD and IPF is irreversible and therapeutic approaches to slow down disease progression remain limited (8, 9).

1.1.1 COPD

COPD is characterized by progressive and irreversible airflow limitation caused by chronic airway inflammation with subsequent airway remodeling and the destruction of the alveolar walls resulting in lung emphysema. The main risk factor for the development of COPD is clearly a history of continuous tobacco smoking which is the reason why smoking cessation should be encouraged in every smoking COPD patient (8). However, since COPD also occurs in never-smokers, other factors such as occupational exposure to organic dusts, air pollution and a specific hereditary defect in the α1-antitrypsin gene need to be taken into account (10-13).

COPD patients present with respiratory symptoms of various degrees, the most prevalent ones being chronic cough, increased sputum production, progredient dyspnea and wheezing as consequence of the airflow limitation. Complications include

exacerbations of lung function decline, chronic respiratory insufficiency, cachexia secondary to increased respiratory muscle work and pulmonary hypertension (8, 14).
The formal diagnosis of COPD is made by spirometry with an initial assessment of the Tiffeneau index after bronchodilator application, which is calculated by the Forced Expiratory Volume in 1 second (FEV_1) divided by the Forced Vital Capacity (FVC). Once COPD is diagnosed, the subsequent classification into Global Initiative for Chronic Obstructive Lung Disease (GOLD) groups A-D relevant for therapy relies on the age-adjusted FEV_1, the amount of exacerbations and the impact of the symptoms on quality of life assessed by the mMRC and CAT questionnaire (8).

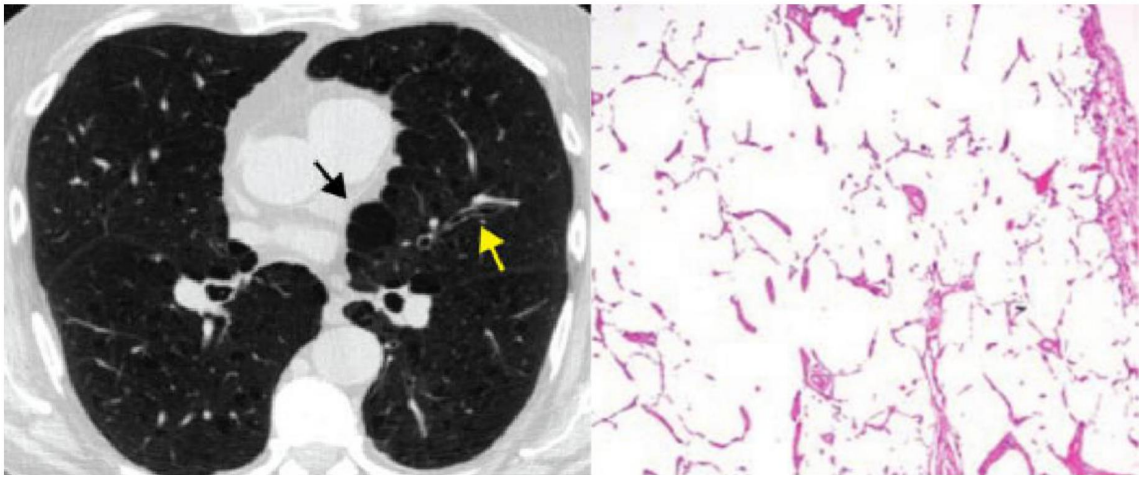

Figure I1: Radiologic and histologic characteristic of COPD

CT scan (left) shows airway thickening (yellow arrow) and emphysema (black arrow), histology (right, hematoxylin and eosin stain) shows severe emphysema with loss of alveolar septa. Modified images with permission of John Wiley and Sons and American Society for Clinical Investigation (15, 16).

The current pharmacological therapy of COPD focuses on bronchodilators, mainly anticholinergic drugs and β_2-agonists, which are both available in short-acting and long-acting formulas, and in later stages on anti-inflammatory inhaled corticosteroids (8, 17). Antibiotics and the phosphodiesterase inhibitor Roflumilast are occasionally used in patients with frequent exacerbations. Mucolytics can help to control symptoms. Nonpharmacologic treatment options like pulmonary rehabilitation programs, physical exercise and vaccinations against influenza and pneumococcus have also been shown to be beneficial. For patients with respiratory insufficiency, oxygen therapy and assisted ventilation should be considered (8).

1.1.1.2 Pathogenesis of COPD

The pathologic hallmarks of COPD are chronic airway inflammation and remodeling as well as pulmonary emphysema. Large airway inflammation in the context of chronic bronchitis is characterized by submucosal gland hypertrophy and disruption of the mucociliary clearance which is responsible for the productive cough patients suffer from, but probably not for airflow limitation (18, 19). Airflow limitation seems to be mainly caused by small airway disease and emphysema, specifically the loss and narrowing of terminal bronchioles which has been shown to precede the emphysematous destruction (20, 21). The initial step is usually the repeated inhalation of injurious substances, mainly tobacco smoke, which leads to ongoing inflammatory infiltration of airways and alveolar walls (22, 23). Along with the oxidative stress caused by smoking, this inflicts damage to the structural cells of the lung such as alveolar epithelial cells which subsequently undergo apoptosis (24-26). The list of further pathobiological processes driving disease progression is extensive. Some examples include impaired lung development in utero, genetic and epigenetic alterations and interactions with the lung microbiome (11, 27, 28). Upon ongoing inflammation and cellular damage in the lung, abnormal tissue repair and remodeling start to take place (29). One key remodeling feature observed in COPD is vast degradation of the extracellular matrix (ECM). The main effectors of this cleavage are neutrophil elastase and matrix metalloproteinases (MMP), whose control by anti-proteinases is disturbed in COPD (22, 30). Historically, elastin has been recognized as the chief ECM component insulted resulting in reduced elastic recoil (23). However, recent studies also identified other matrix proteins as differentially expressed in COPD around the small airways as well as in the emphysematous parenchyma (31-35). Fibroblasts are the main ECM-producing cell type in the lung and one of the chief effectors of tissue homeostasis and repair following injury (36). In addition to altered ECM synthesis, which is likely attributable to fibroblast dysfunction, primary fibroblasts from lungs of COPD patients show features of diminished repair capacity along with increased senescence and increased secretion of inflammatory cytokines (37-40). A more profound understanding of the molecular background and mediators driving these alterations is needed and will pave avenues for future therapeutic strategies.

1.1.2 IPF

IPF is a specific form of idiopathic interstitial pneumonia of unknown etiology. It is characterized by progressive scarring of the lungs resulting in respiratory failure within few years in most patients. Adult patients with chronic exertional dyspnea, dry cough, finger clubbing and inspiratory crackles should be evaluated regarding IPF (41, 42). In the clinical course, which appears to vary remarkably, patients gradually develop a restrictive lung disorder with reduced FVC and reduced diffusion across the blood-air barrier (7). Clinical deteriorations are caused by acute exacerbations, right heart and respiratory failure similar to end-stage COPD (41, 43, 44). The diagnosis of IPF is made when three criteria are fulfilled:

1. Known causes (e.g. connective tissue disease, drug toxicity, occupational environmental exposure) have to be excluded.
2. A pattern of usual interstitial pneumonia (UIP) has to be present in high-resolution computed tomography (HRCT).
3. If surgical lung biopsy has been undertaken, the histologic results have to be concordant with the HRCT imaging (41).

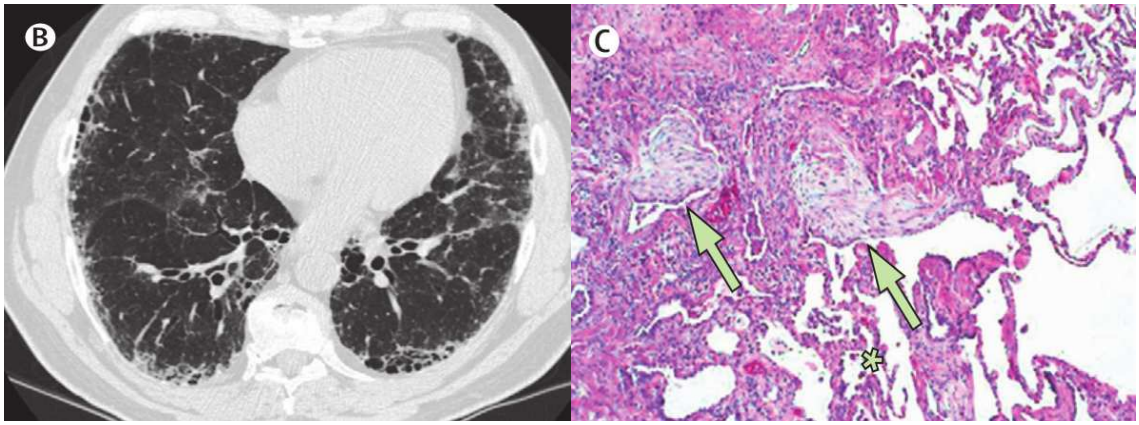

Figure I2: Radiologic and histologic characteristic of IPF

HRCT imaging (left) shows UIP pattern with honeycombing and subpleural thickening, histology (right, hematoxylin and eosin stain) shows dense fibrosis with fibroblastic foci (arrows) and mild interstitial inflammation. Modified images with permission of Elsevier (45).

Given the devastating and incurable nature of IPF, the lack of therapeutic options is alarming. The usual approach to treat interstitial lung diseases with steroids and immunomodulatory agents like Azathioprin is ineffective, in some constellations even harmful (46, 47). In the last years, two drugs with antifibrotic properties, Pirfenidone

and Nintedanib, were introduced (48, 49). In 2015, an international practice guideline gave a conditional recommendation for the use of these drugs because of studies showing improved clinical parameters. However, they do not seem to decrease mortality (9). In the treatment of acute exacerbations, corticosteroids are used based on a weak recommendation (50). Regarding supportive care, the guideline endorses the use of pulmonary rehabilitation as well as oxygen for resting hypoxemia. As a last resort, the only therapeutic intervention to improve survival is lung transplantation (41).

1.1.2.2 Pathogenesis of IPF

Central to the pathology of IPF are marked fibrotic changes which distort normal lung architecture in a heterogeneous temporospatial pattern. Usually, these remodeling processes begin to manifest in the subpleural regions with the deposition of collagen. Professional collagen-producing fibroblasts are organized in reticular foci at the edge between healthy-looking and diseased lung tissue (46). These cellular conglomerates are often located close to hyperplastic or apoptotic alveolar epithelial cells (51, 52). This spatial association underlines the prevailing hypothesis of IPF as a disease driven by deranged epithelial-mesenchymal crosstalk. It is assumed that repetitive injury to alveolar epithelial cells is the initial step in this respect. Alike COPD, cigarette smoking is recognized as one of the major risk factors, but also gastroesophageal reflux, endoplasmatic reticulum stress and oxidative stress have been subject to discussions (46, 53-55). Notably, there are familial forms of pulmonary fibrosis which present with mutations in genes encoding for epithelial proteins, like mucin 5B, highlighting genetic predispositions for the development of IPF (56, 57). Upon injury in the context of IPF, alveolar epithelial cells secrete cytokines such as the profibrotic transforming growth factor β_1 (TGF-β) acting on the surrounding cells. Furthermore, the basement membrane is continuously damaged because alveolar epithelial cells fail to regenerate properly, and the coagulation cascade is ongoingly activated (45, 58). All these factors contribute to the differentiation of fibroblasts into highly synthetically active myofibroblasts, which account for the increased ECM production (46, 52). A special characteristic of myofibroblasts present in IPF lungs is the enhanced resistance to apoptosis which is suggested to be an explanation why the scarring does not resolve like in physiologic wound healing (59). Interestingly, the composition and stiffness of the ECM deposited in IPF appears to propagate the profibrotic phenotype of fibroblasts (46, 60). Several contributing factors to disease development, like gastric reflux, oxidative stress and an

overactive coagulation cascade are amenable to therapy. However, studies using anti-acid drugs, antioxidants or anticoagulants could hardly show any clinical benefit (61-63). The same holds true for drugs used against pulmonary hypertension with the observation of pathological vasculature found in IPF lungs (64, 65). Collectively, there is an urgent need for new therapeutic targets in IPF. Investigating fibroblasts as the main effector of ECM production seems to be a promising strategy.

1.1.3 Similarities between COPD and IPF

Although COPD and IPF are often regarded as highly dissimilar diseases with the obstructive disorder with tissue loss, COPD, on one side and the restrictive disorder with tissue increase, IPF, on the other side, there is a growing number of reports describing overlap of these diseases, even in individual patients (45, 66). In fact, the scientific field is discussing whether a disease entity called combined pulmonary fibrosis and emphysema (CPFE) should be recognized (67). The major risk factor for CPFE is heavy cigarette smoking. A review of Jankowich et al. described that a compelling number of 98% of CPFE patients have a smoking history (68). Interestingly, spirometric parameters of CPFE patient are often normal, so HRCT imaging is used to establish the diagnosis (Fig. **I3**). The management of CPFE requires precaution because patients are more prone to develop pulmonary hypertension and lung cancer compared to patients suffering from COPD or IPF alone (67, 69, 70).

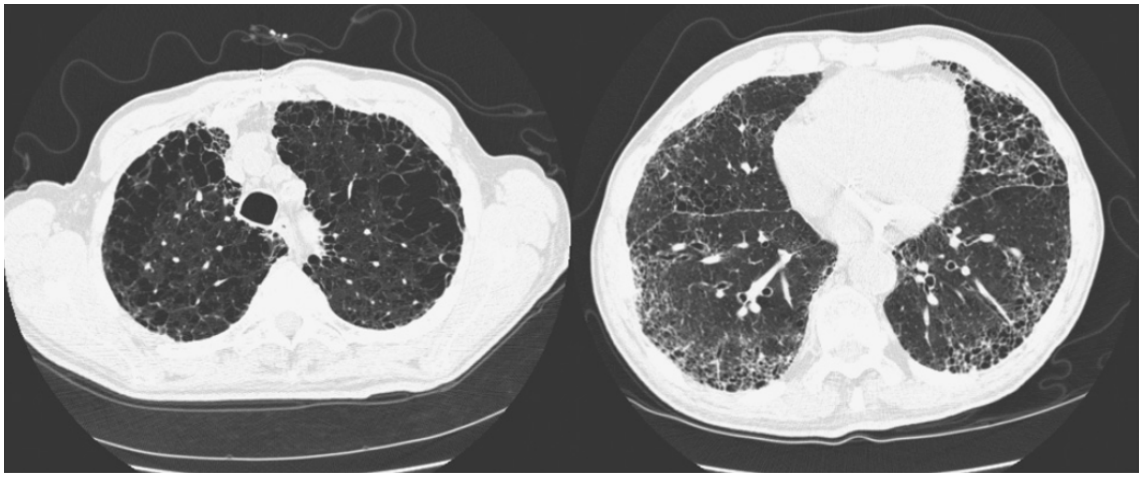

Figure I3: Chest HRCT of a CPFE patient

HRCT imaging shows upper-lobe emphysema (left) and lower-lobe pulmonary fibrosis (right) in a patient with CPFE. Modified images with permission of El Sevier (68).

As an explanation for the clinical picture described, it is worth noting that COPD and IPF share several pathophysiological principles (71). One of the best described similarities is the concept that both diseases partly represent accelerated and abnormal aging of the lung (72, 73). Astonishingly, a recent report described familial early-onset combined fibrosis and emphysema caused by a mutation in telomerase, a protein that is a key regulator of cellular regeneration in the face of aging processes (74). As a feature of lung aging in the context of chronic lung diseases, Meiners et al. proposed dysregulation of the ECM. In both COPD and IPF, ECM composition and turnover and along with this, the biology of the main professional ECM-synthesizing and -organizing cells, fibroblasts, is substantially deranged (32, 72). This has severe implications on the regenerative potential of the lung. In addition to the dynamics of cell-ECM interaction, lung regeneration is determined by endogenous progenitor cells and signaling pathways (75). Also, when it comes to altered cellular signaling, COPD and IPF display remarkable similarities. Both profibrotic such as TGF-β and "Wingless-related integration site"-3A (WNT3A) and proinflammatory cytokines such as Tumor Necrosis Factor-α (TNF-α), Interleukin-6 (IL-6) and Interleukin-1β (IL-1β) have been shown to be involved in the pathogenesis in both diseases (76-81). Another group of dysregulated signaling pathways are developmental pathways, like Notch and WNT signaling (82-84).

1.2 WNT pathway

1.2.1 Signal transduction and functions

The WNT pathway refers to a group of 19 secreted glycoproteins, the so-called WNTs, that share specific amino acids sequences and are able to initiate an intracellular signaling cascade by binding to one of 10 Frizzled (FZD) receptors (85, 86). In a simplified way, WNT signaling can be divided into a canonical pathway that relies on intracellular signal transduction activating the key mediator β-catenin, and non-canonical pathways that signal independently of β-catenin (Fig. **I4**). When the canonical WNT signaling pathway is inactive (i.e. no WNT present), cytosolic β-catenin is constantly marked for proteasomal degradation by the so-called "β-catenin destruction complex" consisting of "glycogen synthase kinase" (GSK)-3β, "adenomatosis polyposis coli" (APC), axin and casein kinase (CK)-1 (85). The first step in the activation of canonical WNT signaling is binding of a WNT to a FZD receptor and a "low density lipoprotein receptor related proteins receptor" (LRP) 5/6 located on the cell membrane (87). Subsequently, the β-catenin destruction complex is inhibited by the signaling intermediate dishevelled (DVL). β-catenin accumulates in the cytosol and is translocated into the nucleus. There it binds to the group of "T-cell factor/lymphoid enhancer factor-1" (TCF/LEF) transcription factors promoting transcription of classical WNT target genes like *AXIN2* (85, 88).

Non-canonical WNT signaling is activated by binding of a WNT to a receptor (independently of LRP5/6 receptors) which could be either one of the FZD receptors and/or an alternative receptor like Ryk, Ror1 or 2 (89). Downstream of these receptors lay a multitude of signaling cascades such as the Rho-kinase, c-Jun N-terminal kinase (JNK) or the YAP/TAZ pathway (90, 91). Owing to this heterogeneity, it is difficult to define clear target genes of non-canonical WNT signaling. Interestingly, non-canonical WNT signaling has been shown to antagonize canonical WNT/β-catenin signaling in various ways (92-94).

Whether canonical or non-canonical WNT signaling is transmitted, was originally thought to be determined by the WNT binding on the cell surface. Although this process was discovered to be more complex and highly dependent on cell type and receptor recruitment, some WNTs are still considered to mainly trigger canonical (e.g. WNT3A) or non-canonical WNT (e.g. WNT5A) signaling (89, 90, 95).

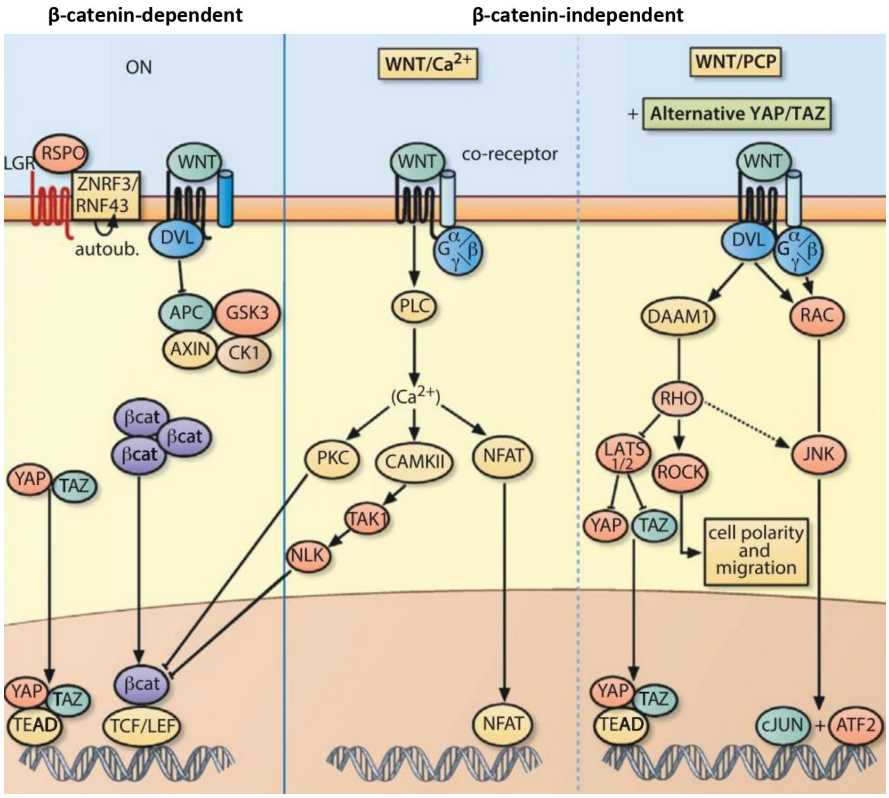

Figure I4: Overview of WNT signaling cascades

Canonical (β-catenin-dependent) and non-canonical (β-catenin-independent) WNT pathways are triggered based on WNT and (co-)receptor interaction. Modified images with permission of El Sevier (96).

Balanced WNT signaling is indispensable for a multitude of biological processes during embryogenesis (86, 88). In lung development, WNT signaling controls lung progenitor specification, epithelial-mesenchymal interaction and branching of the distal airways (97-100). However, it has been recognized for a long time that the WNT pathway also affects adult tissue homeostasis orchestrating cellular processes like proliferation, migration and differentiation (88, 101). Considering this, it is easy to conceive that dysregulated WNT signaling contributes to disease pathogenesis. In fact, one of the best-described implications of WNT signaling in human disease is a mutation of APC leading to inappropriate accumulation of β-catenin promoting a hereditary form of colon cancer called familial adenomatous polyposis (102, 103).

1.2.2 Involvement in chronic lung diseases

The first study describing deranged WNT signaling in chronic lung pathologies was conducted by Chilosi et al. who detected enhanced β-catenin staining in bronchiolar lesions and fibroblastic foci in IPF samples (104). These findings were supported by unbiased gene expression profiling detecting a so-called "WNT signature" in IPF (83). Further research created a more comprehensive view showing that in addition to β-catenin other components of the WNT pathway such as WNT7B, WNT10A and FZD receptors like *FZD2* and *FZD3* are increasingly expressed in IPF lung tissue compared to donor lung tissue (81, 96, 105-107). It is worth noting that also modulators of WNT signaling are differentially expressed in IPF, for instance dickkopf (DKK) proteins, "inhibitor of β-catenin and TCF-4" (ICAT) and micro-RNA (miR/miRNA) targeting FZD receptors (108-111). Furthermore, increased gene expression of *WNT3A*, *FZD7*, *FZD8* and the WNT coreceptors *LRP5/6* among other WNT components in peripheral blood mononuclear cells (PBMC) has been associated to disease progression (112). Promisingly, numerous studies presented alleviated experimental fibrosis using pharmacological inhibitors or antibodies to target transcriptional coactivators of β-catenin, the β-catenin destruction complex or the WNT target gene "WNT1-inducible signaling protein–1" (WISP1) (105, 113, 114). However, when therapeutically modulating the canonical WNT pathway, it must be considered that a certain expression level of β-catenin seems essential for proper epithelial repair. Thus, determining an adequate equilibrium between too much profibrotic and too little regenerative WNT/β-catenin signaling remains an ongoing challenge (115, 116).

A disease which displays insufficient regeneration in the form of lung emphysema and reduced canonical WNT signaling in the epithelium is COPD, as shown by diminished nuclear β-catenin staining and reduced WNT target gene expression in specimen of human COPD lungs compared to donors (117-121). Several underlying mechanisms have been proposed. Ezzie et al. described that WNT pathway components might be a target of miRNA dysregulated in COPD and Jiang et al. suggested that WNT/β-catenin signaling is controlled by the COPD susceptibility gene "family with sequence similarity 13, member A" (*FAM13A*) (122, 123). Fascinatingly, FAM13A null mice were protected against emphysema induced by either cigarette smoke or elastase while the protection against the latter could be reversed by inhibition of β-catenin signaling (123). Other studies focused on WNT signaling components upstream of β-catenin. Specifically, decreased expression levels of FZD4 and increased levels of non-canonical

WNT5A have been delineated with a negative regulatory effect on WNT/β-catenin signaling. In these studies, low FZD4 expression and high WNT5A expression impaired alveolar epithelial cell function in terms of wound healing, differentiation capacity and organoid formation (94, 124, 125). Finally, the immanent therapeutic potential of WNT/β-catenin signaling in COPD was highlighted by studies using reactivation of WNT/β-catenin signaling via inhibition of GSK-3β, an enzyme of the β-catenin destruction complex. This intervention resulted in restored lung architecture in a murine model of COPD and notably, in patient-derived three dimensional-lung tissue cultures (117, 119).

An aspect of WNT signaling that is of emerging interest, but still less extensively studied, is the non-canonical branch of the pathway (121). In the context of IPF, Vuga et al. were first to describe that the prototype of a non-canonical WNT, WNT5A, is enhanced in fibroblasts isolated from patients with UIP, the pathologic correlate to IPF, compared to normal lung fibroblasts (126). Further studies showed that in fibrotic lung disease, WNT5A is expressed in a variety of structural cells, WNT5A expression is increased (even in normal-looking parenchyma belonging to IPF specimen) and that WNT5A is secreted in extracellular vesicles (109, 127, 128). Interestingly, in the IPF patient cohort investigated by Lam et al., *WNT5A* in PBMCs was among the top hits of WNT pathway components associated to disease progression (112). As receptors transmitting non-canonical WNT signals in IPF, FZD7 and FZD8 have been proposed (129, 130).

In COPD, fascinatingly, observations of upregulated non-canonical WNT signaling have been made as well. Bronchial biopsy specimen and epithelial cells of COPD patients are enriched with WNT4, which was described to have proinflammatory effects in the setting of bronchitis independently of β-catenin (131, 132). The induction of *WNT5B*, another WNT known to predominantly trigger non-canonical WNT signaling, by TGF-β stimulation was more pronounced in fibroblasts from COPD patients compared to fibroblasts from patients without COPD, whereas immunohistochemistry studies showed enhanced WNT5B signal in the bronchial epithelial layer (133, 134). On the cellular level, WNT5B increased the expression of remodeling genes in bronchial epithelial cells and of proinflammatory genes in lung fibroblasts (134, 135). Moreover, a single nucleotide polymorphism of the FZD8 receptor was associated with chronic mucus hypersecretion, a feature of chronic bronchitis. Functionally, Spanjer et al.

delineated that FZD8 concerts different proinflammatory stimuli in lung fibroblasts (136). Recent studies finally investigated the expression of the prototype ligand for non-canonical WNT signaling, WNT5A, in COPD and found an upregulation in lung homogenate of murine models and COPD patients as well as in patients` sera (94, 135, 137). Intriguingly, antibody-mediated inhibition of WNT5A in a murine model of COPD resulted in improved lung architecture and function along with restored epithelial cell markers (94).

The same study compared WNT5A expression in different structural cells of the lung indicating that a large proportion of WNT5A in the lung is derived from fibroblasts, which is in accordance with the studies carried out in IPF (94, 126, 127). However, the understanding of the background of elevated WNT5A in chronic lung diseases is poor and there are remarkable gaps in the knowledge regarding the autocrine function of WNT5A on fibroblasts.

2 Aim of the study

COPD and IPF are severe and ultimately fatal diseases. While COPD mostly harms in a slowly progressing way, yet with a high prevalence all over the world, IPF occurs less often, but has a prognosis worse than many types of cancer with a median survival of ~ 3 years (7, 13). Both disorders lack causal therapies with disease management focusing on symptom relief and deceleration of disease progression (9, 13). Pathological features that COPD and IPF have in common are among others aberrant fibroblast function and altered signaling of development pathways, such as the WNT pathway (71, 72, 121). Promisingly, modulation of WNT/β-catenin signaling has been shown to be beneficial in murine models of COPD and pulmonary fibrosis (105, 114, 117, 138, 139). However, the role of non-canonical WNT signaling in COPD and IPF is less clearly determined. Here, we aimed to further understand the role of non-canonical WNT signaling for the following reasons: 1) The expression of the non-canonical WNT WNT5A is not only upregulated in the whole lung of COPD and IPF patients, but also 2) specifically in fibroblasts isolated from lungs of individuals that suffer from these diseases (94, 109, 126, 127). Yet, there is scarce evidence about what causes the increased WNT5A levels in the lung and the consequences on development and progression of COPD and IPF that arise from it.

Thus, we frame two research questions for the present study:

1) **Do COPD- and IPF-relevant stimuli induce WNT5A expression in lung fibroblasts?**
2) **Does WNT5A stimulation lead to aberrant lung fibroblast function?**

To answer this, we analyzed:

- Regulation of WNT5A mRNA and protein expression in human lung fibroblasts by profibrotic (TGF-β, WNT3A) and proinflammatory (TNF-α, IL-1β, IL-6) stimuli as well as soluble components of cigarette smoke
- Impact of WNT5A treatment on gene expression, proliferation, differentiation and attachment of human lung fibroblasts

3 Material and Methods

3.1 Materials

3.1.1 Recombinant protein

Protein:	Company:	Product code:
hTGF-β1	R&D, Minneapolis, MN, USA	240B
hWNT3A	R&D, Minneapolis, MN, USA	5036-WN
hTNF-α	R&D, Minneapolis, MN, USA	210-TA
hIL-6	R&D, Minneapolis, MN, USA	206-IL
hIL-1β	R&D, Minneapolis, MN, USA	201-LB
h/mWNT5A	R&D, Minneapolis, MN, USA	645-W

3.1.2 Antibodies

Antibody:	Company:	Application:
Anti-WNT5A (rat) *MAB645*	R&D Systems Minneapolis, MN, USA	1:750 in Roti-Block, non-reducing, non-denaturating conditions
Anti-BSA (mouse) *SC57504*	Santa Cruz Biotechnology Santa Cruz, CA, USA	1:500 in Roti-Block, non-reducing, non-denaturating conditions
Anti-β-actin, HRP-labelled (mouse) *A5228*	Sigma-Aldrich St. Louis, MO, USA	1:50000 in 5% milk
Anti-Cyclin D1 (rabbit), *92G2*	Cell Signaling Danvers, MA, USA	1:1000 in Roti-Block
Anti-α-SMA (mouse), *A5228*	Sigma-Aldrich St. Louis, MO, USA	1:1000 in Roti-Block
Anti-rat *NA935V*	GE Healthcare Chicago, IL, USA	1:4000 in 5% milk
Anti-mouse *NA931V*	GE Healthcare Chicago, IL, USA	1:4000 in 5% milk
Anti-rabbit *NA934V*	GE Healthcare Chicago, IL, USA	1:10000 in 5% milk

3.1.3 Primer sequences

Gene:	Sequence (5' to 3'):
HPRT_fw	AAGGACCCCACGAAGTGTTG
HPRT_rv	GGCTTTGTATTTTGCTTTTCCA
WNT5A_fw	CCAAGGGCTCCTACGAGAGTGC
WNT5A_rv	CACATCAGCCAGGTTGTACACCG
IL8_fw	CAGGAAGAAACCACCGGAAG
IL8_rv	AACTGCACCTTCACACAGAG
COMP_fw	ATGCAGACTGCGTCCTAGAG
COMP_rv	GTCACGCAGTTGTCCTTACG
ELN_fw	GGCCATTCCTGGTGGAGTTCC
ELN_rv	AACTGGCTTAAGAGGTTTGCCTCC
TNS1_fw	TCAAGTGGAAGAACTTGTTTGCTT
TNS1_rv	CACGACAATATAGTGGAGGCACA
TSPAN2_fw	TCTATGTGGGGCTGTATGTTCT
TSPAN2_rv	TCACCAGGAGGCAGGTAAAA
Acta2_fw	CGAGATCTCACTGACTACCTCATGA
Acta2_rv	AGAGCTACATAACACAGTTTCTCCTTGA
Axin2_fw	AGAAATGCATCGCAGTGTGAAG
Axin2_rv	GGTGGGTTCTCGGGAAATG
CyclinD1_fw	CCGAGAAGCTGTGCATCTACAC
CyclinD1_rv	AGGTTCCACTTGAGCTTGTTCAC

Primer pairs were ordered from Eurofins MWG Operon; Ebersberg, Germany.

3.1.4 Pharmacological inhibitors

Pharmacological inhibitor:	Company:	Product Number:
SB216763	Tocris	1616
SC514	Tocris	3318
7-Oxozeaenol	Tocris	3604
U0126	Tocris	1144

3.1.5 Reagents and chemicals

10x PCR Buffer II	Applied Biosystems, Thermo Fisher; Waltham, MA, USA
Acryl-bisacrylamide mix (Rotiphorese gel 30 (37,5:1))	Carl Roth; Karlsruhe, Germany
Amicon-Ultra-filters	Merck; Darmstadt, Germany
APS	AppliChem; Darmstadt, Germany
Bromophenol blue	AppliChem; Darmstadt, Germany
BSA in PBS	Sigma-Aldrich; St. Louis, MO, USA
Collagenase I	Biochrom, Merck; Darmstadt, Germany
COmplete Mini Prot. Inh.	Roche; Basel, Switzerland
Cyanine-3 dye	Agilent Technologies; Santa Clara, CA, USA
DAPI	Sigma-Aldrich; St. Louis, MO, USA
dNTPs	Thermo Fisher; Waltham, USA
DTT	AppliChem; Darmstadt, Germany
DMEM-F12	Gibco, Thermo Fisher Scientific; Waltham, MA, USA
DMSO	Carl Roth; Karlsruhe, Germany
EDTA	AppliChem; Darmstadt, Germany
EGTA	Sigma-Aldrich; St. Louis, MO, USA
Ethanol	AppliChem; Darmstadt, Germany
Falcon Cell Strainer filters	BD; Franklin Lakes, NJ, USA
FCS	PAN-Biotech; Aidenbach, Germany
Glycerol	AppliChem; Darmstadt, Germany
Glycine	AppliChem; Darmstadt, Germany
H_2O, RNase free	Peqlab, VWR Life Science; Erlangen, Germany
LightCycler® 480 SYBR Green I Master	Roche; Basel, Switzerland
Lipofectamine 2000	Thermo Fisher Scientific; Waltham, MA, USA
Methanol	AppliChem; Darmstadt, Germany
$MgCl_2$	Applied Biosystems, Thermo Fisher; Waltham, MA, USA
Minisart filter	Sartorius; Göttingen, Germany
MuLV reverse transcriptase	Applied Biosystems, Thermo Fisher; Waltham, MA, USA
NaCl	Sigma-Aldrich; St. Louis, MO, USA
$Na_4P_2O_7$	Sigma-Aldrich; St. Louis, MO, USA
Non-fat dried milk powder	AppliChem; Darmstadt, Germany

NP-40	AppliChem; Darmstadt, Germany
Opti-MEM	Gibco, Thermo Fisher Scientific; MA, USA
peqGOLD Total RNA kit	Peqlab, VWR Life Science; Erlangen, Germany
Pierce ECL substrate	Thermo Fisher Scientific; Waltham, MA, USA
Pierce BCA Assay Kit	Thermo Fisher Scientific; Waltham, MA, USA
Protein marker V	VWR Life Science; Erlangen, Germany
Random hexamers	Invitrogen, Thermo Fisher Scientific; Waltham, USA
Research cigarettes (3R4F)	Kentucky Tobacco Research and Development Center at the University of Kentucky; Lexington, KY, USA
RNase inhibitor	Applied Biosystems, Thermo Fisher; Waltham, MA, USA
Roti®-Block	Carl Roth; Karlsruhe, Germany
P/S	Gibco, Thermo Fisher Scientific; Waltham, MA, USA
PFA 4%	Carl Roth; Karlsruhe, Germany
PhosSTOP phosph. inh.	Roche; Basel, Switzerland
SDS	Carl Roth; Karlsruhe, Germany
Sodium deoxycholate	Sigma-Aldrich; St. Louis, MO, USA
Stripping buffer Restore Plus for Western blot	Thermo Fisher Scientific; Waltham, MA, USA
SuperSignal West Dura	Thermo Fisher Scientific; Waltham, MA, USA
SuperSignal West Femto	Thermo Fisher Scientific; Waltham, MA, USA
SurePrint G3 Human GE 8x60K Microarrays	Agilent Technologies; Santa Clara, CA, USA
TEMED	AppliChem; Darmstadt, Germany
Tris	AppliChem; Darmstadt, Germany
Trypsin	Gibco, Thermo Fisher Scientific; Waltham, MA, USA
Tween-20	AppliChem; Darmstadt, Germany

3.1.6 Equipment and software

24-well plates Costar® for adhesion assay	Corning, Sigma-Aldrich; St. Louis, MO, USA
2100 Bioanalyzer	Agilent Technologies; Santa Clara, CA, USA
AxioVision LE 4.8	Zeiss; Jena, Germany
ChemiDoc XRS+	Bio-Rad; Hercules, CA, USA
Chromatography paper	GE Healthcare; Chicago, IL, USA

Whatman 3 mm	
Electrophoresis chamber Mini-PROTEAN Tetra Cell	Bio-Rad; Hercules, CA, USA
Feature Extraction 10.7.3.1	Agilent Technologies; Santa Clara, CA, USA
GraphPad PRISM	GraphPad Software; San Diego, CA, USA
Image Lab software	Bio-Rad; Hercules, CA, USA
Light Cycler 480 II	Roche; Basel, Switzerland
LSM Microscope 710	Zeiss; Jena, Germany
MasterCycler nexus	Eppendorf; Hamburg, Germany
NanoDrop 1000	Peqlab, VWR Life Science; Erlangen, Germany
Nitrocellulose membrane (0.2 µm)	Bio-Rad; Hercules, CA, USA
Plate Reader Sunrise	Tecan; Männedorf, Switzerland
Scan Control A.8.4.1	Agilent Technologies; Santa Clara, CA, USA

3.2 Cell culture

3.2.1 Fibroblast isolation

Primary human lung fibroblasts were kindly provided by the CPC Munich bioArchive whose employees performed the herein described procedures. Fibroblasts were obtained from human lungs that couldn't be entirely transplanted to a recipient or from patients undergoing thoracic surgery due to lung cancer whose adjacent tumor-free lung tissue was processed. Surgeries were performed at University Hospital of the LMU, Großhadern, Munich and at Asklepios Clinic Gauting. Participants provided written informed consent to participate in this study, in accordance with approval by the local ethics committee of the LMU (Project 333–10, 455–12). Lung fibroblasts were isolated using the outgrowth method. Resected lungs were cut into pieces of 1-2 cm^2 followed by 2 h of digestion at 37°C with Collagenase I to degrade collagen in the extracellular matrix. Next, digested samples underwent filtration through Falcon Cell Strainer filters with a pore size of 70 µm to remove large tissue clumps. The cell containing filtrate was centrifuged at 400 g at 4 °C for 5 min. The obtained pellet was resuspended in "Dulbecco's Modified Eagle Medium: Nutrient Mixture F-12" (DMEM-F12) supplemented with 20% (v/v) fetal calf serum (FCS), 100 U/ml penicillin and 100 mg/l

streptomycin (P/S) and seeded on 10 cm cell culture dishes for expanding. Medium was changed every other day and cells were split at 80-90% confluency.

3.2.2 Fibroblast culture

All experiments were carried out using primary human fibroblasts if not described differently. Fibroblasts isolated as described above were expanded in 75 cm^2-flasks in DMEM-F12 supplemented with 10% (v/v) FCS and P/S in the concentrations described in chapter 3.2.1 in an incubator with a temperature of 37°C and an atmosphere with 5% CO_2, 19.5% O_2 and 95% relative humidity. Medium was changed every 2-3 days. For experimental procedures, cells were detached by treatment with 0.1% Trypsin in ethylenediaminetetraacetic acid (EDTA). After complete detachment, the reaction was stopped adding 10% (v/v) FCS DMEM-F12. The cells in the suspension were counted using a Neubauer chamber and seeded at a density of 20.000 cells/cm^2 on appropriate cell culture dishes. The next day, medium was changed to 0.1% (v/v) FCS starvation medium for growth arrest overnight before treatment.

Recombinant proteins were dissolved in 0.1% bovine serum albumin (BSA) in phosphate-buffered saline (PBS), thus control cells were treated with the respective amount of 0.1% BSA in PBS. If used, pharmacological inhibitors or the vehicle substance dimethyl sulfoxide (DMSO) were applied 30 min before stimulation of cells with growth factors, for instance TGF-β.

3.2.3 siRNA transfection

Fibroblasts were seeded as described in chapter 3.2.2. The next day, cells were transfected for 6 h with 50 pmol WNT5A-small interfering ribonucleic acid (siRNA) (*sc-41112*; Santa Cruz Biotech; Dallas, TX, USA) or scrambled (scr) siRNA (*sc-37007*; Santa Cruz Biotech; Dallas, TX, USA) using Lipofectamine RNAiMAX transfection reagent dissolved in serum- and antibiotics-free Opti-MEM. Afterwards, transfection medium was replaced by 10% FCS DMEM-F12 full growth medium overnight and subsequently treated with TGF-β.

3.2.4 Cigarette smoke extract (CSE) preparation

Six research cigarettes (Research-grade cigarettes (3R4F)) were constantly bubbled through 100ml of serum- and antibiotics-free DMEM-F12 medium (Fig. **M1**) followed by sterile filtration through a 0.20 µm Minisart filter. This CSE was frozen at -20°C before use to reduce batch-to-batch variation and considered to be 100% CSE. Before treatment, CSE was diluted to the desired concentration with starvation medium and supplemented with FCS (final concentration 0.1% (v/v)) and P/S (final concentration (1% (v/v)). Cells were photographed after the indicated culture time to assess toxic effects of CSE.

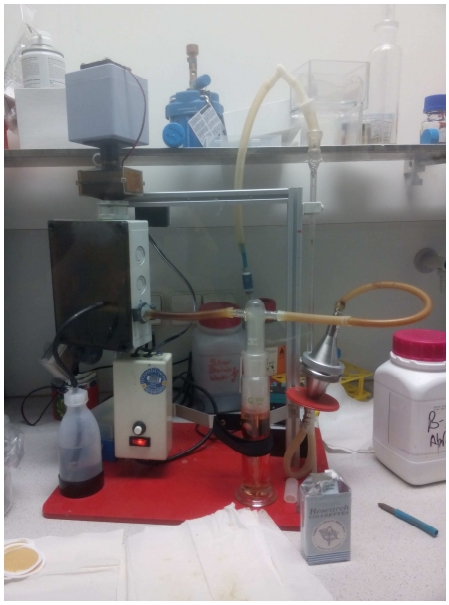

Figure M1: Pump for the generation of cigarette smoke extract

The experimental setup was kindly provided by the Meiners lab at CPC Großhadern. One burning research cigarette is fixed in the black box on the left and smoked at constant airflow by the pump in the back of the setup. Smoke is bubbled through cell culture medium in a flask placed between the smoking box and the pump. The pump is protected from smoke particles by an interposed filter. Filter papers are changed after every smoked cigarette (compare used ones on the left).

3.3 Immunoblotting

3.3.1 Supernatant concentration

Supernatants collected from cultured cells were concentrated ten-fold using Amicon-Ultra-0.5 ml centrifugal filters. 500 µl of supernatant was loaded on filter devices that were placed in a microcentrifuge tube provided with the filters. Following 30 min of centrifugation at 14.000 g, the filter devices were inversely placed in a fresh microcentrifuge tube and centrifuged for 2 min at 2.000 g to recover the concentrate which was stored at -20°C before further use.

3.3.2 Protein isolation

Lung fibroblasts were lysed on ice for 5 min with radioimmunoprecipitation assay (RIPA) buffer or, when a stronger detergent was desirable, with sodiumdodecylsulphate (SDS) buffer supported by scraping with a pipet tip. For one well of a 6-well plate, 125 µl of lysis buffer was used. Lysates were centrifuged at 13.000 rotations per minute (rpm) for 10 min and supernatants were collected. Samples were stored at -20°C before further use.

RIPA buffer (pH adjusted to 7.4):

20 mM Tris HCl
1 mM EDTA
1 mM EGTA
150 mM NaCl
2.5 mM $Na_4P_2O_7$
1% (w/v) sodium deoxycholate $C_{24}H_{39}NaO_4$
1% (v/v) NP-40

SDS buffer (pH adjusted to 6.8):

62.5 mM Tris
2% (w/v) SDS

Before use, to 10 ml of RIPA or SDS buffer one tablet of cOmplete Mini Protease Inhibitor and one tablet of PhosSTOP phosphatase inhibitor were added.

To determine the protein concentration in the lysate, the colorimetric bicinchoninic acid (BCA) assay with Pierce BCA Protein Assay Kit was carried out according to the manufacturer's protocol. The BCA assay relies on two principles. First, Cu^{2+} ions are reduced by peptide bonds to Cu^{+} ions (biuret reaction). The amount of reduced Cu herein is straight proportional to the amount of peptide bonds. Next, the Cu^{+} ions form a complex with BCA in purple color. Analysis was performed by scanning the used 96-well plate with Plate Reader Sunrise. To normalize the absorbance, a standard curve using provided BSA was created and protein concentrations in the samples were determined by interpolation of absorbance. All samples were diluted 1:5 to save lysates, tested in duplicates and absorbance was averaged.

Prior to loading to the SDS-PAGE gel, 7.5 – 10 µg of protein per sample was diluted with the respective lysis buffer to 30 µl and mixed 3:1 with 4x Laemmli loading buffer. Next, samples were boiled at 95°C for 10 min to denaturate the proteins, so that in combination with the equally negative charge reassured by SDS in the Laemmli buffer, proteins were only to be separated according to their molecular weight during the electrophoresis. If an antibody worked best in non-reducing, non-denaturating conditions (compare chapter 3.1.2), no DTT was added to the Laemmli buffer and the samples were not boiled. To determine the molecular weight of the detected bands at the end of the immunoblotting procedure, a prestained Protein Marker V was always run alongside of the samples.

Laemmli loading buffer:

Chemical:	Concentration:
Tris (pH 6,8)	150 mM
SDS	275 mM
Glycerol	3.5 % (w/v)
Bromophenol blue	0.02 %
Dithiothreitol (DTT)	400 mM

3.3.3 SDS polyacrylamide gel electrophoresis (SDS-PAGE)

SDS-PAGE was performed in an electrophoresis chamber filled with running buffer to separate proteins depending on their molecular weight. Proteins with a higher molecular weight run slower through the polymerized acrylamide gel than smaller proteins. The gel consists of a stacking gel that gathers all proteins in the sample at the same point in the gel before the actual separation step and a running gel where the proteins run towards the positive electrode represented by the bottom of the gel. Electrophoresis was performed at a voltage of initially 120 V for 60 min followed by 150 V for 20-30 min.

Stacking Gel:		**Running Gel (10% polyacrylamide):**	
68%	distilled H_2O	40%	distilled H_2O
17%	acryl-bisacrylamide mix (30%)	33%	acryl-bisacrylamide mix (30%)
13%	1.5 M Tris (pH 6.8)	25%	1.5 M Tris (pH 8.8)
1%	10% (w/v) SDS	1%	10% (w/v) SDS
1%	10% (w/v) ammonium persulfate	1%	10% (w/v) ammonium persulfate
0.1%	TEMED	0.04%	TEMED

All percentages given are volume concentrations, if not indicated differently.
Preparing the gel, ammonium persulfate and Tetramethylethylenediamine (TEMED) had to be added as the last step since these compounds start the acrylamide polymerization.

Running buffer:

Tris/HCL pH 7.4	250 mM
Glycine	1.92 M
SDS	1% (w/v)

3.3.4 Immunoblotting

After completed electrophoresis, the proteins were transferred from the gel to a nitrocellulose membrane (0.2 µm) via wet electroblotting. The gel was placed vertically in an electrophoresis chamber filled with transfer buffer. To assure proper transfer without air bubbles, the gels were fixed in a stack made up of a support grid, sponges and chromatography paper. Additionally, the electrophoresis chamber was cooled with ice packs to mitigate heat generation. Electroblotting eventually was performed at 100 V for 60 min.

Afterwards, the nitrocellulose membranes carrying the proteins were briefly rinsed with triphosphate buffered saline (TBS) supplemented with 0.05% Tween-20 (=TBST) and subsequently blocked with 5% non-fat dried milk powder in TBST or Roti®-Block depending on how the following primary antibody was dissolved (compare 3.1.2). This minimized unspecific binding of the antibodies on the membranes. Primary antibody incubation was performed overnight at 4°C or for 1-2 h at room temperature to detect the protein of interest. After four washing steps for 5 min with TBST, the membrane was incubated for 1 h at room temperature with the secondary antibody, which was tagged with horseradish peroxidase (HRP) and directed against the species of origin of the primary antibody. Next, the membrane was again washed with TBST four times for 5 min and proceeded to visualization.

Enhanced chemiluminescence (ECL) substrates for the HRP tagged to the secondary antibody were applied to the membrane. Pierce ECL, SuperSignal West Dura Extended or SuperSignal West Femto Maximum Sensitivity Western blotting substrates were used with increasing signal intensity from ECL over Dura to Femto depending on the strength of the chemiluminescent signal which was detected by ChemiDoc XRS+. If membranes were to be incubated with a different antibody afterwards, stripping buffer Restore Plus was added for 10 min and subsequently the membrane was briefly washed with TBST.

All the procedures were performed at room temperature, if not indicated differently.

Transfer buffer:		**Transfer buffer 10x:**	
Transfer Buffer 10x	10%	Tris/HCl	50 mM
Methanol	200 ml	Glycine	400 mM

TBS:

Tris/HCl pH 7.4	10 mM
NaCl	150mM

3.3.5 Quantification

Densitometric analysis was carried out with Image Lab software. Optical density of the specific band of interest was determined and normalized to the loading control. For cell lysates, β-actin abundance served as a loading control, for supernatants, equal loading was verified by protein expression of BSA, which is part of FCS.

3.4 Quantitative Real-Time Polymerase Chain Reaction (qRT-PCR)

3.4.1 RNA isolation and quantification

RNA isolation from primary human lung fibroblasts was carried out with the peqGOLD Total RNA kit according to the manufacturer's instructions. Cells were lysed using the provided lysis buffer supported by scraping with a pipet tip to detach all cells from the culture plate. Deoxyribonucleic acid (DNA) was removed by precipitating the nucleic acids in the lysate with ethanol and centrifugation through a specialized DNA binding column, RNA isolation was performed with serial centrifugation trough RNA binding columns. A DNase digestion step removed remaining contaminating DNA. Ultimately, the RNA bound to the column was eluted with 42 µl of RNase free water.

RNA concentration and purity were determined using NanoDrop ND-1000 spectral photometer. RNA concentration was calculated from the absorption at a wavelength of 260 nm, which is the absorption peak for RNA. In addition, the absorbance at the absorbance peak of proteins at 280 nm was measured and a ratio of A260/A280 was computed to determine the degree of protein contamination in the isolated RNA sample. A value of >2.0 for A260/A280 was considered appropriate for reverse transcription.

3.4.2 Reverse transcription

Reverse transcription with MasterCycler nexus was performed to convert and amplify isolated RNA into complementary DNA (cDNA) which is suitable for further qPCR. Up to 2000 ng of RNA sample were diluted to 20 µl and heated up at 70°C for 10 min to degrade secondary structure into single-stranded RNA followed by 5 min incubation on ice to assure enzyme stability for the reverse transcriptase used later. Next, the denatured RNA samples were mixed with 20 µl of reverse transcription master mix containing

Reagent:	**Volume:**
10x PCR Buffer II	4 µl
$MgCl_2$	8 µl
dNTPs	2 µl
random hexamers	2 µl
H_2O, RNase free	1 µl
RNase inhibitor	1 µl
MuLV reverse transcriptase	2 µl

Random hexamers served as primers at random points on the RNA strand and annealed at 20°C for 10 min. The reverse transcriptase started the reaction at 43°C for 75 min with $MgCl_2$ as a cofactor and deoxynucleic triphosphates (dNTP) as substrates. Finally, the reverse transcriptase degraded at 99°C for 5 min to finish the transcription. The resulting cDNA concentrate was further diluted 1:5 and stored at -20°C.

3.4.3 qPCR (quantitative Polymerase Chain Reaction)

qPCR was performed to determine the amount of a specific cDNA using the SYBR Green I method. SYBR Green is a fluorescent cyanine dye that binds to the minor groove of double-stranded DNA (dsDNA), a process that enhances the emission of its fluorescent signal by more than the factor 1000. The fluorescent signal intensity is proportional to the amount of dsDNA, which allows the quantification of the specific sequences that are amplified by qPCR (140). Specificity was assured by proper primers (compare chapter 3.4.4.) starting the action of the thermostable Taq polymerase in the LightCycler® 480 SYBR Green I Master. We performed the qPCR in 96-well plates with 2.5 µl cDNA solution per experimental condition and 7.5 µl of the master mix containing

Reagent:	**Volume:**
LightCycler® 480 SYBR Green I Master	5 µl
forward primer (10 µM)	0.25 µl
reverse primer (10 µM)	0.25 µl
distilled water	2 µl

Step:		**Temperature:**	**Duration:**
1	warming-up of LightCycler	50°C	2 min
1	denaturation of double-stranded DNA	95°C	5 min
2	denaturation of double-stranded DNA	95°C	5 sec
2	primer annealing	59°C	5 sec
2	amplification of DNA by Taq polymerase	72°C	10 sec
3	melting curve	95°C	5 sec
3	melting curve	60°C	1 min
3	melting curve	60-97°C	continuous
4	cooling	4°C	30 sec

The procedures belonging to step 2 were repeated 45 times doubling the amount amplification product in every cycle. qPCR analysis with Light Cycler 480 II (Roche; Basel, Switzerland) delivered a cycle threshold (C_t) when the emitted fluorescence and thus the amount of amplified cDNA started to be significantly increased compared to the background signal which was representative of the amount of cDNA present in the

sample. All samples were measured in duplicates and averaged. Next, the C_t values of the target gene were normalized to the C_t of the constitutively expressed Hypoxanthine-guanine phosphoribosyltransferase (HPRT)(141). C_t (target gene) was subtracted from C_t (HPRT) and considered ΔC_t, Subtracting ΔC_t (control) from ΔC_t (treatment) was determined as $\Delta\Delta C_t$. Presented like this, a positive $\Delta\Delta C_t$ value signifies an upregulation upon treatment and vice versa. Owing to the calculation, ΔC_t and $\Delta\Delta C_t$ represent logarithmic values.

With qPCR analysis, you aim to decipher the amount of a specific amplicon. However, primer dimers also incorporate SYBR Green and can consequently distort the results. To control for primer quality, a duplicate of no template controls (only master mix, no cDNA sample) was run with every experiment. High C_t values or undetectable signal in the no template control indicated only few or no primer dimers. Additionally, melting curve analysis was performed to define the melting temperatures of the amplification product. Gradually increasing the temperature after 45 cycles releases the bound dye with a maximum decline in fluorescent signal at the melting temperature of the amplified dsDNA (140). A single sharp peak is indicative for specific primers, side peaks suggest distinct formation of primer dimers and/or amplified side products. (Fig. **M2**).

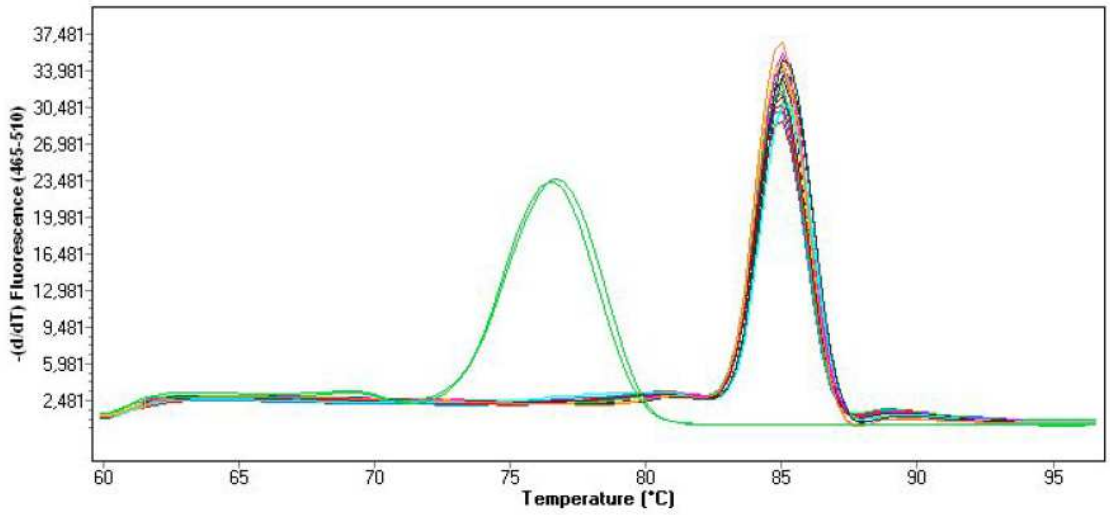

Figure M2: Melting curves for amplified Plasminogen activator inhibitor-1 (PAI-1)

Example melting curves of PAI-1 amplicon from cDNA from primary human lung fibroblasts. The peak at around 76 °C represents neglectable primer dimers in the no template control (turquoise) considering that the samples' melting curves (other colors) only have a single sharp peak at their designated melting temperature (~ 86 °C) and no additional peaks at 76 °C.

3.4.4 Primer design

Primers were designed with the NCBI Primer-BLAST tool (https://www.ncbi.nlm.nih.gov/tools/primer-blast/). Nucleotide sequences for the target genes were obtained from the NCBI nucleotide database (https://www.ncbi.nlm.nih.gov/nuccore/). Primer design was carried out taking account of the following parameters that were harmonized with our qPCR protocol:

- PCR product size: minimum 80 – maximum 150 base pairs
- primer melting temperatures: minimum 61°C – optimum 64°C – maximal 72°C
- melting temperature difference between forward and reverse primer: ≤5°C
- exon junction span: Primer must span an exon-exon junction, in order not to amplify contaminating DNA
- splice variant handling: choose “allow primers to amplify mRNA splice variants”

Primer pairs were delivered in lyophilized form and reconstituted with RNase free water according to the manufacturer’s instructions. Primer efficiency was tested by qPCR of serially diluted primary human lung fibroblast cDNA. If a doubling efficiency of 1.9 – 2.1 was achieved and the melting curve analysis showed no major side product or primer dimer amplification, the primers were regarded as appropriate for qPCR.

3.5 Microarray analysis

Primary human lung fibroblasts were stimulated with WNT5A (100 ng/ml) or BSA control for 6 and for 24 h followed by RNA isolation as described in chapter 3.4.1. Samples were sent to IMGM Laboratories (Martinsried, Germany) which provided the Agilent Microarray Analysis. RNA concentration and purity were determined using NanoDrop ND-1000 spectral photometer as described in chapter 3.4.1. A ratio of A260/280 > 1.6 was considered suitable for microarray analysis. RNA integrity was determined with the 2100 Bioanalyzer. This system utilizes capillary electrophoresis of RNA samples and calculates among other factors the 28S/18S-rRNA ratio to determine the level of RNA degradation. Eventually, a RNA integrity number between 1 and 10 is issued with a value of 1 meaning severe degradation and 10 meaning perfect RNA integrity. A value higher than 7.5 was required for the continuation of the microarray analysis. Our samples fulfilled all criteria described above. Next, 100 ng of RNA per sample underwent reverse transcription to cDNA followed by *in vitro* transcription. In the latter step, samples were labelled with fluorescent Cyanine-3 dye. To assure

sufficient cRNA (RNA transcribed from cDNA) yield, purity, integrity and dye incorporation, the samples were analyzed via NanoDrop and the 2100 Bioanalyzer as described above. Next, 600 ng per Cyanine-3 labelled cRNA sample were subject to hybridization on specific DNA probes on Agilent SurePrint G3 Human Gene Expression 8x60K Microarrays on 65°C for 17 h. After washing and drying, Scan Control A.8.4.1 software was used to scan fluorescent signal intensities to detect fluorescently labelled cRNA that had bound to the probes on the microarray chip. Further quantification and computational analysis were processed with Feature Extraction 10.7.3.1 software and delivered to our lab.

We created heatmaps using R software (http://www.cran.r-project.org/). *In silico* analysis of protein-protein interactions was performed using String database Version 10.0 (http://string-db.org/), functional annotation analysis was performed with DAVID Bioinformatics tool 6.8 Beta (https://www.david.ncifcrf.gov/summary.jsp).

3.6 Adhesion assay

Three different experimental setups were chosen to assess attachment of primary human lung fibroblasts to cell culture plates. In setup 1, cells were stimulated for 48 h with or without WNT5A followed by detachment with trypsin and seeding on a 24-well plate. In setup 2, cells were treated with or without WNT5A for 5 days directly on a 24-well plate, stimulation medium was changed every 2-3 days. After 5 days, cells were detached with 5 mM EDTA (pH 7.6) and gentle shaking of the cell culture dish until no attached fibroblasts were visible on light microscopy. Subsequently, previously untreated primary human lung fibroblasts were seeded on the extracellular matrix deposited on the well plate. In setup 3, previously untreated primary human lung fibroblasts were trypsinized and reseeded in medium with or without added WNT5A. In all setups, cellular adhesion to cell culture plates was stopped after 30 min by removing the seeding medium and washing with PBS. Next, 4% paraformaldehyde (PFA) was applied for 15 min for fixation. 4′,6-diamidino-2-phenylindole (DAPI) was used for 10 min to stain nuclei of attached cells. Entire wells were scanned with immunofluorescence LSM Microscope 71 and DAPI signal was quantified with AxioVision LE 4.8 software.

For all experimental setups, an equal number of up to 100.000 fibroblasts was seeded, the WNT5A concentration was 500 ng/ml and all conditions were tested in triplicates.

3.7 Statistical analysis

If not indicated differently, results in brackets (like ΔCt values) are presented as control vs treatment plus standard deviation (stdev). GraphPad PRISM was used to carry out the following calculations:

For paired observations from cell culture experiments, statistical significance was determined using two-tailed paired Student's t-test. Unpaired observations such as gene expression data in COPD and control lungs were assessed by Mann-Whitney U-test for the sample size was too small to perform a Shapiro-Wilk test on normal distribution. ΔΔCt values were analyzed by two-tailed, one-sample t-test.

When multiple values were to be tested against each other, One-Way-Analysis of Variance (ANOVA) with repeated measures followed by Newman-Keuls Multiple Comparison Test was applied, when multiple values were only to be compared to control conditions, Dunnett's Multiple Comparison Test succeeded One-Way-ANOVA. Analysis of correlation between gene expression and lung function parameters was carried out by Spearman test. Significance was assumed when $p<0.05$.

4 Results

4.1 Regulation of WNT5A in primary human fibroblasts

4.1.1 Influence of profibrotic and proinflammatory cytokines

First, we aimed to decipher whether in primary human lung fibroblasts, expression of WNT5A is regulated by profibrotic (TGF-β (2 ng/ml) and WNT3A (100 ng/ml)) and/or proinflammatory (TNF-α (10 ng/ml), IL-6 (10 ng/ml)) and IL-1β (1 ng/ml)) cytokines, that have been implicated in the pathogenesis of chronic lung diseases and in the induction of WNT5A (compare chapter 1.1.3). The concentrations of the recombinant proteins were selected in accordance with existing studies (142, 143). Since the concentrations of IL-1β were used on airway smooth muscle cells but not on lung fibroblasts, we performed dose-response experiments showing that only a concentration of 1 ng/ml of IL-1β was able to significantly increase *IL-8* mRNA expression (Suppl. Fig 1, (143)).

We observed that TGF-β significantly upregulated WNT5A expression both on mRNA level as determined by qRT-PCR (ΔCt: 4.01±0.91 vs 6.26±0.25, $p<0.05$, n=3; Fig. **1A**) and protein in the corresponding supernatants as measured by immunoblotting followed by densitometric analysis (fold of control: 3.33±1.61, $p<0.05$, n=5; Fig. **1B**). Moreover, WNT3A significantly increased *WNT5A* mRNA expression (ΔCt: 3.37±0.42 vs 4.45±0.04, $p<0.05$, n=3; Fig. **1C**) and showed a tendency to increase secretion of WNT5A protein compared to untreated fibroblasts (fold of control: 4.76±2.76, p=0.147, n=3; Fig. **1D**).

Treatment with the proinflammatory cytokines TNF-α, IL-6 or IL-1β in the used concentrations did not significantly alter *WNT5A* mRNA levels (Fig. **2A**) or secreted WNT5A (Fig. **2B**) 24 h after treatment.

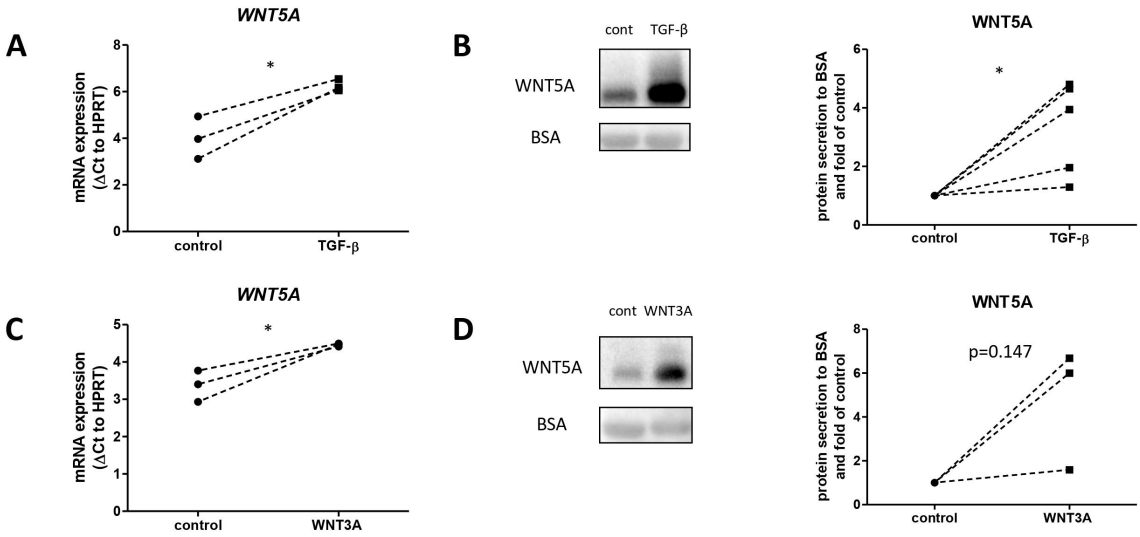

Figure 1: Profibrotic cytokines upregulate WNT5A expression.

Primary human lung fibroblasts were stimulated with TGF-β (2 ng/ml, **A** and **B**) or WNT3A (100 ng/ml **C** and **D**) and subject to qRT-PCR to determine mRNA levels after 24 h. *WNT5A* gene expression is shown as relative to the housekeeping gene HPRT (**A** and **C**). Supernatants were collected after 48 h of treatment and subject to immunoblotting followed by densitometric analysis to assess WNT5A protein secretion. Representative blots are shown (**B** and **D**). Statistical analysis was performed using two-tailed paired Student's t-test, *p<0.05. Results are presented as mean + stdev of 3-5 independent experiments.

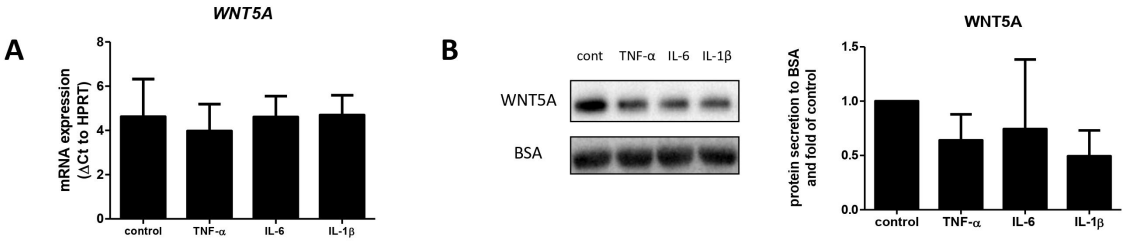

Figure 2: Proinflammatory cytokines do not significantly alter WNT5A expression.

Primary human lung fibroblasts were treated with TNF-α (10 ng/ml), IL-6 (10 ng/ml) and IL-1β (1 ng/ml) for 24 h. *WNT5A* mRNA expression was assessed via qRT-PCR (**A**), WNT5A protein secretion via immunoblotting of concentrated supernatants followed by densitometric analysis (**B**). Statistical analysis was performed using One-Way-ANOVA with repeated measures followed by Dunnett's Multiple Comparison Test. All results are shown as mean + stdev of 3 independent experiments.

4.1.2 Signaling pathways involved in TGF-β-induced upregulation of WNT5A

As TGF-β treatment resulted in the most robust induction of WNT5A expression, we decided to further study the mechanisms of TGF-β-induced upregulation of WNT5A in primary human lung fibroblasts. Similar to the WNT cascade, TGF-β can signal via canonical and non-canonical pathways. The canonical pathway is "Small Mothers Against Decapentaplegic" (SMAD)-dependent, whereas the non-canonical pathways rely on Ras/Erk-, TGF-β activated kinase 1 (TAK1)/ "Nuclear Factor kappa-light-chain-enhancer of activated B cells" (NF-κB)- and/or phosphatidylinositol-3-kinase (PI3K)/Akt-dependent pathways (144). There is ample evidence on interactions of TGF-β and WNT signaling in the lung field (107, 130, 133, 134, 145, 146). To investigate the pathways involved in WNT5A-induction by TGF-β, we added pharmacological inhibitors targeting pathways known to be both downstream of TGF-β and/or upstream of WNT5A prior to treatment with TGF-β (2 ng/ml) (Fig. **3**) (145, 147). Stimulation time for all the experiments described below was 24 h.

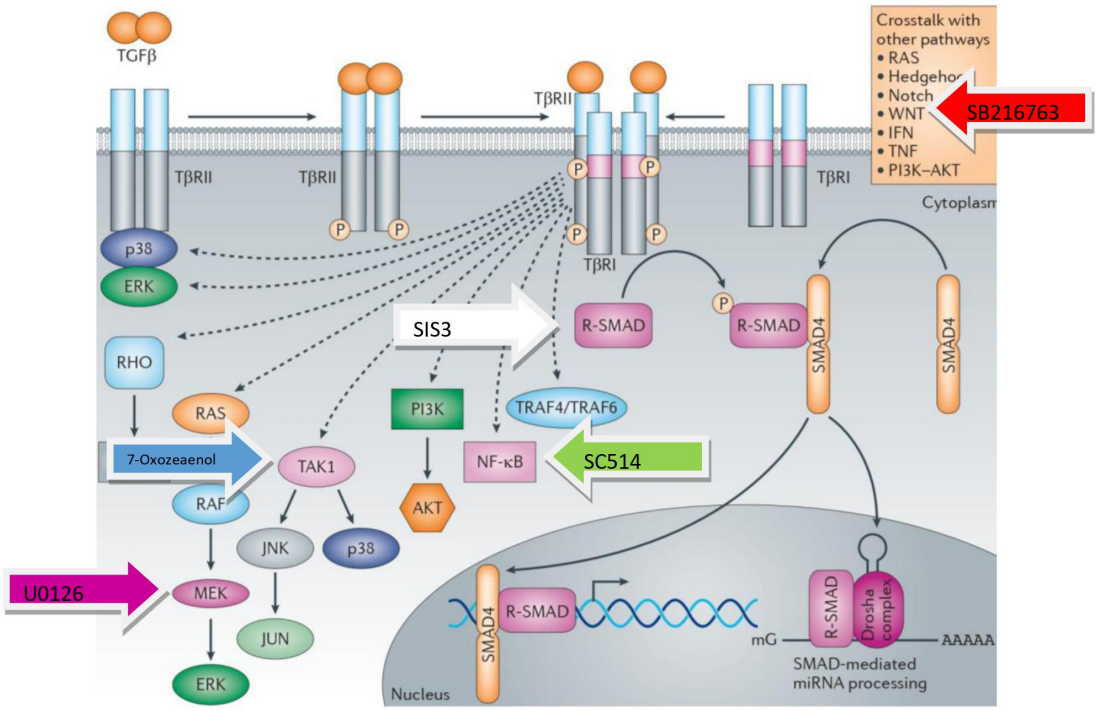

Figure 3: Targets of the used kinase inhibitors in the TGF-β signaling cascade

Inhibitors used: SMAD3 inhibitor SIS3 (white arrow), GSK-3β inhibitor SB216763 (5 µM, red arrow), Inhibitor of nuclear factor kappa-B kinase subunit beta (IKK-β, upstream of NF-κB) inhibitor SC514 (10 µM, green arrow), TAK1 inhibitor 7-Oxozeaenol (0.5 µM, blue arrow), Mitogen-activated protein kinase kinase 1/2 (MEK1/2) inhibitor U0126 (3 µM, purple arrow). Concentrations were used in line with previous studies (142, 148, 149). Modified image with permission of Springer Nature (144).

We also targeted SMAD3-phosphorylation, a critical event in canonical TGF-β signaling, by treating fibroblasts with SIS3. However, in our experimental setup, we found that the doses used were either not sufficiently high to change phospho-SMAD3 levels or toxic to the cells when concentrations were increased (personal communication), thus we focused on non-canonical TGF-β pathways.

Treatment of primary human lung fibroblasts with the GSK-3β inhibitor SB216763 resulted in a significant upregulation of *WNT5A* mRNA expression compared to vehicle control (ΔCt: 4.51±0.81 vs 5.20±0.56, $p<0.05$, n=4; Fig. **4A**). Inhibition of IKK-β, a kinase regulating NF-κB signaling, by SC514 did not alter *WNT5A* mRNA levels at baseline or after TGF-β treatment (Fig. **4B**). Conversely, decreasing the activity of TAK1 by 7-Oxozeaenol significantly lowered the increase of *WNT5A* transcript upon TGF-β stimulation compared to TGF-β treatment alone (ΔCt: 6.06±0.68 vs 5.35±0.48, $p<0.05$, n=4; Fig. **4C**). Using the MEK1/2 kinase inhibitor U0126 did neither alter *WNT5A* mRNA levels on baseline nor upon TGF-β stimulation (Fig. **4D**).

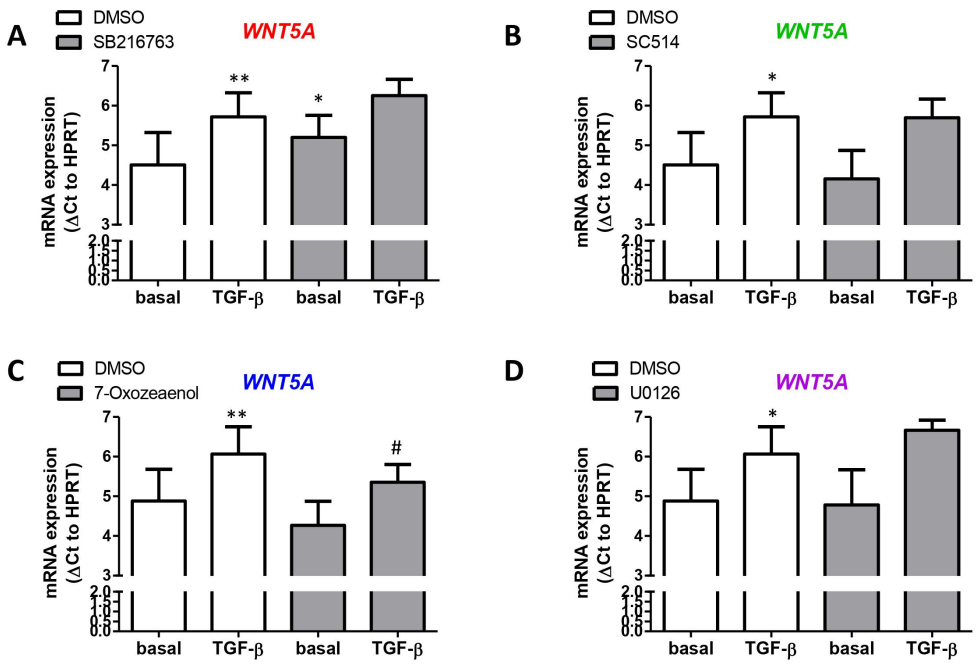

Figure 4: TGF-β induced upregulation of *WNT5A* mRNA is dependent on TAK1.

Primary human lung fibroblasts were treated with TGF-β (2 ng/ml) for 24 h in presence or absence of the GSK-3β inhibitor SB216763 (**A**), the IKK-β inhibitor SC514 (**B**), the TAK1 inhibitor 7-Oxoezeaenol (**C**) or the MEK1/2 inhibitor U0126 (**D**). The respective color code and concentrations of the inhibitors are indicated in figure 3. *WNT5A* mRNA levels were determined via qRT-PCR. Statistical analysis was performed using One-Way-ANOVA with repeated measures followed by Newman-Keuls Multiple Comparison Test, *$p<0.05$, **$p<0.01$ compared to basal + DMSO; #$p<0.05$ compared to TGF-β + DMSO. Results are presented as mean + stdev of 4 independent experiments.

Next, we analyzed the secretion of WNT5A into the cell culture medium (Fig. **5A**). In line with the observations on mRNA level, GSK-3β inhibition significantly increased baseline levels of secreted WNT5A to a similar extent than TGF-β (fold of TGF-β stimulation: 0.28±0.10 vs 1.09±0.38, $p<0.05$, n=3; Fig. **5B**). Inhibition of IKK-β led to a pronounced attenuation of TGF-β-increased WNT5A abundance in the supernatants (fold of TGF-β stimulation: 0.27±0.20, $p<0.001$, n=3; Fig. **5C**). Inhibition of TAK1 resulted in a similar effect (fold of TGF-β stimulation: 0.49±0.18, $p<0.01$, n=3; Fig. **5D**). Treatment with U0126 had no influence on basal or TGF-β-stimulated WNT5A secretion (Fig. **5E**). Finally, intracellular WNT5A protein expression was determined following the application of SB216763 or SC514 with or without TGF-β stimulation. Consistent with our supernatant data, inhibiting IKK-β resulted in an attenuation of TGF-β-induced intracellular WNT5A protein by TGF-β, whereas SB216763 did not exert effects on baseline or on TGF-β-stimulated WNT5A protein expression (Fig. **5F**).

Collectively, TGF-β induced *WNT5A* mRNA expression dependent on TAK1, whereas protein secretion was dependent on TAK1 and IKK-β and intracellular protein expression dependent on IKK-β. Contrarily, inhibition of GSK-3β increased *WNT5A* mRNA levels and secretion. MEK1/2 did not seem to be involved in the upregulation of WNT5A by TGF-β in primary human lung fibroblasts.

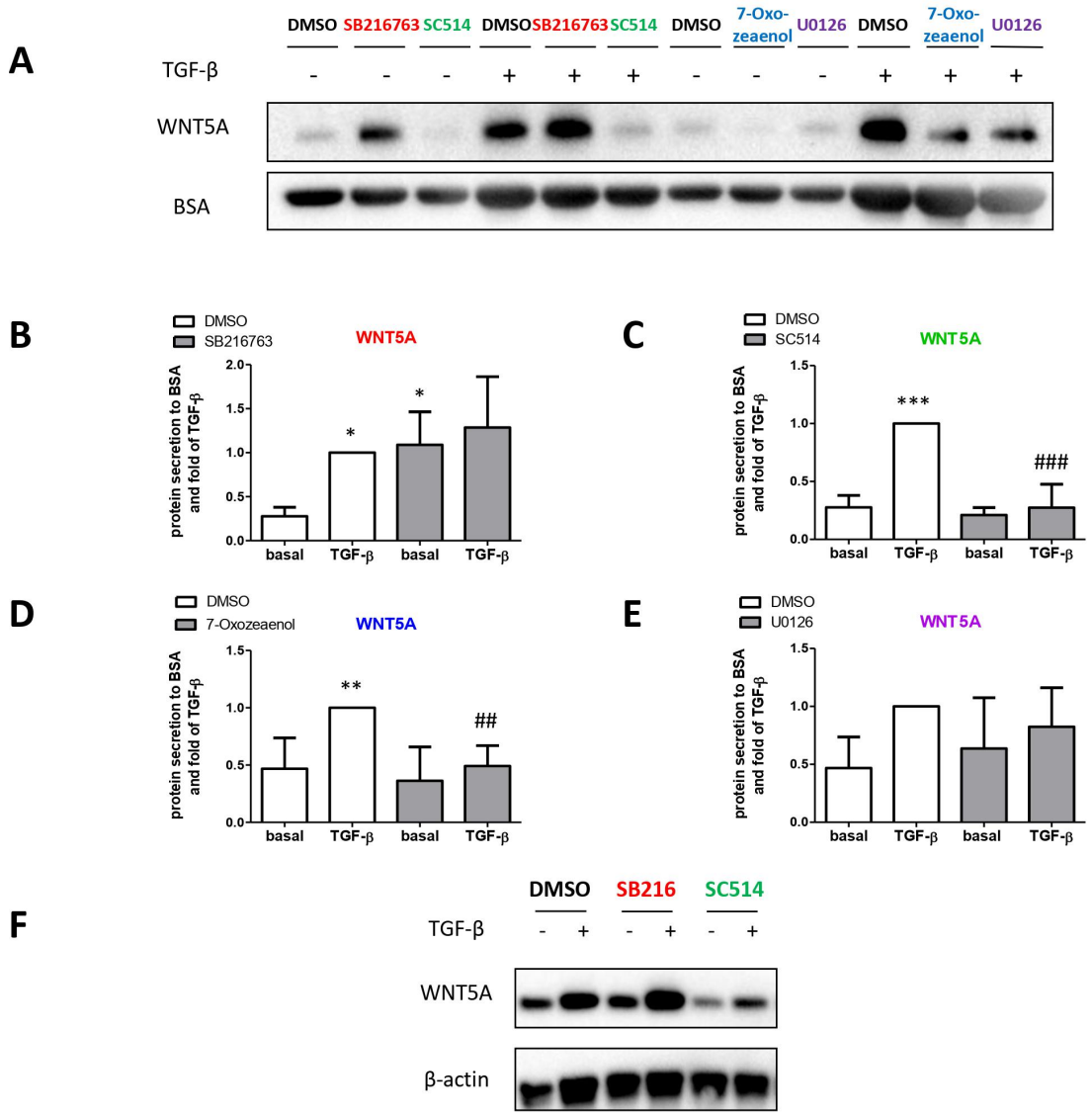

Figure 5: TGF-β induced upregulation of WNT5A protein is dependent on TAK1 and IKK-β

Primary human lung fibroblasts were treated with TGF-β (2 ng/ml) for 24 h in presence or absence the GSK-3β inhibitor SB216763, the IKK-β inhibitor SC514, the TAK1 inhibitor 7-Oxoezeaenol or the MEK1/2 inhibitor U0126. The respective color code and concentrations of the inhibitors are indicated in figure 3. WNT5A protein secretion was assessed via immunoblotting of concentrated supernatants (**A**). Densitometric quantification was performed normalizing to TGF-β stimulation without inhibitors because of high variability of baseline WNT5A in the supernatants. Effect of SB216763 (**B**), SC514 (**C**), 7-Oxozeaenol (**D**) or U0126 (**E**) on WNT5A secretion. Statistical analysis was performed using One-Way-ANOVA with repeated measures followed by Newman-Keuls Multiple Comparison Test, *p<0.05, **p<0.01, ***p<0.001 compared to untreated fibroblasts; ##p<0.01, ###p<0.001 compared to TGF-β without inhibitor added. Results are presented as mean + stdev of 3 independent experiments. Intracellular WNT5A protein expression was determined via immunoblotting of cell lysates of 2 independent experiments, β-actin was used as a loading control (**F**).

4.1.3 Influence of cigarette smoke extract on WNT5A expression

Cigarette smoke exposure is the major risk factor for the development of COPD and IPF. Previous work from our group demonstrated that WNT5A expression is elevated in lung homogenate of mice after both short (3 days) and long term (4 months) exposure to cigarette smoke (94). We aimed to transfer these findings to primary human lung fibroblasts to mimic the *in vivo* situation of a smoker's lung by treating the cells with different concentrations of cigarette smoke extract (CSE). In addition, we combined the CSE treatment with TGF-β stimulation to model a local environment with elevated TGF-β levels as found for example in the small airways of COPD patients and in fibrotic connective tissue in IPF patients (150, 151). We chose the relatively low dose of 5% CSE to avoid exceeding the maximal ability of fibroblasts to express WNT5A and to reduce potential cellular toxicity (152).

Initially, we aimed to decipher general effects of CSE on fibroblasts. Increasing concentrations up to 15% CSE did not alter fibroblast morphology (Fig. **6A**).
Already the low concentration of 5% CSE for 24 h was able to induce *IL-8* mRNA expression, which was used as a positive control (153) (ΔCt: -2.09±2.74 vs -1.34±2.86, $p<0.01$, n=4; Fig. **6B**).

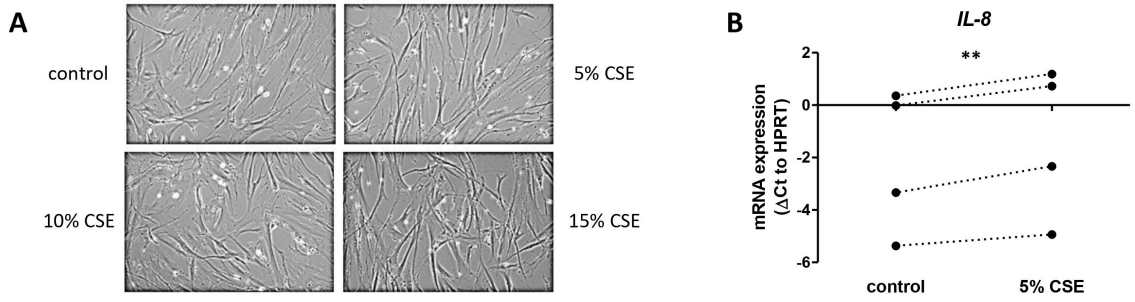

Figure 6: CSE upregulates *IL-8* mRNA but does not alter fibroblast morphology.

Primary human lung fibroblasts were treated with 5%, 10% or 15% CSE for 24 h. Fibroblast morphology as assessed by light microscopy (**A**). *IL-8* mRNA expression was measured by qRT-PCR as a positive control upon stimulation with 5% CSE (**B**). Statistical analysis was performed using two-tailed paired Student's t-test, **p<0.01, n=4.

Nevertheless, 24 h of CSE treatment had no clear effect on *WNT5A* mRNA levels. TGF-β (a positive control) significantly enhanced *WNT5A* mRNA (ΔCt: 5.03±1.41 vs 6.33±1.13; $p<0.001$, n=4), but there was no difference between the cotreatment of TGF-β and 5% CSE compared to TGF-β treatment alone. (Fig. **7A**).

However, prolonged treatment with CSE for 48 h showed a slight, though not significant upregulation of intracellular WNT5A protein. Remarkably, the combined treatment of TGF-β and 5% CSE resulted in an additive effect over solely TGF-β stimulation (fold of TGF-β stimulation: 1.31±0.29, $p<0.01$, n=4; Fig. **7B**).
The effect of 5% CSE potentiating the induction of WNT5A by TGF-β was even more pronounced when determining the amount of secreted WNT5A after 48 h (fold of TGF-β stimulation: 1.48±0.26, $p<0.001$, n=4; Fig. **7C**).

Taken together, we demonstrate that CSE discreetly increases WNT5A protein expression in primary human lung fibroblasts at baseline, whereas low doses of CSE strongly potentiate the ability of TGF-β to induce WNT5A protein intra- and extracellularly.

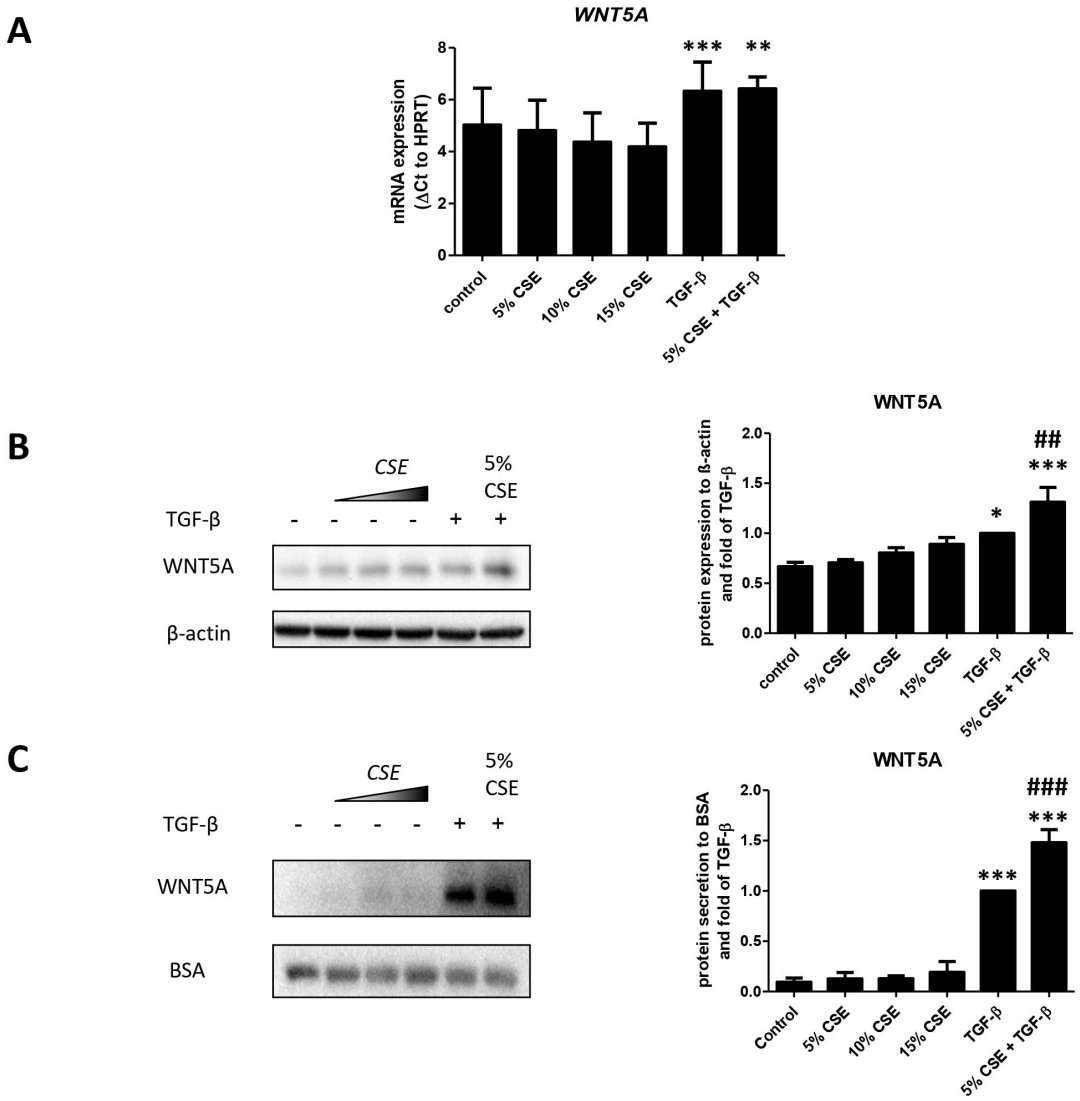

Figure 7: CSE enhances TGF-β-mediated upregulation of WNT5A protein

Primary human lung fibroblasts were stimulated with 5%, 10% or 15% CSE, TGF-β (2 ng/ml) or a combination of 5% CSE and TGF-β (2 ng/ml) for 24 h for mRNA and 48 h for intracellular and secreted protein. *WNT5A* transcript levels were determined by qRT-PCR (**A**), intracellular (**B**) and secreted (**C**) WNT5A protein expression by immunoblotting followed by densitometric analysis. Protein data is presented relative to TGF-β treatment without CSE because of low baseline expression of WNT5A. Statistical analysis was performed using One-Way-ANOVA with repeated measures followed by Newman-Keuls Multiple Comparison Test, *p<0.05, **p<0.01, ***p<0.001 compared to untreated fibroblasts; ##p<0.01, ###p<0.001 compared to TGF-β without CSE added. Results are presented as mean + stdev of 4 independent experiments.

4.2 Function of WNT5A on primary human lung fibroblasts

4.2.1 Microarray analysis of WNT5A-treated fibroblasts

To investigate how WNT5A acts on primary human lung fibroblasts, we first postulated that WNT5A alters gene expression in fibroblasts. We performed a microarray analysis treating fibroblasts with 100 ng/ml of recombinant WNT5A for 6 and 24 h, respectively. The concentration of WNT5A was chosen according to the manufacturer's instructions. Indeed, we discovered 259 genes to be upregulated and 191 to be downregulated at the 6 h timepoint (Fig. **8A**) and 104 to be upregulated and 220 to be downregulated at the 24 h timepoint (Fig. **8B**) (defined cut-off at >1.3x fold change with a significance level of $p<0.05$).

The 20 genes that were most prominently increased and decreased after 6 h are presented in Fig. **8C**, the respective heatmap for the 24 h timepoint is shown in Fig. **8D**.

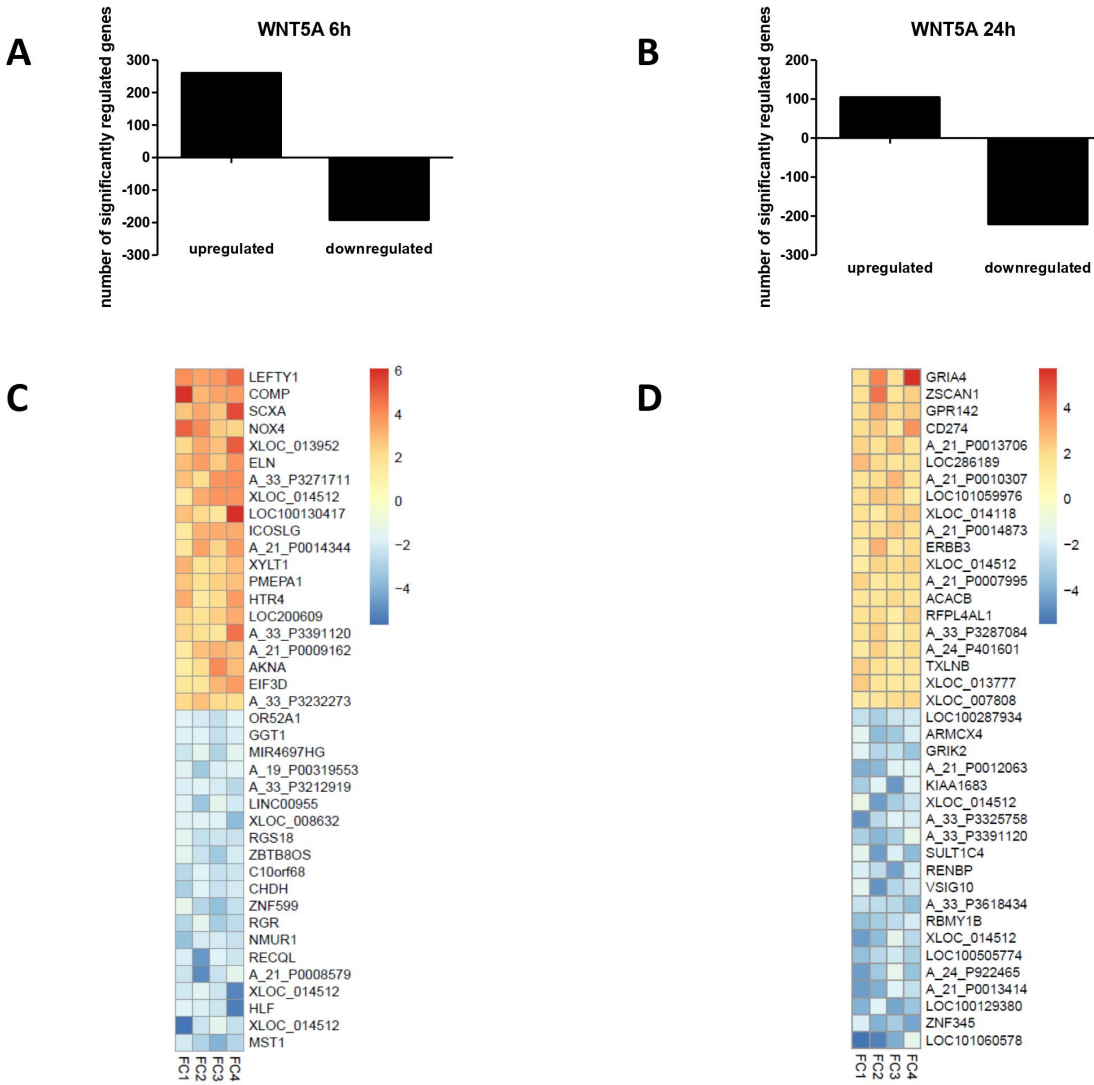

Figure 8: WNT5A alters gene expression in primary human lung fibroblasts

Primary human lung fibroblasts were treated with WNT5A (100 ng/ml) for 6 h and 24 h and subject to Agilent microarray analysis. Number of regulated genes including splice variants and unknown genes after a stimulation time of 6 h (**A**) and 24 h (**B**) defined by a cut-off of a fold-change>1.3 and a $p<0.05$. Heatmap of the highest up- (presented in red) and downregulated (presented in blue) genes after 6 h (**C**) and 24 h (**D**). n=4.

4.2.2 Identification of WNT5A target genes

We continued focusing on the genes regulated after 6 h of stimulation with WNT5A expecting to identify genes directly regulated by WNT5A. Literature research on the comprehensive list of regulated genes revealed several genes associated with lung disease, four of which were of particular interest as they are involved in either IPF, COPD or in pathophysiologic processes relevant in both diseases.

One of the top hits of the microarray analysis was Cartilage Oligomeric Matrix Protein (*COMP*, 3.97x upregulated, $p<0.01$), an extracellular matrix protein normally expressed in cartilage, but also in fibrotic disorders of the lung and skin (154, 155). Additional interest in *COMP* aroused with the analysis of possible protein-protein interactions among the genes regulated by WNT5A after 6 h by the STRING software. This revealed that COMP protein is connected to several other proteins encoded by WNT5A-controlled genes (Suppl. Fig. 2). The other three genes we concentrated on were Elastin (*ELN*, 3.26x upregulated, $p<0.01$), Tetraspanin-2 (*TSPAN2*, 1.85x upregulated, $p<0.001$) and Tensin-1 (*TNS1*, 1,33x upregulated, $p=0.09$). Elastin is the main component of elastic fibers and upregulated in very severe emphysema (156). Its degradation is a common feature in pulmonary emphysema with breakdown products facilitating disease progression (157). TSPAN2 is a transmembrane protein serving as a buffer for reactive oxygen species that promotes invasion in lung cancer associated with a p53 mutation. (158). Finally, the focal adhesion protein TNS1 has been detected in fibroblastic foci from IPF lungs and Single Nucleotide Polymorphisms (SNPs) of TNS1 have been associated to a higher risk of developing COPD (159-161).

Next, we wanted to confirm these results in independent experiments. After 6 h of WNT5A treatment (100 ng/ml) of primary human lung fibroblasts, all the chosen genes were significantly upregulated (log-fold change ($\Delta\Delta$Ct) *COMP*: 3.03±0.69, $p<0.01$, n=4; Fig. **9A**), ($\Delta\Delta$Ct *ELN*: 1.56±0.65, $p<0.01$, n=5; Fig. **9B**), ($\Delta\Delta$Ct *TSPAN2*: 1.10±0.67, $p<0.05$, n=5; Fig. **9C**), ($\Delta\Delta$Ct *TNS1*: 0.67±0.09, $p<0.001$, n=4; Fig. **9D**).

To examine whether the induction of these genes is persistent over time, we also stimulated lung fibroblasts with the same concentration of WNT5A for 24 h. The microarray data after 24 h of WNT5A stimulation indicated that only *TNS1* was still significantly upregulated compared to control (Suppl. Fig. 3). In fact, we observed that the induction of *COMP* mRNA was stable and significant (ΔΔCt: 2.46±1.33, p<0.01, n=8; Fig. **9A**), while mRNA levels of *ELN* went back to baseline (Fig. **9B**). *TSPAN2* expression was still significantly increased upon 24 h of WNT5A treatment (ΔΔCt: 0.40±0.11, p<0.01, n=4; Fig. **9C**), whereas no differences of *TNS1* mRNA levels could be found (Fig. **9D**).

As described above, TGF-β and WNT signaling are tightly interconnected (107, 130, 133, 134, 145, 146). Therefore, we urged to determine whether the selected microarray genes are also regulated by TGF-β. Interestingly, treatment of lung fibroblasts with 2 ng/ml of TGF-β for 24 h upregulated all examined genes on mRNA level to a much greater extent than WNT5A did (ΔΔCt *COMP*: 10.59±0.07, p<0.001, n=3; Fig. **9A**), (ΔΔCt *ELN*: 7.58±0.73, p<0.01, n=3; Fig. **9B**), (ΔΔCt *TSPAN2*: 7.43±0.48, p<0.01, n=3; Fig. **9C**), (ΔΔCt *TNS1*: 2.54±0.59, p<0.05, n=3; Fig. **9D**).

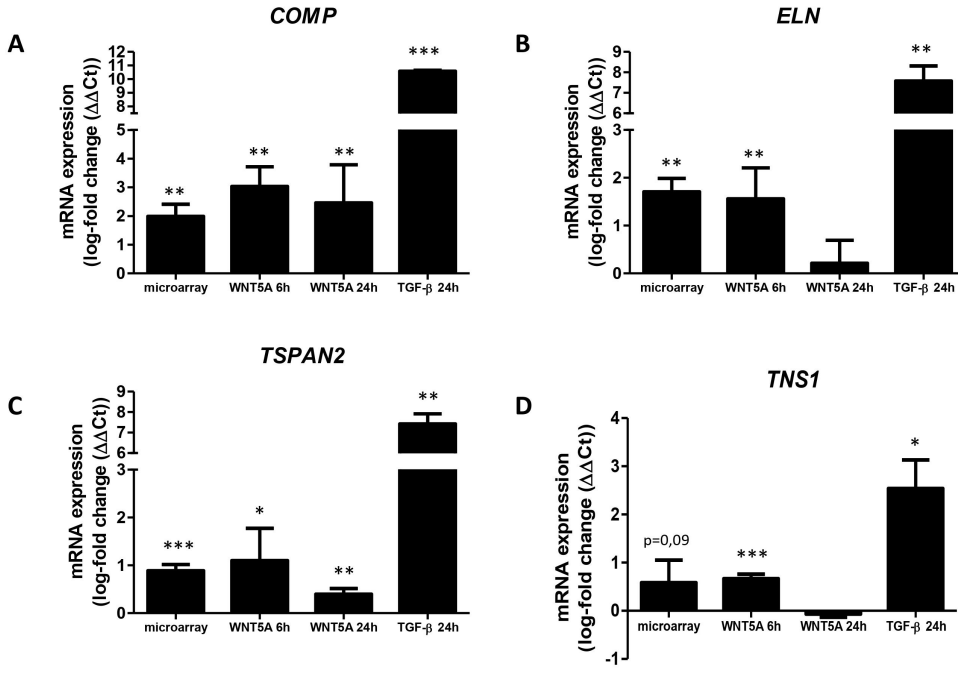

Figure 9: Confirmation and regulation of selected microarray genes

Primary human lung fibroblasts were treated with WNT5A (100 ng/ml) for 6 h and for 24 h or with TGF-β (2 ng/ml) for 24 h, mRNA levels of *COMP* (**A**), *ELN* (**B**), *TSPAN2* (**C**) and *TNS1* (**D**) were subsequently determined via qRT-PCR. In addition, the gene expression data from the microarray (6 h timepoint) is presented. Statistical analysis was performed using two-tailed, one-sample t-test, *p<0.05, **p<0.01, ***p<0.001. Results are shown as mean log-fold change + stdev of 3-8 independent experiments.

Elastic fiber formation is a complex biological process implicating, besides the crosslinking of the main component elastin, a range of microfibrillar and linker proteins like fibrillin-1 (FBN1) and elastin microfibrillar interface-located protein-1 (EMILIN1) (162). Noteworthy, some elastogenesis-related proteins like fibulin-5 (FBLN5) have recently been identified as dysregulated in COPD (163). In addition, there are reports describing an interaction of elastogenesis-related proteins with WNT/β-catenin signaling (164, 165). Hence, we hypothesized that not only elastin, but also other elastogenesis-related genes are directly regulated by WNT5A in lung fibroblasts. However, the mRNA expression of *FBN1*, *FBN2*, *EMILIN1*, *EMILIN2*, *FBLN5*, latent TGF-β binding protein 2 (*LTBP2*), microfibrillar associated protein 4 (*MFAP4*) and biglycan (*BGN*) remained unaltered after 6 h of WNT5A stimulation (Suppl. Fig. 4).

Taken together, these data indicate that the genes encoding for the ECM components *COMP* and *ELN* as well as for the plasma membrane-associated proteins *TSPAN2* and *TNS1* are direct target of WNT5A in primary human lung fibroblasts. Furthermore, we demonstrate that all these four genes are also regulated by TGF-β pointing at a possible connection between non-canonical WNT and TGF-β signaling.

4.2.3 Involvement of WNT5A target genes in disease

To assess whether COMP, ELN, TSPAN2 and TNS1 are differentially expressed in chronic lung diseases, we determined their respective mRNA levels in whole lung homogenate from COPD patients and patients with fibrotic lung disease (not exclusively IPF) compared to tissue from individuals without these diseases (donor).

In COPD patients from our cohort, *COMP* (ΔCt: -3.46±1.83 vs -1.60±1.71, p=0.06, n=6; Fig. **10A**), *ELN* (ΔCt: 1.87±0.82 vs 2.93±0.49, p<0.05, n=6; Fig. **10B**) and *TSPAN2* mRNA levels (ΔCt: -2.78±0.82 vs -1.74±0.25, p<0.05, n=6; Fig. **10C**) were higher expressed than in donors. There was no difference in *TNS1* mRNA abundance between COPD patients and donors (Fig. **10D**).

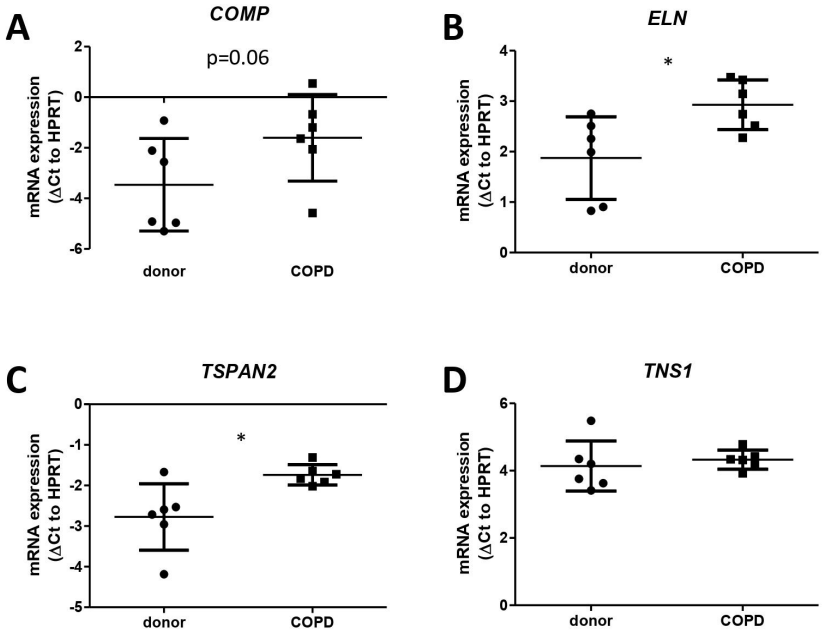

Figure 10: Microarray genes are partly upregulated in COPD

Transcript levels of *COMP* (**A**), *ELN* (**B**), *TSPAN2* (**C**) and *TNS1* (**D**) in whole lung homogenate of patients with end-stage COPD and donors as determined via qRT-PCR. The average patient age in the COPD group was 55.9 years, the average patient age in the control group 41.2 years. Statistical analysis was performed using Mann-Whitney U-test, *p<0.05. Results are shown as mean + stdev of 6 patients per group.

Interestingly, also lung tissue from patients with fibrotic lung disease showed enhanced mRNA levels of *COMP* (ΔCt: -0.71±1.97 vs 1.89±1.07, p<0.01, n=6; Fig. **11A**) and *ELN* (ΔCt: 2.30±0.56 vs 3.61±0.96, p<0.05, n=6; Fig. **11B**) compared to donors. In addition, a tendency to an increase of *TSPAN2* mRNA abundance in fibrotic lung disease patients (Fig. **11C**) and a trend to a decrease in *TNS1* mRNA levels (Fig. **11D**) was observed.

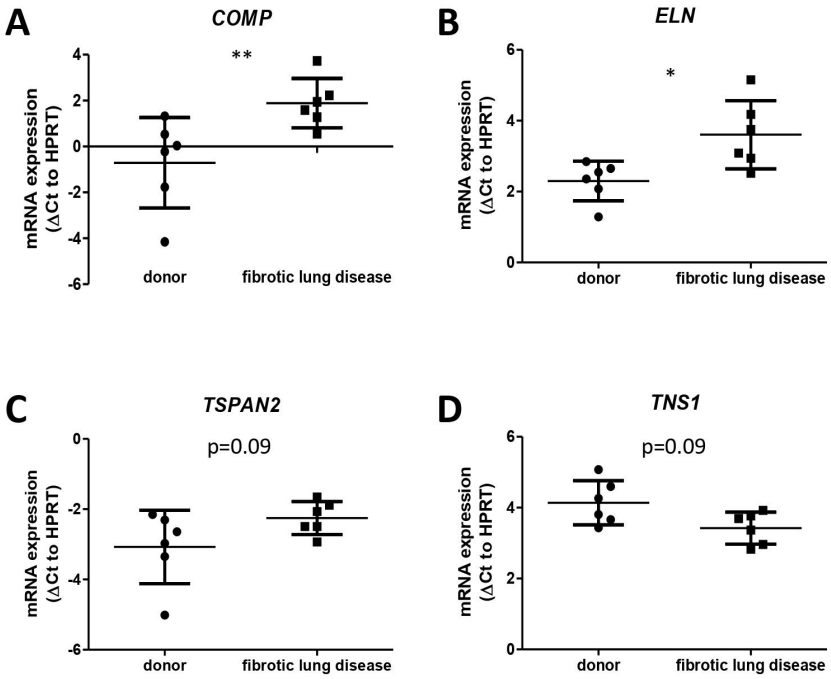

Figure 11: Microarray genes are partly upregulated in fibrotic lung disease

Transcript levels of *COMP* (**A**), *ELN* (**B**), *TSPAN2* (**C**) and *TNS1* (**D**) in whole lung homogenate of patients with end-stage fibrotic lung disease and donors as determined via qRT-PCR. The average patient age in the fibrotic lung disease group was 42.4 years, the average patient age in the control group 49.4 years. Statistical analysis was performed using Mann-Whitney U-test, *p<0.05. Results are shown as mean + stdev of 6 patients per group.

To evaluate whether the alterations in WNT5A target gene expression levels were linked to the clinical presentation of patients, we plotted mRNA expression of the WNT5A target genes against lung function parameters obtained from a published dataset (Series GSE47460). The spirometric parameter FEV_1 was chosen to assess COPD disease severity in 91 control (donor) and 142 COPD patients, FVC values were analyzed in 55 control and 49 IPF patients.

Correlation analysis revealed that *COMP* mRNA levels were significantly associated with both a decline in FEV_1 in COPD and control patients (r=-0.36, p<0.0001; Fig. **12A**) and a decline in FVC in IPF and control patients (r=-0.66, p<0.0001; Fig **12B**). In

line with these observations, examining gene expression data in this microarray, we found *COMP* significantly increased in COPD patients compared to donors as well as in IPF patients compared to donors (Suppl. Fig. 5).

In summary, the WNT5A target genes *COMP*, *ELN*, *TSPAN2* and *TNS1* are differentially expressed in chronic lung diseases. Particular interest applies to COMP, which is associated to a decline in lung function parameters in both COPD and IPF patients.

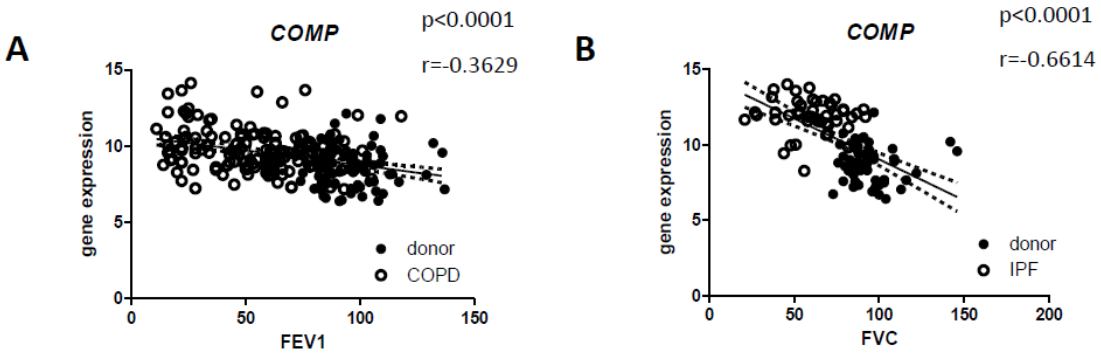

Figure 12: COMP gene expression correlates with a decline in lung function parameters

Data from the published microarray GSE47460 was analyzed. *COMP* mRNA levels from 144 COPD patients and 91 donors were plotted against FEV_1 (**A**), *COMP* mRNA levels from 50 IPF patients and 55 donors were plotted against FVC (**B**). Statistical analysis was performed using Spearman's correlation test.

4.2.4 Effect of WNT5A on fibroblast function

Finally, we aimed to delineate the functional consequences of WNT5A treatment on primary human lung fibroblasts. We started by further analyzing the microarray list of the upregulated genes after 6 h of WNT5A stimulation with DAVID bioinformatics resource. Functional annotation analysis of Gene Ontology terms revealed biological properties shared by WNT5A-induced genes. Intriguingly, extracellular matrix organization, cell adhesion and positive regulation of stress fiber assembly were observed among the strongest enriched terms (Fig. **13**).

Enriched biological properties (DAVID Bioinformatics)	Number of regulated genes	p-value
Extracellular matrix organization	12	0.00001
Cell adhesion	11	0.00065
Blood coagulation	10	0.0073
Positive regulation of smooth muscle migration	3	0.015
Positive regulation of stress fiber assembly	3	0.033
Lung alveolus development	3	0.034
Cellular response to TGF-β stimulus	3	0.046
Apoptotic process	9	0.057

Figure 13: Biological properties are enriched among the genes altered by WNT5A

Functional annotation analysis was performed with DAVID Bioinformatics tool 6.8 Beta. The input consisted of the 178 genes (excluding splice variants and unknown genes) significantly upregulated after 6 h of stimulation of primary human lung fibroblasts with WNT5A (100 ng/ml) (compare microarray Fig. 8). The most significantly enriched biological functions as well as selected functions associated to lung pathologies and fibroblast function are presented.

To clarify whether more ECM components besides COMP and ELN are affected by WNT5A treatment, we tested the gene expression of the fibrotic markers fibronectin 1 (*FN1*), collagen type 1, alpha 1 (*COL1A1*), tenascin C (*TNC*) and connective tissue growth factor (*CTGF*) upon 6 h of WNT5A stimulation but did not observe any differences in mRNA abundance (Suppl. Fig. 6).

The excessive production of ECM in fibrotic chronic lung diseases is heavily attributable to myofibroblasts. Myofibroblasts are an activated type of fibroblast characterized by contractile stress fibers consisting of α-smooth muscle actin (α-SMA). Interestingly, positive regulation of stress fibers showed up in the list of enriched biological properties among the WNT5A target genes (Fig. **13**). To acquire the activated phenotype of a myofibroblast, resident organ fibroblasts are described to proliferate and subsequently differentiate as a response to cytokines like TGF-β (36, 166, 167). We aimed to decipher whether WNT5A is involved in fibroblast proliferation (as determined by levels of the proliferation marker Cyclin D1 (CCND1)). Furthermore, we investigated the potential involvement of WNT5A in TGF-β-induced myofibroblast differentiation (as determined by levels of α-SMA). To test this, we performed siRNA-mediated knockdown of WNT5A upon stimulation with or without TGF-β.

In primary human lung fibroblasts, WNT5A-siRNA was able to significantly knockdown *WNT5A* mRNA levels by 91.47% on baseline and by 92.08% upon TGF-β stimulation (Fig. **14A**). Basal as well as TGF-β-induced secretion of WNT5A in the cell culture medium after 24 and 48 h was also compromised (Fig. **14B**). mRNA expression of the canonical WNT target gene *AXIN2* was not altered upon knockdown of WNT5A at baseline. TGF-β stimulation resulted in a significant decrease of *AXIN2* mRNA expression. However, the TGF-β-induced decrease in *AXIN2* mRNA levels was not altered by WNT5A knockdown (Suppl Fig. 7).

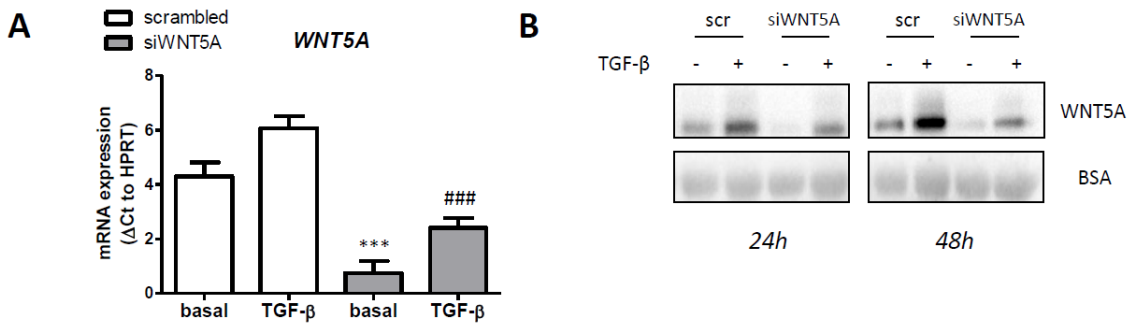

Figure 14: WNT5A-siRNA treatment decreases WNT5A mRNA and secretion

Primary human lung fibroblasts were treated with siWNT5A or scr-siRNA in the absence and presence of TGF-β (2 ng/ml). *WNT5A* mRNA levels after 24 h of TGF-β stimulation were determined via qRT-PCR (**A**). WNT5A protein secretion after 24 and 48 h was assessed via immunoblotting of concentrated supernatants (**B**). Statistical analysis was performed using One-Way-ANOVA with repeated measures followed by Newman-Keuls Multiple Comparison Test, ***p<0.001 compared to basal + scr; ###p<0.001 compared to TGF-β + scr. Results are presented as mean + stdev of 3 independent experiments.

On transcript level, TGF-β significantly induced α-*SMA* levels (ΔCt: 3.33±1.10 vs 7.57±1.16, p<0.001, n=3), an effect which was not affected by knockdown of WNT5A (Fig. **15A**). Expression of the proliferation marker *CCND1*, though, was significantly reduced upon siWNT5A treatment compared to scrambled control (ΔCt: 8.38±0.49 vs 7.45±0.50, p<0.01, n=3; Fig **15A**).

On protein level, knockdown of WNT5A led to a modest, but significant decrease in TGF-β-induced α-SMA abundance (fold of TGF-β: 0.73±0.18, p<0.01, n=3; Fig. **15B+C**). Additionally, basal CCND1 protein levels were suppressed by silencing of WNT5A (fold of control: 0.59±0.21, p<0.05, n=3; Fig. **15B+C**).

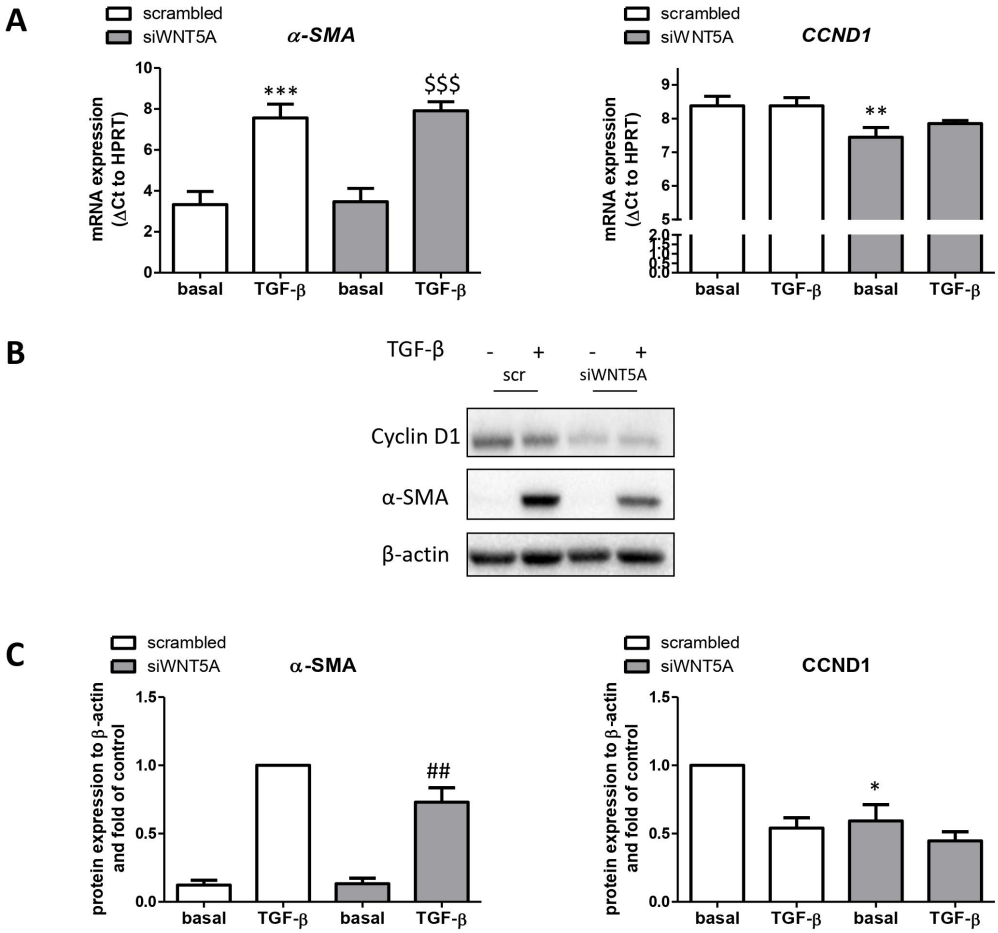

Figure 15: Knockdown of WNT5A reduces fibroblast proliferation and myofibroblast differentiation

Primary human lung fibroblasts were treated with siWNT5A or scr-siRNA in the absence and presence of TGF-β (2 ng/ml). *α-SMA* and *CCND1* mRNA levels after 24 h of TGF-β stimulation were determined via qRT-PCR (**A**). α-SMA and CCND1 protein levels after 48 h was assessed via immunoblotting (**B**). Statistical analysis was performed using One-Way-ANOVA with repeated measures followed by Newman-Keuls Multiple Comparison Test, *p<0.05, **p<0.01, ***p<0.001 compared to basal + scr; ##p<0.01 compared to TGF-β + scr; $$$p<0.001 compared to basal + siWNT5A. Results are presented as mean + stdev of 3 independent experiments.

Given that the GO analysis uncovered cellular adhesion as a possible function activated by WNT5A, we were prompted to study this phenomenon. In initial experiments, we treated primary human lung fibroblasts for 48 h with or without WNT5A. At this timepoint, we expected that proteins with an effect on cellular adhesion had been synthesized and incorporated into the plasma membrane. After the period of 48 h, cells were detached and reseeded. The rate of attachment (a measure of cellular adhesion) was determined by cell count 30 min after the cells were reseeded (compare chapter 3.6). However, no differences in fibroblast attachment were observed between untreated and WNT5A-treated fibroblasts in this experimental set-up (Fig. **16**).

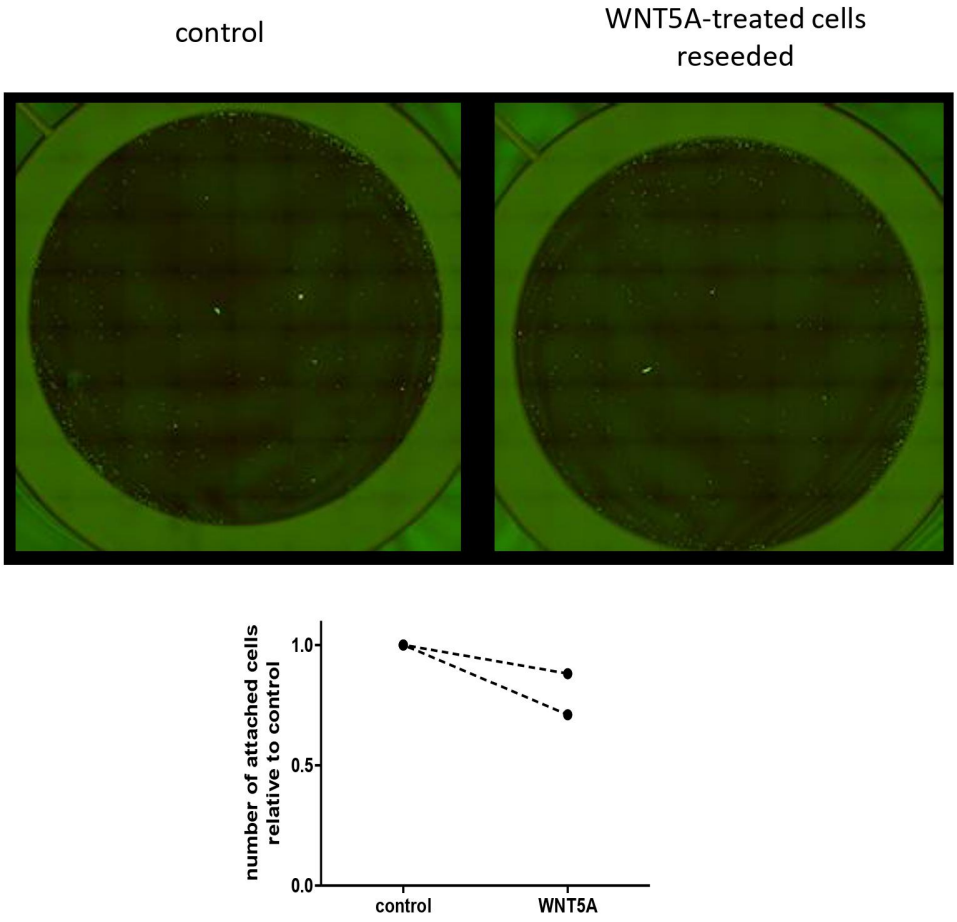

Figure 16: WNT5A pretreatment does not alter fibroblast adhesion

Primary human lung fibroblasts were stimulated with WNT5A (500 ng/ml) for 48 h, detached from the cell culture dish and reseeded on a new well plate. Attachment after 30 min was measured quantifying DAPI staining.

In view of our results that WNT5A increases transcript levels of ECM components, we further hypothesized that stimulation of WNT5A leads to enhanced ECM deposition in vitro which subsequently influences adhesion of native fibroblasts. To test this, primary human lung fibroblasts underwent prolonged treatment with WNT5A (500 ng/ml) for 5 days. Afterwards, cells were detached from the cell culture plate. Subsequently, untreated human lung fibroblasts were seeded on these tissue culture plates. However, there was no change in fibroblast attachment observed comparing the number of cells on the WNT5A-induced matrix compared to matrix of vehicle-treated fibroblasts (data not shown).

Next, we reasoned that WNT5A enhances fibroblast adhesion via rapid posttranslational changes in the cell, such as cytoskeletal rearrangements or the control of focal adhesion complexes as recently demonstrated (168). And indeed, seeding of fibroblasts in WNT5A-supplemented medium significantly increased cellular adhesion to cell culture plates compared to seeding of fibroblasts in normal starvation medium (fold of vehicle-treated cells: 3.34±0.42, $p<0.05$, n=3; Fig. **17**).

Summarizing the effect of WNT5A on the function of primary human lung fibroblasts, knockdown of WNT5A decreases protein and mRNA expression of the proliferation marker Cyclin D1 and attenuates TGF-β-induced increase in α-SMA protein.

Conversely, WNT5A in the seeding medium of fibroblasts enhances fibroblast attachment in vitro.

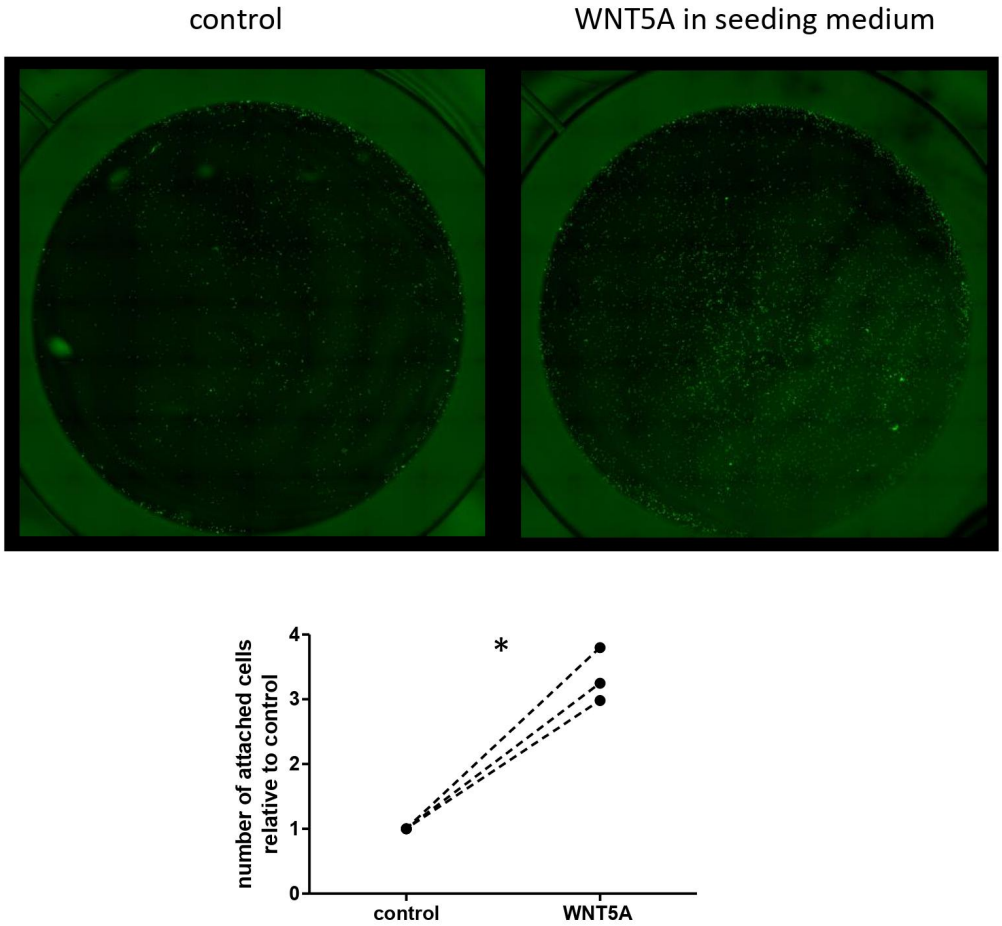

Figure 17: WNT5A in the seeding medium enhances fibroblast adhesion

Previously untreated primary human lung fibroblasts were seeded on a 24-wells plate in the presence or absence of WNT5A (500 ng/ml) in the seeding medium. Attachment after 30 min was measured quantifying DAPI staining. Statistical analysis was performed using two-tailed paired Student's t-test, *$p<0.05$, n=3.

5 Discussion

The chronic lung diseases COPD and IPF constitute a significant individual and global health burden due to their chronic and ultimately fatal clinical course (7, 13, 169). Although clinical phenotypes appear to differ vastly at first sight with COPD being classified as the prototype of an obstructive and IPF being classified as the prototype of a restrictive pulmonary disorder, both conditions have some pathophysiological processes in common and can even occur at the same time in patients (68, 71, 82). For instance, fibroblast-driven tissue remodeling processes are observed both around the airways in COPD and in fibroblastic foci in IPF (36, 166, 170). Furthermore, there is a wide array of studies reporting deranged activity of developmental signaling pathways, such as WNT signaling, in both diseases (75, 81, 105, 117, 132). We aimed to decipher the role of WNT5A, a non-canonical WNT that displays enhanced expression in lungs and particularly fibroblasts of both COPD and IPF patients compared to healthy individuals (94, 127, 128, 135). Intriguingly, Baarsma et al. showed detrimental effects of WNT5A on alveolar epithelial cell regeneration and lung architecture in the context of COPD, while Lam et al. reported an association of IPF disease progression in patients with high WNT5A levels in PBMCs (94, 112). This highlights the importance of intensifying research on WNT5A to further explore its potential as a future drug target in light of the limited options to treat the devastating diseases COPD and IPF.

In the current study, we describe that risk factors and stimuli relevant in COPD and IPF pathogenesis induced WNT5A expression in primary human lung fibroblasts. The profibrotic cytokine TGF-β, the canonical WNT WNT3A and inhibition of GSK-3β increased WNT5A mRNA and protein. To upregulate WNT5A abundance, TGF-β utilized a pathway dependent of TAK1 and NF-κB. Adding soluble components of cigarette smoke to TGF-β treatment resulted in an even stronger increase in WNT5A protein compared to solely TGF-β treatment.

Fibroblast-derived WNT5A, in turn, acts in an autocrine fashion to promote cellular behavior relevant to disease pathogenesis. Specifically, we identified target genes of WNT5A, such as COMP and Elastin, which are differentially expressed in chronic lung diseases, using microarray analysis, *in silico* studies and qRT-PCR experiments. Furthermore, knockdown of WNT5A affected fibroblast proliferation and myofibroblast differentiation. Finally, WNT5A treatment led to increased fibroblast adhesion.

5.1 Regulation of WNT5A in primary human lung fibroblasts

In the healthy lung, immunohistochemical studies showed that WNT5A is expressed by different cell types like alveolar and airway epithelial cells, smooth muscle cells and fibroblasts (127). In IPF lungs, WNT5A is still widely distributed among various cell types, however, notably, the vast majority of fibroblasts and myofibroblasts around fibroblastic foci were positive for WNT5A (109, 127). In line with this, lung fibroblasts isolated from lung tissue of IPF patients express more WNT5A than fibroblasts isolated from donor tissue (126, 127). Similarly, lung fibroblasts isolated from lung tissue of COPD patients also have a higher WNT5A abundance compared to donor fibroblasts (94).

5.1.1 Regulation of WNT5A by TGF-β

We demonstrate that TGF-β is a robust inducer of WNT5A expression in lung fibroblasts. Modulation of TGF-β signaling at various levels in the signaling cascade showed promising results in preclinical and clinical settings to treat COPD and IPF (171-173). Noteworthy, there are also various challenges in TGF-β antagonism owing to its pleiotropic role in biological processes like regulation of inflammation and tissue homeostasis (174). Therefore, we considered it of major interest to study the mechanisms how WNT5A is regulated by TGF-β. This might enable to diversify therapeutic avenues in TGF-β and/or future WNT inhibition resulting in medication available for different subsets of patients.

The TGF-β signaling cascade can broadly be divided into a canonical, SMAD-dependent, and various non-canonical, SMAD-independent, pathways. The essential step in the canonical signaling cascade is the phosphorylation of SMAD2 and SMAD3 with subsequent nuclear translocation of these proteins, where they serve as transcription factors by binding to SMAD-binding elements (SBE). Non-canonical TGF-β signaling involves several other mediators, such as TAK1, NF-κB or PI3K (compare Fig. **3**) (144). Interestingly, several of the downstream effector proteins of TGF-β have been implicated in the regulation of WNT5A, which is highly complex and dependent on the cell type (147, 175). Since the inhibitor of canonical, SMAD-dependent TGF-β, SIS3, was inexplicably toxic in our experimental setup, we focused on non-canonical signaling pathways.

In fact, we show that inhibition of TAK1 by 7-Oxozeaenol attenuates the induction of WNT5A mRNA and protein secretion by TGF-β. This is in concordance with the recent findings that TAK1 controls WNT secretion by TGF-β in cardiac fibroblasts and WNT5A expression in airway smooth muscle cells (145, 176). The latter study showed that β-catenin lies downstream of TAK1 in this process. This prompted us to address the question whether β-catenin is also implied in the regulation of WNT5A in lung fibroblasts. In canonical WNT signaling, transcriptional activity of β-catenin is induced by inhibition of the β-catenin destruction complex leading to cytosolic accumulation and subsequent nuclear translocation of β-catenin (85). The multifunctional enzyme GSK-3β is part of the β-catenin destruction complex and consequently, GSK-3β inhibition by SB216763 has been shown to activate β-catenin in human alveolar epithelial cells (94). Indeed, treatment of lung fibroblasts with SB216763 led to a significant increase in WNT5A mRNA and protein secretion compared to vehicle treatment. However, it appeared that the ability of lung fibroblasts to express WNT5A upon TGF-β stimulation is only marginally potentiated. It is possible that this might be due to a full activation of β-catenin-dependent transcriptional activity upon TGF-β stimulation, which could not be further increased by SB216763 treatment. In corroboration of our result that SB216763 treatment induced WNT5A expression at baseline, we delineate that WNT3A, a predominantly canonical WNT, upregulated WNT5A mRNA and protein secretion which has also been demonstrated by treatment with WNT3A-conditioned medium in airway smooth muscle cells (145). Moreover, adenoviral overexpression of WNT7B, another WNT that has been shown to induce canonical WNT signaling and that is upregulated in IPF, led to an increase in WNT5A protein expression in human lung fibroblasts (106, 127). However, our results are limited by the fact that WNT3A and foremost GSK-3β have multiple downstream effectors or substrates other than β-catenin (95, 148). Additional experiments, for instance, assessing the impact of silencing of β-catenin on WNT5A expression would help supporting our findings.

In addition to β-catenin, TAK1 can also activate NF-κB (p50/p65) signaling (177). In the inactive state, NF-κB is sequestered in the cytoplasm by inhibitory proteins of the IkB family. When NF-κB upstream signaling is activated, IkB proteins are phosphorylated and targeted for proteosomal degradation by IKKs (IkB kinases) (178). In our experimental setup, inhibition of IKK-β by SC514 attenuated the increase in WNT5A protein secretion induced by TGF-β. This is in line with previous studies reporting a regulatory role for NF-κB in increasing WNT5A levels (147, 179, 180). Surprisingly, the proinflammatory cytokines TNF-α and IL-1β, that were used in these studies to induce NF-κB signaling, did not alter WNT5A expression in our experimental setup. NF-κB-driven gene transcription is a tightly regulated process with a large number of upstream pathways diverging into it and a lot of transcription factors interacting in the nucleus (178). Thus, it can be hypothesized that in primary human lung fibroblasts TGF-β signaling activates essential mediators of WNT5A induction that TNF-α and IL-1β do not address. Yet the identification of the exact mechanisms that distinguish the TGF-β response from the TNF-α and IL-1β response of lung fibroblasts are beyond the scope of this study.

Taken together, our findings thus suggest that in primary human lung fibroblasts TGF-β induces WNT5A expression via a signaling cascade involving TAK1 and/or NF-κB. Moreover, GSK-3β and presumably β-catenin signaling control WNT5A expression.

5.1.2 Regulation of WNT5A by CSE

Regarding our initial research question whether stimuli relevant in COPD and IPF induce WNT5A expression in primary human lung fibroblasts, it was compelling to assess a potential effect of the major risk factor for both diseases, cigarette smoke. Promisingly, there is a numerous reports describing altered expression of components of the WNT signaling pathway in either cigarette smoke extract (CSE)-treated cells, specimen obtained from smoking patients and samples from mice exposed to cigarette smoke (94, 117, 118, 124, 132, 134, 181, 182). We thus hypothesized that also in primary human lung fibroblasts, WNT5A expression is regulated by soluble constituents of cigarette smoke. Indeed, we discovered that solely CSE enhanced the amount of WNT5A protein to a modest extent, whereas CSE treatment upregulated WNT5A protein expression when used in cotreatment with TGF-β compared to TGF-β stimulation alone. However, it appears challenging to pin down the exact compounds in CSE which is responsible for the upregulation of WNT5A, as cigarette smoke consists

of thousands of compounds (183). Possible inducers of WNT5A in primary fibroblasts are Nicotine, Nicotine-derived nitrosamine ketone (NNK) and Lipopolysaccharide (LPS), all of which are present in cigarette smoke (181, 184). A study conducted by Whang et al. showed that exposure of bronchial epithelial cells to nicotine or NNK increases WNT5A mRNA expression, whereas Villar et al. presented increased WNT5A protein amount in lung fibroblasts in response to LPS (181, 185). However, it appears unlikely that LPS is responsible for the increase of WNT5A in our experimental setup. Our CSE preparation protocol resembles the one that Pera et al. used and they could not detect LPS in the CSE (186). We decided to use a CSE preparation protocol involving a freezing step before application to reduce batch-to-batch variation which could have resulted in a partial loss of volatile substances present in CSE, such as reactive oxygen species and radicals (187). There is conflicting data on whether storage affects the antiproliferative effect of CSE. Volatilization and lyophilization of CSE, for instance, have been described to reduce growth inhibition whereas short time storage at temperatures up to -70°C did not (188, 189). Nonetheless, we consider our model of CSE use and storage as appropriate to reflect smoke exposure on fibroblasts since mainly soluble compounds of the cigarette smoke will be able to pass the epithelial layer to reach the fibroblasts that are located in the interstitium. In general, interpretation of CSE data between labs remains challenging as the procedure of CSE preparation and storage is still poorly standardized throughout the scientific community with differences in pumps, syringes, cigarette brands and storage conditions being used (190, 191).

In regard of intracellular signaling cascades CSE has been shown to activate, it is intriguing that there are several parallels to non-canonical TGF-β signaling pathways, which we identified as mediators of WNT5A induction. For instance, CSE stimulation of human alveolar epithelial cells transfected with an NF-κB reporter construct led to enhanced luciferase activity and CSE treatment of human bronchial epithelial cells resulted in an increase of phosphorylated Iκ-B (192). Lung fibroblasts isolated from COPD patients express fibronectin when exposed to CSE, an effect that is attenuated by pharmacological inhibition of NF-κB signaling (193). In human airway smooth muscles cells, Pera et al. unraveled a signaling cascade triggered by CSE with subsequent TAK1 and NF-κB activation finally leading to IL-8 secretion which is exactly the mechanism we propose for TGF-β-induced WNT5A (194). This could explain the synergistic effect of combined CSE and TGF-β treatment in the upregulation of WNT5A protein. Another

phenomenon that might be responsible for the increase in WNT5A in response to CSE is the alteration of miRNA levels. miRNAs are short sequences of non-coding RNA that often form loop structures and have a major role in posttranscriptional regulation (195). CSE has been shown to decrease the expression of miR-487b, which negatively regulates WNT5A in the process of lung carcinogenesis (196). Moreover, miR-31 has been discovered to upregulate WNT5A expression and concordantly, miR-31 abundance is elevated by CSE in airway epithelial cells (197). As regulation of protein translation by miRNA does not necessarily rely on mRNA degradation, but also on mere blocking of the respective mRNA, the miRNA alterations evoked by CSE could explain why we observed a change in WNT5A protein levels, but not in WNT5A mRNA levels (195).

5.2 Function of WNT5A on primary human lung fibroblasts

Given the recent findings from our group that fibroblast-derived WNT5A hampers alveolar epithelial cell repair, further interest arose in the function of WNT5A on the WNT5A-synthesizing cells, lung fibroblasts, in respect of the pathogenesis of COPD and IPF. In reference to our initial hypothesis that WNT5A alters fibroblast behavior, we will discuss different aspects of fibroblast biology, how they are altered in disease and to which extent WNT signaling and specifically WNT5A contributes to the disease phenotype.

Fibroblasts are the key cell type in different organs including the lung in the control of ECM homeostasis, but they also serve as essential promotors of wound healing and mediators of inflammation (36). Upon stimulation with various cytokines like TGF-β, fibroblasts can differentiate from a rather proliferative state to a synthetically active, contractile phenotype called myofibroblasts (166). This process mostly occurs during physiological tissue repair processes, such as the closing of a scratch on the skin, but also during the formation of pathological scarring and fibrosis (36, 198).

5.2.1 Effect of WNT5A on ECM expression

Attempting to gain a broad perspective on whether and how WNT5A alters gene expression, we applied a microarray analysis in WNT5A-treated primary human lung fibroblasts. To our knowledge, this is the first study conducting a genome-wide expression analysis examining the impact of WNT5A on structural cells of the human lung. Klapholz-Brown et al. have previously demonstrated that lung fibroblasts are

responsive to the canonical WNT WNT3A, we aimed to unravel whether the same holds true for non-canonical WNT signaling (199). After 6 h stimulation with WNT5A, 259 genes were significantly upregulated which we would hence classify as direct WNT5A target genes in primary human lung fibroblasts. Subsequently, we performed functional annotation analysis and discovered that genes encoding for ECM components were significantly enriched.

The ECM forms an acellular scaffold and is made up of wide array of proteins including proteoglycans and bound cytokines (200). In COPD and IPF, quality and quantity of the ECM is substantially altered (32, 201). Pathological hallmarks of IPF are fibrotic foci that are characterized by excessive and uncoordinated deposition of ECM components like collagen, FN and TNC and accumulating myofibroblasts (51, 202). COPD pathology displays the fascinating feature of emphysematous destruction of alveoli with loss of ECM and remodeling of airways with accumulation of ECM occurring in close proximity (29, 201). It is worth noting that an increase in the tissue volume surrounding small airways is strongly associated to disease progression in COPD patients (203). The composition of the fibrotic alterations surrounding the airways remarkably resembles what is observed in fibrotic areas of IPF lungs with increased FN and TNC levels as immunohistochemical studies have shown (33-35).

Further scrutiny of the list of direct WNT5A targets in lung fibroblast revealed among others two ECM components that we decided to follow up on. We confirmed via qPCR that WNT5A significantly upregulates *COMP* and that this upregulation persists after 24 h of WNT5A treatment. COMP is a collagen-binding extracellular matrix protein that is physiologically found in cartilage and skin and pathologically increased in a fibrotic diseases of liver and skin as well as in IPF (154, 155, 204-206). We confirmed the upregulation of *COMP* mRNA in lung homogenate of IPF patients in our small cohort and interestingly, we found out that this is also the case in COPD patients. Moreover, we showed that in a published cohort (GSE47460), *COMP* mRNA levels are associated with a decline in FVC in IPF patients as well as with a decline in FEV1 in COPD patients. Given that COMP is elevated in many fibrotic disorders, this suggests that COMP is implicated in airway remodeling in COPD. Mechanistically, the action of WNT signaling on COMP expression remains vastly unexplored. A recent study delineated that in a rat model of osteoarthritis, blocking of DKK1 (an antagonist of canonical WNT signaling) led to reduced serum COMP levels accompanied an increase in nuclear β-catenin protein in osteoarthritic knee joint tissue (207). WNT5A has been

reported in different cell types to antagonize β-catenin dependent WNT signaling (90). However, in our experimental setup, we could neither detect an effect of WNT5A knockdown on the target gene of canonical WNT signaling *AXIN2* nor an effect of WNT5A stimulation on active β-catenin levels (data not shown). Thus, we could not provide proof that WNT5A affects β-catenin signaling in human lung fibroblasts. Contrarily, Vuga et al. observed a downregulation in β-catenin protein expression upon WNT5A treatment of human lung fibroblasts, but this difference can be explained by the concentrations of WNT5A they used which were much higher than ours (up to 3 µg/ml compared to 100 ng/ml) (126). In summary, given that in our experimental setup WNT5A appears to signal independently of β-catenin, the signaling pathways involved in the regulation of COMP in particular, and of the newly identified target genes in general, remain subject to future investigation.

In addition to COMP, the microarray indicated elastin, the main component of elastic fibers, as a direct WNT5A target gene. We confirmed this by qPCR. While there is poor evidence regarding the role of elastin in IPF, degradation of elastic fibers and successive loss of elastic recoil with increased lung compliance is a classic feature in COPD pathology (208-210). This was originally raised by the discovery of protease-antiprotease imbalance in α-antitrypsin deficiency patients, a genetic disorder, whose patients suffer from early-onset lung emphysema attributable to inadequate inhibition of elastin-cleaving neutrophil elastase (12, 30). Furthermore, in very severe emphysema, elastin expression is increased which Deslee et al. interpreted as a failed repair attempt due to the incapacity of successful elastic fiber formation in the adulthood (156, 162). Instead, the newly synthesized elastin might be detrimental in COPD assuming that it undergoes cleavage with the resulting elastin fragments driving disease progression (157). Given our results that WNT5A induces *ELN* expression, WNT5A might contribute to the aberrant increase in ELN seen at late disease stages as WNT5A expression in induced sputum rises with disease stage as well (94). In support of this, a therapeutic approach with WNT5A-neutralizing antibodies in the murine model of elastase-induced lung emphysema led to significantly improved lung function parameters and lung architecture (94).

Previous publications have suggested that WNT5A mediates profibrotic stimuli (211-214). WNT5A knockdown studies delineated that WNT5A lies downstream of TGF-β in the expression of FN and Collagen in human airway smooth muscle cells and hepatic myofibroblasts (211, 212). Additionally, the induction of FN by basic Fibroblast

Growth Factor (bFGF) signaling in human lung fibroblasts depends on WNT5A (215). Regarding the impact of solely WNT5A on ECM expression, observations are diverging, but evidence is growing that WNT5A can induce ECM expression as a single stimulus. In human periodontal ligament cells, a fibroblastic cell type, WNT5A upregulates *COL-1* mRNA and soluble collagen (216). Also, in primary human lung fibroblasts, high concentrations of 3 µg/ml of WNT5A increase FN protein levels (126). In human fetal lung fibroblasts, Guan et al. reported an increase in collagen, *FN* and *CTGF* levels, which Spanjer et al. could not observe (129, 130). We unravel that the comparatively low concentration of 100 ng/ml WNT5A enhances the expression of selected ECM components. While *COL1A1*, *FN1*, *TNC* and *CTGF* are unaffected, *COMP* and *ELN* mRNA levels are significantly elevated by WNT5A treatment. We thus propose that from an ECM perspective, WNT5A does not serve as a broad, but rather a fine-tuning profibrotic stimulus. This appears plausible considering the defined stages in embryonic development of the mesodermal compartment that are controlled by WNT5A (217).

5.2.2 Effect of WNT5A on fibroblast function

Before ECM expression and deposition by myofibroblasts take place, either in physiological wound healing or organ fibrosis, fibroblasts need to accumulate around the site of injury. As an explanation for the pathological aggregation of (myo)fibroblasts in IPF, three different origins have been discussed. Firstly, circulating bone marrow-derived fibrocytes were reported to traffic to the diseased lung and contribute to fibrotic remodeling (218, 219). However, it remains controversial whether these migrated cells possess the capacity to express α-SMA indicative of myofibroblast differentiation once they have reached their organ of destination (219, 220). Secondly, the existence of epithelial-to-mesenchymal transition as a source for pulmonary myofibroblasts has been matter of debate, but these assumptions mainly relied on *in vitro* and colocalization studies and couldn't clearly be confirmed with lineage tracing experiments (46, 221, 222). Most popular and widely accepted remains the theory that resident fibroblast populations migrate towards the site of injury and upon confrontation with excessively secreted profibrotic cytokines increasingly proliferate, adhere to fibroblastic clusters and subsequently differentiate into myofibroblasts (36, 45, 46, 223). In COPD, alterations in fibroblast biology appear more complex for there is presumably a discrepancy between fibroblast activation surrounding the airways and fibroblast dysfunction in the

emphysematous parenchyma. Fibroblasts isolated from the peripheral lung of emphysema patients proliferate differently compared to fibroblasts from control patients (39, 224, 225). On the other hand, Lofdahl et al. as well as Karvonen et al. observed that fibroblasts in lung sections from COPD patients express less α-SMA in the distal lung, but more α-SMA around the large airways (33, 226). This heterogeneity in fibroblast phenotype in obstructive pulmonary disease is underpinned by examinations carried out with fibroblasts obtained from asthmatic patients and healthy individuals, which found that both cell morphology, marker expression and transcriptome remarkably differs depending on their original location in the lung (227-229). These findings implicate that also various growth factors such as WNTs might elicit spatially different responses.

We observed that siRNA-mediated knockdown of WNT5A expression led to a decrease in proliferation marker *CCND1* mRNA and protein expression in primary human lung fibroblasts. The effect of WNT5A on proliferation has already been described under various circumstances with diverging results. In a homozygous WNT5A knockout model, hyperproliferation of the pulmonary mesenchymal cell compartment has been described (100). Moreover, WNT5A inhibits hypoxia-induced proliferation of pulmonary artery smooth muscle cells modeling pulmonary hypertension (230). On the other hand, in the context of lung cancer, a large number of WNT5A-positive cells correlated with high expression of the proliferation marker Ki67 and in pancreatic cancer cells, knockdown of WNT5A decreased Thymidine incorporation in these cells indicative of reduced proliferation (231, 232). This divergence is probably attributable to the mechanism that the cellular response to WNT binding is highly dependent on receptor recruitment and the succeeding intracellular pathway induction (93, 95). Interestingly, Bauer et al. have provided evidence that the two different isoforms of WNT5A (i.e. WNT5A-long and WNT5A-short) differentially affect proliferation of cancer cells (233). In primary human lung fibroblasts, exogenously added WNT5A stimulates proliferation shown by increased optical density and metabolic activity (110, 126). These studies, however, did not distinguish between the different isoforms of WNT5A. Our siRNA study adds another mechanism including a proliferation marker which gives further certainty that WNT5A promotes proliferation in lung fibroblasts.

Knockdown of WNT5A furthermore attenuated the induction of α-SMA by TGF-β by 27% indicating that WNT5A is a mediator of fibroblast-to-myofibroblast differentiation. Stimulation with only WNT5A did not induce α-SMA protein after 48 h (data not shown), which is in accordance to previous findings in embryonic lung

fibroblasts and airway smooth muscle cells (130, 234). Nonetheless, WNT5A and WNT11 treatment induces actin polymerization in airway smooth muscle cells, a process which in turn is indispensable for TGF-β-induced α-SMA expression. Knockdown of WNT5A or WNT11 in these cells consequently resulted in a marked attenuation of α-SMA increase by TGF-β (234, 235). It seems possible that similar mechanisms hold true for myofibroblast differentiation in the lung.

Fibroblast-matrix as well as fibroblast-fibroblast interactions are particularly relevant in the generation of fibroblastic foci in IPF (167, 236, 237). Moreover, attachment and detachment at the leading edge is the natural sequence of a migrating cell and enhanced fibroblast migration to sites of injury is observed in IPF (45, 223, 238). As an *in vitro* setup, we aimed to examine the impact of WNT5A on fibroblast attachment to cell culture dishes in various settings and discovered that WNT5A in the seeding medium decidedly enhanced fibroblast adhesion. Similar insights were delivered by a study with skin fibroblasts concluding a role for WNT5A in wound healing. Besides, the authors proposed that the PI3K/Akt pathway and rapid integrin activation mediate adhesive features of fibroblasts induced by WNT5A (239). Of note, enhanced α5-integrin expression in response to WNT5A stimulation has been shown in lung fibroblasts (126). Another mechanism involved could be the modulation of focal adhesion dynamics which has been brought up by several studies. In these publications, WNT5A has been shown to specifically reorganize the cytoskeleton, activate Focal Adhesion Kinase and regulate Paxillin levels, two essential mediators of cellular migration and adhesion (168, 240-242). Candidate targets to further unravel the effect of WNT5A on fibroblast adhesion could potentially be represented by the WNT5A microarray targets TNS1 and TSPAN2. Interestingly, TNS1 has recently been discovered as upregulated in IPF regulating cytoskeletal transformations and focal adhesion kinase signaling (161). TSPAN2, on the other hand, has been demonstrated to regulate motility and invasion in p53-mutated small airway epithelial cells (158).

5.3 Conclusion and perspective

Altogether, our results indicate that TGF-β- and CSE-induced WNT5A modulates distinct aspects of fibroblast activation at various stages. Partly, these changes in fibroblast adhesion, proliferation, differentiation and ECM expression occur in response to WNT5A treatment alone, partly in coordination with TGF-β stimulation. A limitation of our results on the pathways involved in the regulation of WNT5A is that we exclusively used pharmacological kinase inhibitors. Silencing the suggested mediators of WNT5A induction, such as TAK1 and β-catenin, with siRNA would corroborate our findings. Regarding the effect of WNT5A on lung fibroblasts, it would be interesting to examine whether some of the identified WNT5A target genes can be linked to the functional effects of WNT5A. Moreover, our patient data concerning the expression of WNT5A target genes in disease need to be interpreted in context with existing findings because of limited sample sizes and patient characteristics available. A definite strength of our study is that we performed experiments exclusively with primary human cells. Thus, our findings should reflect the situation present in a human lung as closely as *in vitro* monoculture can model. To evaluate the translational potential of WNT5A as a target in chronic lung diseases, additional experiments on other lung cell types or in coculture settings like lung tissue slices or lung organoids will be helpful (119, 243). Promisingly, for *in vivo* manipulation of WNT5A signaling either in murine models or in potential clinical studies, researchers have neutralizing antibodies as well as activating or inhibiting peptides at hand (94, 244, 245). Especially blocking of increased WNT5A to reestablish tissue homeostasis might be beneficial to COPD and/or IPF patients.

6 References

1. Halbert RJ, Natoli JL, Gano A, Badamgarav E, Buist AS, Mannino DM. Global burden of COPD: systematic review and meta-analysis. The European respiratory journal. 2006;28(3):523-32.
2. Buist AS, McBurnie MA, Vollmer WM, Gillespie S, Burney P, Mannino DM, et al. International variation in the prevalence of COPD (the BOLD Study): a population-based prevalence study. Lancet (London, England). 2007;370(9589):741-50.
3. Mathers CD, Loncar D. Projections of global mortality and burden of disease from 2002 to 2030. PLoS medicine. 2006;3(11):e442.
4. Vos T, Flaxman AD, Naghavi M, Lozano R, Michaud C, Ezzati M, et al. Years lived with disability (YLDs) for 1160 sequelae of 289 diseases and injuries 1990-2010: a systematic analysis for the Global Burden of Disease Study 2010. Lancet (London, England). 2012;380(9859):2163-96.
5. Hutchinson J, Fogarty A, Hubbard R, McKeever T. Global incidence and mortality of idiopathic pulmonary fibrosis: a systematic review. The European respiratory journal. 2015;46(3):795-806.
6. Samet JM, Coultas D, Raghu G. Idiopathic pulmonary fibrosis: tracking the true occurrence is challenging. The European respiratory journal. 2015;46(3):604-6.
7. Ley B, Collard HR, King TE, Jr. Clinical course and prediction of survival in idiopathic pulmonary fibrosis. American journal of respiratory and critical care medicine. 2011;183(4):431-40.
8. Vogelmeier CF, Criner GJ, Martinez FJ, Anzueto A, Barnes PJ, Bourbeau J, et al. Global Strategy for the Diagnosis, Management, and Prevention of Chronic Obstructive Lung Disease 2017 Report. GOLD Executive Summary. American journal of respiratory and critical care medicine. 2017;195(5):557-82.
9. Raghu G, Rochwerg B, Zhang Y, Garcia CA, Azuma A, Behr J, et al. An Official ATS/ERS/JRS/ALAT Clinical Practice Guideline: Treatment of Idiopathic Pulmonary Fibrosis. An Update of the 2011 Clinical Practice Guideline. American journal of respiratory and critical care medicine. 2015;192(2):e3-19.
10. Salvi SS, Barnes PJ. Chronic obstructive pulmonary disease in non-smokers. Lancet (London, England). 2009;374(9691):733-43.
11. Tager IB, Ngo L, Hanrahan JP. Maternal smoking during pregnancy. Effects on lung function during the first 18 months of life. American journal of respiratory and critical care medicine. 1995;152(3):977-83.
12. Alpha 1-antitrypsin deficiency: memorandum from a WHO meeting. Bulletin of the World Health Organization. 1997;75(5):397-415.
13. Vestbo J, Hurd SS, Agusti AG, Jones PW, Vogelmeier C, Anzueto A, et al. Global strategy for the diagnosis, management, and prevention of chronic obstructive pulmonary disease: GOLD executive summary. American journal of respiratory and critical care medicine. 2013;187(4):347-65.
14. Kent BD, Mitchell PD, McNicholas WT. Hypoxemia in patients with COPD: cause, effects, and disease progression. International journal of chronic obstructive pulmonary disease. 2011;6:199-208.
15. Taraseviciene-Stewart L, Voelkel NF. Molecular pathogenesis of emphysema. The Journal of clinical investigation. 2008;118(2):394-402.
16. Sheikh K, Coxson HO, Parraga G. This is what COPD looks like. Respirology (Carlton, Vic). 2016;21(2):224-36.

17. Wedzicha JA, Banerji D, Chapman KR, Vestbo J, Roche N, Ayers RT, et al. Indacaterol-Glycopyrronium versus Salmeterol-Fluticasone for COPD. The New England journal of medicine. 2016;374(23):2222-34.
18. Thorley AJ, Tetley TD. Pulmonary epithelium, cigarette smoke, and chronic obstructive pulmonary disease. International journal of chronic obstructive pulmonary disease. 2007;2(4):409-28.
19. Vestbo J, Lange P. Can GOLD Stage 0 provide information of prognostic value in chronic obstructive pulmonary disease? American journal of respiratory and critical care medicine. 2002;166(3):329-32.
20. McDonough JE, Yuan R, Suzuki M, Seyednejad N, Elliott WM, Sanchez PG, et al. Small-airway obstruction and emphysema in chronic obstructive pulmonary disease. The New England journal of medicine. 2011;365(17):1567-75.
21. Hogg JC, McDonough JE, Suzuki M. Small airway obstruction in COPD: new insights based on micro-CT imaging and MRI imaging. Chest. 2013;143(5):1436-43.
22. Celli BR, Decramer M, Wedzicha JA, Wilson KC, Agusti A, Criner GJ, et al. An Official American Thoracic Society/European Respiratory Society Statement: Research questions in chronic obstructive pulmonary disease. American journal of respiratory and critical care medicine. 2015;191(7):e4-e27.
23. Tuder RM, Petrache I. Pathogenesis of chronic obstructive pulmonary disease. The Journal of clinical investigation. 2012;122(8):2749-55.
24. Cosio MG, Saetta M, Agusti A. Immunologic aspects of chronic obstructive pulmonary disease. The New England journal of medicine. 2009;360(23):2445-54.
25. Repine JE, Bast A, Lankhorst I. Oxidative stress in chronic obstructive pulmonary disease. Oxidative Stress Study Group. American journal of respiratory and critical care medicine. 1997;156(2 Pt 1):341-57.
26. Demedts IK, Demoor T, Bracke KR, Joos GF, Brusselle GG. Role of apoptosis in the pathogenesis of COPD and pulmonary emphysema. Respiratory research. 2006;7:53.
27. Tzortzaki EG, Siafakas NM. A hypothesis for the initiation of COPD. The European respiratory journal. 2009;34(2):310-5.
28. Sethi S, Murphy TF. Infection in the pathogenesis and course of chronic obstructive pulmonary disease. The New England journal of medicine. 2008;359(22):2355-65.
29. Hogg JC, Timens W. The pathology of chronic obstructive pulmonary disease. Annual review of pathology. 2009;4:435-59.
30. Turino GM. Proteases in COPD: a critical pathway to injury. Chest. 2007;132(6):1724-5.
31. Hallgren O, Nihlberg K, Dahlback M, Bjermer L, Eriksson LT, Erjefalt JS, et al. Altered fibroblast proteoglycan production in COPD. Respiratory research. 2010;11:55.
32. Kulkarni T, O'Reilly P, Antony VB, Gaggar A, Thannickal VJ. Matrix Remodeling in Pulmonary Fibrosis and Emphysema. American journal of respiratory cell and molecular biology. 2016;54(6):751-60.
33. Lofdahl M, Kaarteenaho R, Lappi-Blanco E, Tornling G, Skold MC. Tenascin-C and alpha-smooth muscle actin positive cells are increased in the large airways in patients with COPD. Respiratory research. 2011;12:48.
34. Annoni R, Lancas T, Yukimatsu Tanigawa R, de Medeiros Matsushita M, de Morais Fernezlian S, Bruno A, et al. Extracellular matrix composition in COPD. The European respiratory journal. 2012;40(6):1362-73.
35. Kranenburg AR, Willems-Widyastuti A, Moori WJ, Sterk PJ, Alagappan VK, de Boer WI, et al. Enhanced bronchial expression of extracellular matrix proteins in

chronic obstructive pulmonary disease. American journal of clinical pathology. 2006;126(5):725-35.
36. McAnulty RJ. Fibroblasts and myofibroblasts: their source, function and role in disease. The international journal of biochemistry & cell biology. 2007;39(4):666-71.
37. Togo S, Holz O, Liu X, Sugiura H, Kamio K, Wang X, et al. Lung fibroblast repair functions in patients with chronic obstructive pulmonary disease are altered by multiple mechanisms. American journal of respiratory and critical care medicine. 2008;178(3):248-60.
38. Dagouassat M, Gagliolo JM, Chrusciel S, Bourin MC, Duprez C, Caramelle P, et al. The cyclooxygenase-2-prostaglandin E2 pathway maintains senescence of chronic obstructive pulmonary disease fibroblasts. American journal of respiratory and critical care medicine. 2013;187(7):703-14.
39. Zhang J, Wu L, Qu JM, Bai CX, Merrilees MJ, Black PN. Pro-inflammatory phenotype of COPD fibroblasts not compatible with repair in COPD lung. Journal of cellular and molecular medicine. 2012;16(7):1522-32.
40. Zandvoort A, Postma DS, Jonker MR, Noordhoek JA, Vos JT, Timens W. Smad gene expression in pulmonary fibroblasts: indications for defective ECM repair in COPD. Respiratory research. 2008;9:83.
41. Raghu G, Collard HR, Egan JJ, Martinez FJ, Behr J, Brown KK, et al. An official ATS/ERS/JRS/ALAT statement: idiopathic pulmonary fibrosis: evidence-based guidelines for diagnosis and management. American journal of respiratory and critical care medicine. 2011;183(6):788-824.
42. Cottin V, Cordier JF. Velcro crackles: the key for early diagnosis of idiopathic pulmonary fibrosis? The European respiratory journal. 2012;40(3):519-21.
43. Olson AL, Swigris JJ, Lezotte DC, Norris JM, Wilson CG, Brown KK. Mortality from pulmonary fibrosis increased in the United States from 1992 to 2003. American journal of respiratory and critical care medicine. 2007;176(3):277-84.
44. Martinez FJ, Safrin S, Weycker D, Starko KM, Bradford WZ, King TE, Jr., et al. The clinical course of patients with idiopathic pulmonary fibrosis. Annals of internal medicine. 2005;142(12 Pt 1):963-7.
45. King TE, Jr., Pardo A, Selman M. Idiopathic pulmonary fibrosis. Lancet (London, England). 2011;378(9807):1949-61.
46. Wolters PJ, Collard HR, Jones KD. Pathogenesis of idiopathic pulmonary fibrosis. Annual review of pathology. 2014;9:157-79.
47. Raghu G, Anstrom KJ, King TE, Jr., Lasky JA, Martinez FJ. Prednisone, azathioprine, and N-acetylcysteine for pulmonary fibrosis. The New England journal of medicine. 2012;366(21):1968-77.
48. Noble PW, Albera C, Bradford WZ, Costabel U, Glassberg MK, Kardatzke D, et al. Pirfenidone in patients with idiopathic pulmonary fibrosis (CAPACITY): two randomised trials. Lancet (London, England). 2011;377(9779):1760-9.
49. Richeldi L, du Bois RM, Raghu G, Azuma A, Brown KK, Costabel U, et al. Efficacy and safety of nintedanib in idiopathic pulmonary fibrosis. The New England journal of medicine. 2014;370(22):2071-82.
50. Juarez MM, Chan AL, Norris AG, Morrissey BM, Albertson TE. Acute exacerbation of idiopathic pulmonary fibrosis-a review of current and novel pharmacotherapies. Journal of thoracic disease. 2015;7(3):499-519.
51. Kuhn C, 3rd, Boldt J, King TE, Jr., Crouch E, Vartio T, McDonald JA. An immunohistochemical study of architectural remodeling and connective tissue synthesis in pulmonary fibrosis. The American review of respiratory disease. 1989;140(6):1693-703.

52. Fernandez IE, Eickelberg O. New cellular and molecular mechanisms of lung injury and fibrosis in idiopathic pulmonary fibrosis. Lancet (London, England). 2012;380(9842):680-8.
53. Oh CK, Murray LA, Molfino NA. Smoking and idiopathic pulmonary fibrosis. Pulmonary medicine. 2012;2012:808260.
54. Lee JS, Collard HR, Raghu G, Sweet MP, Hays SR, Campos GM, et al. Does chronic microaspiration cause idiopathic pulmonary fibrosis? The American journal of medicine. 2010;123(4):304-11.
55. Kinnula VL, Fattman CL, Tan RJ, Oury TD. Oxidative stress in pulmonary fibrosis: a possible role for redox modulatory therapy. American journal of respiratory and critical care medicine. 2005;172(4):417-22.
56. Seibold MA, Wise AL, Speer MC, Steele MP, Brown KK, Loyd JE, et al. A common MUC5B promoter polymorphism and pulmonary fibrosis. The New England journal of medicine. 2011;364(16):1503-12.
57. Nogee LM, Dunbar AE, 3rd, Wert SE, Askin F, Hamvas A, Whitsett JA. A mutation in the surfactant protein C gene associated with familial interstitial lung disease. The New England journal of medicine. 2001;344(8):573-9.
58. Queisser MA, Kouri FM, Konigshoff M, Wygrecka M, Schubert U, Eickelberg O, et al. Loss of RAGE in pulmonary fibrosis: molecular relations to functional changes in pulmonary cell types. American journal of respiratory cell and molecular biology. 2008;39(3):337-45.
59. Maher TM, Evans IC, Bottoms SE, Mercer PF, Thorley AJ, Nicholson AG, et al. Diminished prostaglandin E2 contributes to the apoptosis paradox in idiopathic pulmonary fibrosis. American journal of respiratory and critical care medicine. 2010;182(1):73-82.
60. Parker MW, Rossi D, Peterson M, Smith K, Sikstrom K, White ES, et al. Fibrotic extracellular matrix activates a profibrotic positive feedback loop. The Journal of clinical investigation. 2014;124(4):1622-35.
61. Kreuter M, Wuyts W, Renzoni E, Koschel D, Maher TM, Kolb M, et al. Antacid therapy and disease outcomes in idiopathic pulmonary fibrosis: a pooled analysis. The Lancet Respiratory medicine. 2016;4(5):381-9.
62. Noth I, Anstrom KJ, Calvert SB, de Andrade J, Flaherty KR, Glazer C, et al. A placebo-controlled randomized trial of warfarin in idiopathic pulmonary fibrosis. American journal of respiratory and critical care medicine. 2012;186(1):88-95.
63. Martinez FJ, de Andrade JA, Anstrom KJ, King TE, Jr., Raghu G. Randomized trial of acetylcysteine in idiopathic pulmonary fibrosis. The New England journal of medicine. 2014;370(22):2093-101.
64. King TE, Jr., Behr J, Brown KK, du Bois RM, Lancaster L, de Andrade JA, et al. BUILD-1: a randomized placebo-controlled trial of bosentan in idiopathic pulmonary fibrosis. American journal of respiratory and critical care medicine. 2008;177(1):75-81.
65. Zisman DA, Schwarz M, Anstrom KJ, Collard HR, Flaherty KR, Hunninghake GW. A controlled trial of sildenafil in advanced idiopathic pulmonary fibrosis. The New England journal of medicine. 2010;363(7):620-8.
66. Cottin V, Nunes H, Brillet PY, Delaval P, Devouassoux G, Tillie-Leblond I, et al. Combined pulmonary fibrosis and emphysema: a distinct underrecognised entity. The European respiratory journal. 2005;26(4):586-93.
67. Lin H, Jiang S. Combined pulmonary fibrosis and emphysema (CPFE): an entity different from emphysema or pulmonary fibrosis alone. Journal of thoracic disease. 2015;7(4):767-79.
68. Jankowich MD, Rounds SI. Combined pulmonary fibrosis and emphysema syndrome: a review. Chest. 2012;141(1):222-31.

69. Cottin V, Le Pavec J, Prevot G, Mal H, Humbert M, Simonneau G, et al. Pulmonary hypertension in patients with combined pulmonary fibrosis and emphysema syndrome. The European respiratory journal. 2010;35(1):105-11.
70. Kwak N, Park CM, Lee J, Park YS, Lee SM, Yim JJ, et al. Lung cancer risk among patients with combined pulmonary fibrosis and emphysema. Respiratory medicine. 2014;108(3):524-30.
71. Chilosi M, Poletti V, Rossi A. The pathogenesis of COPD and IPF: distinct horns of the same devil? Respiratory research. 2012;13:3.
72. Meiners S, Eickelberg O, Konigshoff M. Hallmarks of the ageing lung. The European respiratory journal. 2015;45(3):807-27.
73. Faner R, Rojas M, Macnee W, Agusti A. Abnormal lung aging in chronic obstructive pulmonary disease and idiopathic pulmonary fibrosis. American journal of respiratory and critical care medicine. 2012;186(4):306-13.
74. Alder JK, Guo N, Kembou F, Parry EM, Anderson CJ, Gorgy AI, et al. Telomere length is a determinant of emphysema susceptibility. American journal of respiratory and critical care medicine. 2011;184(8):904-12.
75. Rock J, Konigshoff M. Endogenous lung regeneration: potential and limitations. American journal of respiratory and critical care medicine. 2012;186(12):1213-9.
76. Morty RE, Konigshoff M, Eickelberg O. Transforming growth factor-beta signaling across ages: from distorted lung development to chronic obstructive pulmonary disease. Proceedings of the American Thoracic Society. 2009;6(7):607-13.
77. Fernandez IE, Eickelberg O. The impact of TGF-beta on lung fibrosis: from targeting to biomarkers. Proceedings of the American Thoracic Society. 2012;9(3):111-6.
78. Barnes PJ. The cytokine network in chronic obstructive pulmonary disease. American journal of respiratory cell and molecular biology. 2009;41(6):631-8.
79. Aumiller V, Balsara N, Wilhelm J, Gunther A, Konigshoff M. WNT/beta-catenin signaling induces IL-1beta expression by alveolar epithelial cells in pulmonary fibrosis. American journal of respiratory cell and molecular biology. 2013;49(1):96-104.
80. Le TT, Karmouty-Quintana H, Melicoff E, Le TT, Weng T, Chen NY, et al. Blockade of IL-6 Trans signaling attenuates pulmonary fibrosis. Journal of immunology (Baltimore, Md : 1950). 2014;193(7):3755-68.
81. Konigshoff M, Balsara N, Pfaff EM, Kramer M, Chrobak I, Seeger W, et al. Functional Wnt signaling is increased in idiopathic pulmonary fibrosis. PloS one. 2008;3(5):e2142.
82. Kusko RL, Brothers JF, 2nd, Tedrow J, Pandit K, Huleihel L, Perdomo C, et al. Integrated Genomics Reveals Convergent Transcriptomic Networks Underlying Chronic Obstructive Pulmonary Disease and Idiopathic Pulmonary Fibrosis. American journal of respiratory and critical care medicine. 2016;194(8):948-60.
83. Selman M, Pardo A, Kaminski N. Idiopathic pulmonary fibrosis: aberrant recapitulation of developmental programs? PLoS medicine. 2008;5(3):e62.
84. Boucherat O, Morissette MC, Provencher S, Bonnet S, Maltais F. Bridging Lung Development with Chronic Obstructive Pulmonary Disease. Relevance of Developmental Pathways in Chronic Obstructive Pulmonary Disease Pathogenesis. American journal of respiratory and critical care medicine. 2016;193(4):362-75.
85. Baarsma HA, Konigshoff M, Gosens R. The WNT signaling pathway from ligand secretion to gene transcription: molecular mechanisms and pharmacological targets. Pharmacology & therapeutics. 2013;138(1):66-83.
86. Logan CY, Nusse R. The Wnt signaling pathway in development and disease. Annual review of cell and developmental biology. 2004;20:781-810.

87. Liu G, Bafico A, Aaronson SA. The mechanism of endogenous receptor activation functionally distinguishes prototype canonical and noncanonical Wnts. Molecular and cellular biology. 2005;25(9):3475-82.
88. Clevers H. Wnt/beta-catenin signaling in development and disease. Cell. 2006;127(3):469-80.
89. van Amerongen R. Alternative Wnt pathways and receptors. Cold Spring Harbor perspectives in biology. 2012;4(10).
90. Kikuchi A, Yamamoto H, Sato A, Matsumoto S. Wnt5a: its signalling, functions and implication in diseases. Acta physiologica (Oxford, England). 2012;204(1):17-33.
91. Park HW, Kim YC, Yu B, Moroishi T, Mo JS, Plouffe SW, et al. Alternative Wnt Signaling Activates YAP/TAZ. Cell. 2015;162(4):780-94.
92. Ishitani T, Kishida S, Hyodo-Miura J, Ueno N, Yasuda J, Waterman M, et al. The TAK1-NLK mitogen-activated protein kinase cascade functions in the Wnt-5a/Ca(2+) pathway to antagonize Wnt/beta-catenin signaling. Molecular and cellular biology. 2003;23(1):131-9.
93. Mikels AJ, Nusse R. Purified Wnt5a protein activates or inhibits beta-catenin-TCF signaling depending on receptor context. PLoS biology. 2006;4(4):e115.
94. Baarsma HA, Skronska-Wasek W, Mutze K, Ciolek F, Wagner DE, John-Schuster G, et al. Noncanonical WNT-5A signaling impairs endogenous lung repair in COPD. The Journal of experimental medicine. 2016.
95. van Amerongen R, Mikels A, Nusse R. Alternative wnt signaling is initiated by distinct receptors. Science signaling. 2008;1(35):re9.
96. Skronska-Wasek W, Gosens R, Konigshoff M, Baarsma HA. WNT receptor signalling in lung physiology and pathology. Pharmacology & therapeutics. 2018.
97. Goss AM, Tian Y, Tsukiyama T, Cohen ED, Zhou D, Lu MM, et al. Wnt2/2b and beta-catenin signaling are necessary and sufficient to specify lung progenitors in the foregut. Developmental cell. 2009;17(2):290-8.
98. Ota C, Baarsma HA, Wagner DE, Hilgendorff A, Konigshoff M. Linking bronchopulmonary dysplasia to adult chronic lung diseases: role of WNT signaling. Molecular and cellular pediatrics. 2016;3(1):34.
99. Konigshoff M, Eickelberg O. WNT signaling in lung disease: a failure or a regeneration signal? American journal of respiratory cell and molecular biology. 2010;42(1):21-31.
100. Li C, Xiao J, Hormi K, Borok Z, Minoo P. Wnt5a participates in distal lung morphogenesis. Developmental biology. 2002;248(1):68-81.
101. Nabhan AN, Brownfield DG, Harbury PB, Krasnow MA, Desai TJ. Single-cell Wnt signaling niches maintain stemness of alveolar type 2 cells. Science (New York, NY). 2018;359(6380):1118-23.
102. Kinzler KW, Nilbert MC, Su LK, Vogelstein B, Bryan TM, Levy DB, et al. Identification of FAP locus genes from chromosome 5q21. Science (New York, NY). 1991;253(5020):661-5.
103. Nishisho I, Nakamura Y, Miyoshi Y, Miki Y, Ando H, Horii A, et al. Mutations of chromosome 5q21 genes in FAP and colorectal cancer patients. Science (New York, NY). 1991;253(5020):665-9.
104. Chilosi M, Poletti V, Zamo A, Lestani M, Montagna L, Piccoli P, et al. Aberrant Wnt/beta-catenin pathway activation in idiopathic pulmonary fibrosis. The American journal of pathology. 2003;162(5):1495-502.
105. Konigshoff M, Kramer M, Balsara N, Wilhelm J, Amarie OV, Jahn A, et al. WNT1-inducible signaling protein-1 mediates pulmonary fibrosis in mice and is upregulated in humans with idiopathic pulmonary fibrosis. The Journal of clinical investigation. 2009;119(4):772-87.

106. Meuten T, Hickey A, Franklin K, Grossi B, Tobias J, Newman DR, et al. WNT7B in fibroblastic foci of idiopathic pulmonary fibrosis. Respiratory research. 2012;13:62.
107. Oda K, Yatera K, Izumi H, Ishimoto H, Yamada S, Nakao H, et al. Profibrotic role of WNT10A via TGF-beta signaling in idiopathic pulmonary fibrosis. Respiratory research. 2016;17:39.
108. Pfaff EM, Becker S, Gunther A, Konigshoff M. Dickkopf proteins influence lung epithelial cell proliferation in idiopathic pulmonary fibrosis. The European respiratory journal. 2011;37(1):79-87.
109. Rydell-Tormanen K, Zhou XH, Hallgren O, Einarsson J, Eriksson L, Andersson-Sjoland A, et al. Aberrant nonfibrotic parenchyma in idiopathic pulmonary fibrosis is correlated with decreased beta-catenin inhibition and increased Wnt5a/b interaction. Physiological reports. 2016;4(5).
110. Huang C, Xiao X, Yang Y, Mishra A, Liang Y, Zeng X, et al. MicroRNA-101 attenuates pulmonary fibrosis by inhibiting fibroblast proliferation and activation. The Journal of biological chemistry. 2017.
111. Akhmetshina A, Palumbo K, Dees C, Bergmann C, Venalis P, Zerr P, et al. Activation of canonical Wnt signalling is required for TGF-beta-mediated fibrosis. Nature communications. 2012;3:735.
112. Lam AP, Herazo-Maya JD, Sennello JA, Flozak AS, Russell S, Mutlu GM, et al. Wnt coreceptor Lrp5 is a driver of idiopathic pulmonary fibrosis. American journal of respiratory and critical care medicine. 2014;190(2):185-95.
113. Shi J, Li F, Luo M, Wei J, Liu X. Distinct Roles of Wnt/beta-Catenin Signaling in the Pathogenesis of Chronic Obstructive Pulmonary Disease and Idiopathic Pulmonary Fibrosis. Mediators of inflammation. 2017;2017:3520581.
114. Henderson WR, Jr., Chi EY, Ye X, Nguyen C, Tien YT, Zhou B, et al. Inhibition of Wnt/beta-catenin/CREB binding protein (CBP) signaling reverses pulmonary fibrosis. Proceedings of the National Academy of Sciences of the United States of America. 2010;107(32):14309-14.
115. Tanjore H, Degryse AL, Crossno PF, Xu XC, McConaha ME, Jones BR, et al. beta-catenin in the alveolar epithelium protects from lung fibrosis after intratracheal bleomycin. American journal of respiratory and critical care medicine. 2013;187(6):630-9.
116. Gottardi CJ, Konigshoff M. Considerations for targeting beta-catenin signaling in fibrosis. American journal of respiratory and critical care medicine. 2013;187(6):566-8.
117. Kneidinger N, Yildirim AO, Callegari J, Takenaka S, Stein MM, Dumitrascu R, et al. Activation of the WNT/beta-catenin pathway attenuates experimental emphysema. American journal of respiratory and critical care medicine. 2011;183(6):723-33.
118. Wang R, Ahmed J, Wang G, Hassan I, Strulovici-Barel Y, Hackett NR, et al. Down-regulation of the canonical Wnt beta-catenin pathway in the airway epithelium of healthy smokers and smokers with COPD. PloS one. 2011;6(4):e14793.
119. Uhl FE, Vierkotten S, Wagner DE, Burgstaller G, Costa R, Koch I, et al. Preclinical validation and imaging of Wnt-induced repair in human 3D lung tissue cultures. The European respiratory journal. 2015;46(4):1150-66.
120. Guo L, Wang T, Wu Y, Yuan Z, Dong J, Li X, et al. WNT/beta-catenin signaling regulates cigarette smoke-induced airway inflammation via the PPARdelta/p38 pathway. Laboratory investigation; a journal of technical methods and pathology. 2016;96(2):218-29.
121. Baarsma HA, Konigshoff M. 'WNT-er is coming': WNT signalling in chronic lung diseases. Thorax. 2017.

122. Ezzie ME, Crawford M, Cho JH, Orellana R, Zhang S, Gelinas R, et al. Gene expression networks in COPD: microRNA and mRNA regulation. Thorax. 2012;67(2):122-31.
123. Jiang Z, Lao T, Qiu W, Polverino F, Gupta K, Guo F, et al. A Chronic Obstructive Pulmonary Disease Susceptibility Gene, FAM13A, Regulates Protein Stability of beta-Catenin. American journal of respiratory and critical care medicine. 2016;194(2):185-97.
124. Skronska-Wasek W, Mutze K, Baarsma HA, Bracke KR, Alsafadi HN, Lehmann M, et al. Reduced Frizzled Receptor 4 Expression Prevents WNT/beta-catenin-driven Alveolar Lung Repair in COPD. American journal of respiratory and critical care medicine. 2017.
125. Wu X, van Dijk EM, Ng-Blichfeldt JP, Bos IST, Ciminieri C, Konigshoff M, et al. Mesenchymal WNT-5A/5B Signaling Represses Lung Alveolar Epithelial Progenitors. Cells. 2019;8(10).
126. Vuga LJ, Ben-Yehudah A, Kovkarova-Naumovski E, Oriss T, Gibson KF, Feghali-Bostwick C, et al. WNT5A is a regulator of fibroblast proliferation and resistance to apoptosis. American journal of respiratory cell and molecular biology. 2009;41(5):583-9.
127. Newman DR, Sills WS, Hanrahan K, Ziegler A, Tidd KM, Cook E, et al. Expression of WNT5A in Idiopathic Pulmonary Fibrosis and its Control by TGF-beta and WNT7B in Human Lung Fibroblasts. The journal of histochemistry and cytochemistry : official journal of the Histochemistry Society. 2015.
128. Martin-Medina A, Lehmann M, Burgy O, Hermann S, Baarsma HA, Wagner DE, et al. Increased Extracellular Vesicles Mediate WNT-5A Signaling in Idiopathic Pulmonary Fibrosis. American journal of respiratory and critical care medicine. 2018.
129. Guan S, Zhou J. Frizzled-7 mediates TGF-beta-induced pulmonary fibrosis by transmitting non-canonical Wnt signaling. Experimental cell research. 2017.
130. Spanjer AI, Baarsma HA, Oostenbrink LM, Jansen SR, Kuipers CC, Lindner M, et al. TGF-beta-induced profibrotic signaling is regulated in part by the WNT receptor Frizzled-8. FASEB journal : official publication of the Federation of American Societies for Experimental Biology. 2016.
131. Durham AL, McLaren A, Hayes BP, Caramori G, Clayton CL, Barnes PJ, et al. Regulation of Wnt4 in chronic obstructive pulmonary disease. FASEB journal : official publication of the Federation of American Societies for Experimental Biology. 2013;27(6):2367-81.
132. Heijink IH, de Bruin HG, van den Berge M, Bennink LJ, Brandenburg SM, Gosens R, et al. Role of aberrant WNT signalling in the airway epithelial response to cigarette smoke in chronic obstructive pulmonary disease. Thorax. 2013;68(8):709-16.
133. Baarsma HA, Spanjer AI, Haitsma G, Engelbertink LH, Meurs H, Jonker MR, et al. Activation of WNT/beta-catenin signaling in pulmonary fibroblasts by TGF-beta(1) is increased in chronic obstructive pulmonary disease. PloS one. 2011;6(9):e25450.
134. Heijink IH, de Bruin HG, Dennebos R, Jonker MR, Noordhoek JA, Brandsma CA, et al. Cigarette smoke-induced epithelial expression of WNT-5B: implications for COPD. The European respiratory journal. 2016;48(2):504-15.
135. van Dijk EM, Menzen MH, Spanjer AI, Middag LD, Brandsma CA, Gosens R. Non-canonical WNT-5B signalling induces inflammatory responses in human lung fibroblasts. American journal of physiology Lung cellular and molecular physiology. 2016:ajplung.00226.2015.
136. Spanjer AI, Menzen MH, Dijkstra AE, van den Berge M, Boezen HM, Nickle DC, et al. A pro-inflammatory role for the Frizzled-8 receptor in chronic bronchitis. Thorax. 2016.

137. Feller D, Kun J, Ruzsics I, Rapp J, Sarosi V, Kvell K, et al. Cigarette Smoke-Induced Pulmonary Inflammation Becomes Systemic by Circulating Extracellular Vesicles Containing Wnt5a and Inflammatory Cytokines. Frontiers in immunology. 2018;9:1724.
138. Kim TH, Kim SH, Seo JY, Chung H, Kwak HJ, Lee SK, et al. Blockade of the Wnt/beta-catenin pathway attenuates bleomycin-induced pulmonary fibrosis. The Tohoku journal of experimental medicine. 2011;223(1):45-54.
139. Cui W, Zhang Z, Zhang P, Qu J, Zheng C, Mo X, et al. Nrf2 attenuates inflammatory response in COPD/emphysema: Crosstalk with Wnt3a/beta-catenin and AMPK pathways. Journal of cellular and molecular medicine. 2018.
140. Wilhelm J, Pingoud A. Real-time polymerase chain reaction. Chembiochem : a European journal of chemical biology. 2003;4(11):1120-8.
141. de Kok JB, Roelofs RW, Giesendorf BA, Pennings JL, Waas ET, Feuth T, et al. Normalization of gene expression measurements in tumor tissues: comparison of 13 endogenous control genes. Laboratory investigation; a journal of technical methods and pathology. 2005;85(1):154-9.
142. Klee S, Lehmann M, Wagner DE, Baarsma HA, Konigshoff M. WISP1 mediates IL-6-dependent proliferation in primary human lung fibroblasts. Scientific reports. 2016;6:20547.
143. Baarsma HA, Meurs H, Halayko AJ, Menzen MH, Schmidt M, Kerstjens HA, et al. Glycogen synthase kinase-3 regulates cigarette smoke extract- and IL-1beta-induced cytokine secretion by airway smooth muscle. American journal of physiology Lung cellular and molecular physiology. 2011;300(6):L910-9.
144. Akhurst RJ, Hata A. Targeting the TGFbeta signalling pathway in disease. Nature reviews Drug discovery. 2012;11(10):790-811.
145. Kumawat K, Menzen MH, Slegtenhorst RM, Halayko AJ, Schmidt M, Gosens R. TGF-beta-activated kinase 1 (TAK1) signaling regulates TGF-beta-induced WNT-5A expression in airway smooth muscle cells via Sp1 and beta-catenin. PloS one. 2014;9(4):e94801.
146. Kwak HJ, Park DW, Seo JY, Moon JY, Kim TH, Sohn JW, et al. The Wnt/beta-catenin signaling pathway regulates the development of airway remodeling in patients with asthma. Experimental & molecular medicine. 2015;47:e198.
147. Katoh M, Katoh M. Transcriptional mechanisms of WNT5A based on NF-kappaB, Hedgehog, TGFbeta, and Notch signaling cascades. International journal of molecular medicine. 2009;23(6):763-9.
148. Baarsma HA, Engelbertink LH, van Hees LJ, Menzen MH, Meurs H, Timens W, et al. Glycogen synthase kinase-3 (GSK-3) regulates TGF-beta(1)-induced differentiation of pulmonary fibroblasts. British journal of pharmacology. 2013;169(3):590-603.
149. Bain J, Plater L, Elliott M, Shpiro N, Hastie CJ, McLauchlan H, et al. The selectivity of protein kinase inhibitors: a further update. The Biochemical journal. 2007;408(3):297-315.
150. Aubert JD, Dalal BI, Bai TR, Roberts CR, Hayashi S, Hogg JC. Transforming growth factor beta 1 gene expression in human airways. Thorax. 1994;49(3):225-32.
151. Khalil N, O'Connor RN, Flanders KC, Unruh H. TGF-beta 1, but not TGF-beta 2 or TGF-beta 3, is differentially present in epithelial cells of advanced pulmonary fibrosis: an immunohistochemical study. American journal of respiratory cell and molecular biology. 1996;14(2):131-8.
152. Kanaji N, Basma H, Nelson A, Farid M, Sato T, Nakanishi M, et al. Fibroblasts that resist cigarette smoke-induced senescence acquire profibrotic phenotypes.

American journal of physiology Lung cellular and molecular physiology. 2014;307(5):L364-73.
153. Miglino N, Roth M, Lardinois D, Sadowski C, Tamm M, Borger P. Cigarette smoke inhibits lung fibroblast proliferation by translational mechanisms. The European respiratory journal. 2012;39(3):705-11.
154. Vuga LJ, Milosevic J, Pandit K, Ben-Yehudah A, Chu Y, Richards T, et al. Cartilage oligomeric matrix protein in idiopathic pulmonary fibrosis. PloS one. 2013;8(12):e83120.
155. Agarwal P, Schulz JN, Blumbach K, Andreasson K, Heinegard D, Paulsson M, et al. Enhanced deposition of cartilage oligomeric matrix protein is a common feature in fibrotic skin pathologies. Matrix biology : journal of the International Society for Matrix Biology. 2013;32(6):325-31.
156. Deslee G, Woods JC, Moore CM, Liu L, Conradi SH, Milne M, et al. Elastin expression in very severe human COPD. The European respiratory journal. 2009;34(2):324-31.
157. Houghton AM, Quintero PA, Perkins DL, Kobayashi DK, Kelley DG, Marconcini LA, et al. Elastin fragments drive disease progression in a murine model of emphysema. The Journal of clinical investigation. 2006;116(3):753-9.
158. Otsubo C, Otomo R, Miyazaki M, Matsushima-Hibiya Y, Kohno T, Iwakawa R, et al. TSPAN2 is involved in cell invasion and motility during lung cancer progression. Cell reports. 2014;7(2):527-38.
159. Soler Artigas M, Wain LV, Repapi E, Obeidat M, Sayers I, Burton PR, et al. Effect of five genetic variants associated with lung function on the risk of chronic obstructive lung disease, and their joint effects on lung function. American journal of respiratory and critical care medicine. 2011;184(7):786-95.
160. Shih YP, Sun P, Wang A, Lo SH. Tensin1 positively regulates RhoA activity through its interaction with DLC1. Biochimica et biophysica acta. 2015;1853(12):3258-65.
161. Bernau K, Torr EE, Evans MD, Aoki JK, Ngam CR, Sandbo N. Tensin 1 Is Essential for Myofibroblast Differentiation and Extracellular Matrix Formation. American journal of respiratory cell and molecular biology. 2017;56(4):465-76.
162. Wagenseil JE, Mecham RP. New insights into elastic fiber assembly. Birth defects research Part C, Embryo today : reviews. 2007;81(4):229-40.
163. Brandsma CA, van den Berge M, Postma DS, Jonker MR, Brouwer S, Pare PD, et al. A large lung gene expression study identifying fibulin-5 as a novel player in tissue repair in COPD. Thorax. 2015;70(1):21-32.
164. Chen X, Song X, Yue W, Chen D, Yu J, Yao Z, et al. Fibulin-5 inhibits Wnt/beta-catenin signaling in lung cancer. Oncotarget. 2015;6(17):15022-34.
165. Berendsen AD, Fisher LW, Kilts TM, Owens RT, Robey PG, Gutkind JS, et al. Modulation of canonical Wnt signaling by the extracellular matrix component biglycan. Proceedings of the National Academy of Sciences of the United States of America. 2011;108(41):17022-7.
166. Scotton CJ, Chambers RC. Molecular targets in pulmonary fibrosis: the myofibroblast in focus. Chest. 2007;132(4):1311-21.
167. Hinz B, Phan SH, Thannickal VJ, Galli A, Bochaton-Piallat ML, Gabbiani G. The myofibroblast: one function, multiple origins. The American journal of pathology. 2007;170(6):1807-16.
168. Wang C, Zhao Y, Su Y, Li R, Lin Y, Zhou X, et al. C-Jun N-terminal kinase (JNK) mediates Wnt5a-induced cell motility dependent or independent of RhoA pathway in human dental papilla cells. PloS one. 2013;8(7):e69440.

169. McGarvey LP, John M, Anderson JA, Zvarich M, Wise RA. Ascertainment of cause-specific mortality in COPD: operations of the TORCH Clinical Endpoint Committee. Thorax. 2007;62(5):411-5.
170. Rutgers SR, Timens W, Kauffman HF, Postma DS. Markers of active airway inflammation and remodelling in chronic obstructive pulmonary disease. Clinical and experimental allergy : journal of the British Society for Allergy and Clinical Immunology. 2001;31(2):193-205.
171. Podowski M, Calvi C, Metzger S, Misono K, Poonyagariyagorn H, Lopez-Mercado A, et al. Angiotensin receptor blockade attenuates cigarette smoke-induced lung injury and rescues lung architecture in mice. The Journal of clinical investigation. 2012;122(1):229-40.
172. Taniguchi H, Ebina M, Kondoh Y, Ogura T, Azuma A, Suga M, et al. Pirfenidone in idiopathic pulmonary fibrosis. The European respiratory journal. 2010;35(4):821-9.
173. Minagawa S, Lou J, Seed RI, Cormier A, Wu S, Cheng Y, et al. Selective targeting of TGF-beta activation to treat fibroinflammatory airway disease. Science translational medicine. 2014;6(241):241ra79.
174. Lee CM, Park JW, Cho WK, Zhou Y, Han B, Yoon PO, et al. Modifiers of TGF-beta1 effector function as novel therapeutic targets of pulmonary fibrosis. The Korean journal of internal medicine. 2014;29(3):281-90.
175. Katula KS, Joyner-Powell NB, Hsu CC, Kuk A. Differential regulation of the mouse and human Wnt5a alternative promoters A and B. DNA and cell biology. 2012;31(11):1585-97.
176. Blyszczuk P, Muller-Edenborn B, Valenta T, Osto E, Stellato M, Behnke S, et al. Transforming growth factor-beta-dependent Wnt secretion controls myofibroblast formation and myocardial fibrosis progression in experimental autoimmune myocarditis. European heart journal. 2016.
177. Sakurai H, Miyoshi H, Toriumi W, Sugita T. Functional interactions of transforming growth factor beta-activated kinase 1 with IkappaB kinases to stimulate NF-kappaB activation. The Journal of biological chemistry. 1999;274(15):10641-8.
178. Hayden MS, Ghosh S. Shared principles in NF-kappaB signaling. Cell. 2008;132(3):344-62.
179. Rauner M, Stein N, Winzer M, Goettsch C, Zwerina J, Schett G, et al. WNT5A is induced by inflammatory mediators in bone marrow stromal cells and regulates cytokine and chemokine production. Journal of bone and mineral research : the official journal of the American Society for Bone and Mineral Research. 2012;27(3):575-85.
180. Ge XP, Gan YH, Zhang CG, Zhou CY, Ma KT, Meng JH, et al. Requirement of the NF-kappaB pathway for induction of Wnt-5A by interleukin-1beta in condylar chondrocytes of the temporomandibular joint: functional crosstalk between the Wnt-5A and NF-kappaB signaling pathways. Osteoarthritis and cartilage. 2011;19(1):111-7.
181. Whang YM, Jo U, Sung JS, Ju HJ, Kim HK, Park KH, et al. Wnt5a is associated with cigarette smoke-related lung carcinogenesis via protein kinase C. PloS one. 2013;8(1):e53012.
182. Hussain M, Rao M, Humphries AE, Hong JA, Liu F, Yang M, et al. Tobacco smoke induces polycomb-mediated repression of Dickkopf-1 in lung cancer cells. Cancer research. 2009;69(8):3570-8.
183. Talhout R, Schulz T, Florek E, van Benthem J, Wester P, Opperhuizen A. Hazardous compounds in tobacco smoke. International journal of environmental research and public health. 2011;8(2):613-28.
184. Hasday JD, Bascom R, Costa JJ, Fitzgerald T, Dubin W. Bacterial endotoxin is an active component of cigarette smoke. Chest. 1999;115(3):829-35.

185. Villar J, Cabrera-Benitez NE, Ramos-Nuez A, Flores C, Garcia-Hernandez S, Valladares F, et al. Early activation of pro-fibrotic WNT5A in sepsis-induced acute lung injury. Critical care (London, England). 2014;18(5):568.
186. Pera T, Gosens R, Lesterhuis AH, Sami R, van der Toorn M, Zaagsma J, et al. Cigarette smoke and lipopolysaccharide induce a proliferative airway smooth muscle phenotype. Respiratory research. 2010;11:48.
187. Ballweg K, Mutze K, Konigshoff M, Eickelberg O, Meiners S. Cigarette smoke extract affects mitochondrial function in alveolar epithelial cells. American journal of physiology Lung cellular and molecular physiology. 2014;307(11):L895-907.
188. Nakamura Y, Romberger DJ, Tate L, Ertl RF, Kawamoto M, Adachi Y, et al. Cigarette smoke inhibits lung fibroblast proliferation and chemotaxis. American journal of respiratory and critical care medicine. 1995;151(5):1497-503.
189. Nyunoya T, Monick MM, Klingelhutz A, Yarovinsky TO, Cagley JR, Hunninghake GW. Cigarette smoke induces cellular senescence. American journal of respiratory cell and molecular biology. 2006;35(6):681-8.
190. Lee H, Park JR, Kim EJ, Kim WJ, Hong SH, Park SM, et al. Cigarette smoke-mediated oxidative stress induces apoptosis via the MAPKs/STAT1 pathway in mouse lung fibroblasts. Toxicology letters. 2016;240(1):140-8.
191. Carp H, Janoff A. Possible mechanisms of emphysema in smokers. In vitro suppression of serum elastase-inhibitory capacity by fresh cigarette smoke and its prevention by antioxidants. The American review of respiratory disease. 1978;118(3):617-21.
192. Hellermann GR, Nagy SB, Kong X, Lockey RF, Mohapatra SS. Mechanism of cigarette smoke condensate-induced acute inflammatory response in human bronchial epithelial cells. Respiratory research. 2002;3:22.
193. Krimmer DI, Burgess JK, Wooi TK, Black JL, Oliver BG. Matrix proteins from smoke-exposed fibroblasts are pro-proliferative. American journal of respiratory cell and molecular biology. 2012;46(1):34-9.
194. Pera T, Atmaj C, van der Vegt M, Halayko AJ, Zaagsma J, Meurs H. Role for TAK1 in cigarette smoke-induced proinflammatory signaling and IL-8 release by human airway smooth muscle cells. American journal of physiology Lung cellular and molecular physiology. 2012;303(3):L272-8.
195. Lee D, Shin C. MicroRNA-target interactions: new insights from genome-wide approaches. Annals of the New York Academy of Sciences. 2012;1271:118-28.
196. Xi S, Xu H, Shan J, Tao Y, Hong JA, Inchauste S, et al. Cigarette smoke mediates epigenetic repression of miR-487b during pulmonary carcinogenesis. The Journal of clinical investigation. 2013;123(3):1241-61.
197. Xi S, Yang M, Tao Y, Xu H, Shan J, Inchauste S, et al. Cigarette smoke induces C/EBP-beta-mediated activation of miR-31 in normal human respiratory epithelia and lung cancer cells. PloS one. 2010;5(10):e13764.
198. Martin P. Wound healing--aiming for perfect skin regeneration. Science (New York, NY). 1997;276(5309):75-81.
199. Klapholz-Brown Z, Walmsley GG, Nusse YM, Nusse R, Brown PO. Transcriptional program induced by Wnt protein in human fibroblasts suggests mechanisms for cell cooperativity in defining tissue microenvironments. PloS one. 2007;2(9):e945.
200. Dunsmore SE, Rannels DE. Extracellular matrix biology in the lung. The American journal of physiology. 1996;270(1 Pt 1):L3-27.
201. Salazar LM, Herrera AM. Fibrotic response of tissue remodeling in COPD. Lung. 2011;189(2):101-9.

202. Estany S, Vicens-Zygmunt V, Llatjos R, Montes A, Penin R, Escobar I, et al. Lung fibrotic tenascin-C upregulation is associated with other extracellular matrix proteins and induced by TGFbeta1. BMC pulmonary medicine. 2014;14:120.
203. Hogg JC, Chu F, Utokaparch S, Woods R, Elliott WM, Buzatu L, et al. The nature of small-airway obstruction in chronic obstructive pulmonary disease. The New England journal of medicine. 2004;350(26):2645-53.
204. Agarwal P, Zwolanek D, Keene DR, Schulz JN, Blumbach K, Heinegard D, et al. Collagen XII and XIV, new partners of cartilage oligomeric matrix protein in the skin extracellular matrix suprastructure. The Journal of biological chemistry. 2012;287(27):22549-59.
205. DiCesare PE, Morgelin M, Carlson CS, Pasumarti S, Paulsson M. Cartilage oligomeric matrix protein: isolation and characterization from human articular cartilage. Journal of orthopaedic research : official publication of the Orthopaedic Research Society. 1995;13(3):422-8.
206. Magdaleno F, Arriazu E, Ruiz de Galarreta M, Chen Y, Ge X, Conde de la Rosa L, et al. Cartilage oligomeric matrix protein participates in the pathogenesis of liver fibrosis. Journal of hepatology. 2016.
207. Weng LH, Wang CJ, Ko JY, Sun YC, Wang FS. Control of Dkk-1 ameliorates chondrocyte apoptosis, cartilage destruction, and subchondral bone deterioration in osteoarthritic knees. Arthritis and rheumatism. 2010;62(5):1393-402.
208. Cha SI, Groshong SD, Frankel SK, Edelman BL, Cosgrove GP, Terry-Powers JL, et al. Compartmentalized expression of c-FLIP in lung tissues of patients with idiopathic pulmonary fibrosis. American journal of respiratory cell and molecular biology. 2010;42(2):140-8.
209. Blaauboer ME, Boeijen FR, Emson CL, Turner SM, Zandieh-Doulabi B, Hanemaaijer R, et al. Extracellular matrix proteins: a positive feedback loop in lung fibrosis? Matrix biology : journal of the International Society for Matrix Biology. 2014;34:170-8.
210. Shifren A, Mecham RP. The stumbling block in lung repair of emphysema: elastic fiber assembly. Proceedings of the American Thoracic Society. 2006;3(5):428-33.
211. Kumawat K, Menzen MH, Bos IS, Baarsma HA, Borger P, Roth M, et al. Noncanonical WNT-5A signaling regulates TGF-beta-induced extracellular matrix production by airway smooth muscle cells. FASEB journal : official publication of the Federation of American Societies for Experimental Biology. 2013;27(4):1631-43.
212. Beljaars L, Daliri S, Dijkhuizen C, Poelstra K, Gosens R. WNT-5A regulates TGF-beta-related activities in liver fibrosis. American journal of physiology Gastrointestinal and liver physiology. 2017;312(3):G219-g27.
213. Xiong WJ, Hu LJ, Jian YC, Wang LJ, Jiang M, Li W, et al. Wnt5a participates in hepatic stellate cell activation observed by gene expression profile and functional assays. World journal of gastroenterology. 2012;18(15):1745-52.
214. Burgy O, Konigshoff M. The WNT signaling pathways in wound healing and fibrosis. Matrix biology : journal of the International Society for Matrix Biology. 2018.
215. Ge Z, Li B, Zhou X, Yang Y, Zhang J. Basic fibroblast growth factor activates beta-catenin/RhoA signaling in pulmonary fibroblasts with chronic obstructive pulmonary disease in rats. Molecular and cellular biochemistry. 2016.
216. Hasegawa D, Wada N, Maeda H, Yoshida S, Mitarai H, Tomokiyo A, et al. Wnt5a Induces Collagen Production by Human Periodontal Ligament Cells Through TGFbeta1-Mediated Upregulation of Periostin Expression. Journal of cellular physiology. 2015;230(11):2647-60.

217. Kumawat K, Gosens R. WNT-5A: signaling and functions in health and disease. Cellular and molecular life sciences : CMLS. 2016;73(3):567-87.
218. Phillips RJ, Burdick MD, Hong K, Lutz MA, Murray LA, Xue YY, et al. Circulating fibrocytes traffic to the lungs in response to CXCL12 and mediate fibrosis. The Journal of clinical investigation. 2004;114(3):438-46.
219. Hashimoto N, Jin H, Liu T, Chensue SW, Phan SH. Bone marrow-derived progenitor cells in pulmonary fibrosis. The Journal of clinical investigation. 2004;113(2):243-52.
220. Kisseleva T, Uchinami H, Feirt N, Quintana-Bustamante O, Segovia JC, Schwabe RF, et al. Bone marrow-derived fibrocytes participate in pathogenesis of liver fibrosis. Journal of hepatology. 2006;45(3):429-38.
221. Willis BC, Liebler JM, Luby-Phelps K, Nicholson AG, Crandall ED, du Bois RM, et al. Induction of epithelial-mesenchymal transition in alveolar epithelial cells by transforming growth factor-beta1: potential role in idiopathic pulmonary fibrosis. The American journal of pathology. 2005;166(5):1321-32.
222. Rock JR, Barkauskas CE, Cronce MJ, Xue Y, Harris JR, Liang J, et al. Multiple stromal populations contribute to pulmonary fibrosis without evidence for epithelial to mesenchymal transition. Proceedings of the National Academy of Sciences of the United States of America. 2011;108(52):E1475-83.
223. Selman M, King TE, Pardo A. Idiopathic pulmonary fibrosis: prevailing and evolving hypotheses about its pathogenesis and implications for therapy. Annals of internal medicine. 2001;134(2):136-51.
224. Noordhoek JA, Postma DS, Chong LL, Vos JT, Kauffman HF, Timens W, et al. Different proliferative capacity of lung fibroblasts obtained from control subjects and patients with emphysema. Experimental lung research. 2003;29(5):291-302.
225. Holz O, Zuhlke I, Jaksztat E, Muller KC, Welker L, Nakashima M, et al. Lung fibroblasts from patients with emphysema show a reduced proliferation rate in culture. The European respiratory journal. 2004;24(4):575-9.
226. Karvonen HM, Lehtonen ST, Harju T, Sormunen RT, Lappi-Blanco E, Makinen JM, et al. Myofibroblast expression in airways and alveoli is affected by smoking and COPD. Respiratory research. 2013;14:84.
227. Kotaru C, Schoonover KJ, Trudeau JB, Huynh ML, Zhou X, Hu H, et al. Regional fibroblast heterogeneity in the lung: implications for remodeling. American journal of respiratory and critical care medicine. 2006;173(11):1208-15.
228. Zhou X, Wu W, Hu H, Milosevic J, Konishi K, Kaminski N, et al. Genomic differences distinguish the myofibroblast phenotype of distal lung fibroblasts from airway fibroblasts. American journal of respiratory cell and molecular biology. 2011;45(6):1256-62.
229. Pechkovsky DV, Hackett TL, An SS, Shaheen F, Murray LA, Knight DA. Human lung parenchyma but not proximal bronchi produces fibroblasts with enhanced TGF-beta signaling and alpha-SMA expression. American journal of respiratory cell and molecular biology. 2010;43(6):641-51.
230. Yu XM, Wang L, Li JF, Liu J, Li J, Wang W, et al. Wnt5a inhibits hypoxia-induced pulmonary arterial smooth muscle cell proliferation by downregulation of beta-catenin. American journal of physiology Lung cellular and molecular physiology. 2013;304(2):L103-11.
231. Huang CL, Liu D, Nakano J, Ishikawa S, Kontani K, Yokomise H, et al. Wnt5a expression is associated with the tumor proliferation and the stromal vascular endothelial growth factor--an expression in non-small-cell lung cancer. Journal of clinical oncology : official journal of the American Society of Clinical Oncology. 2005;23(34):8765-73.

232. Ripka S, Konig A, Buchholz M, Wagner M, Sipos B, Kloppel G, et al. WNT5A--target of CUTL1 and potent modulator of tumor cell migration and invasion in pancreatic cancer. Carcinogenesis. 2007;28(6):1178-87.
233. Bauer M, Benard J, Gaasterland T, Willert K, Cappellen D. WNT5A encodes two isoforms with distinct functions in cancers. PloS one. 2013;8(11):e80526.
234. Koopmans T, Kumawat K, Halayko AJ, Gosens R. Regulation of actin dynamics by WNT-5A: implications for human airway smooth muscle contraction. Scientific reports. 2016;6:30676.
235. Kumawat K, Koopmans T, Menzen MH, Prins A, Smit M, Halayko AJ, et al. Cooperative signaling by TGF-beta1 and WNT-11 drives sm-alpha-actin expression in smooth muscle via Rho kinase-actin-MRTF-A signaling. American journal of physiology Lung cellular and molecular physiology. 2016;311(3):L529-37.
236. Matthes SA, LaRouere TJ, Horowitz JC, White ES. Plakoglobin expression in fibroblasts and its role in idiopathic pulmonary fibrosis. BMC pulmonary medicine. 2015;15:140.
237. Hinz B, Pittet P, Smith-Clerc J, Chaponnier C, Meister JJ. Myofibroblast development is characterized by specific cell-cell adherens junctions. Molecular biology of the cell. 2004;15(9):4310-20.
238. Ridley AJ, Schwartz MA, Burridge K, Firtel RA, Ginsberg MH, Borisy G, et al. Cell migration: integrating signals from front to back. Science (New York, NY). 2003;302(5651):1704-9.
239. Kawasaki A, Torii K, Yamashita Y, Nishizawa K, Kanekura K, Katada M, et al. Wnt5a promotes adhesion of human dermal fibroblasts by triggering a phosphatidylinositol-3 kinase/Akt signal. Cellular signalling. 2007;19(12):2498-506.
240. Matsumoto S, Fumoto K, Okamoto T, Kaibuchi K, Kikuchi A. Binding of APC and dishevelled mediates Wnt5a-regulated focal adhesion dynamics in migrating cells. The EMBO journal. 2010;29(7):1192-204.
241. Kurayoshi M, Yamamoto H, Izumi S, Kikuchi A. Post-translational palmitoylation and glycosylation of Wnt-5a are necessary for its signalling. The Biochemical journal. 2007;402(3):515-23.
242. Kurayoshi M, Oue N, Yamamoto H, Kishida M, Inoue A, Asahara T, et al. Expression of Wnt-5a is correlated with aggressiveness of gastric cancer by stimulating cell migration and invasion. Cancer research. 2006;66(21):10439-48.
243. Dye BR, Hill DR, Ferguson MA, Tsai YH, Nagy MS, Dyal R, et al. In vitro generation of human pluripotent stem cell derived lung organoids. eLife. 2015;4.
244. Safholm A, Tuomela J, Rosenkvist J, Dejmek J, Harkonen P, Andersson T. The Wnt-5a-derived hexapeptide Foxy-5 inhibits breast cancer metastasis in vivo by targeting cell motility. Clinical cancer research : an official journal of the American Association for Cancer Research. 2008;14(20):6556-63.
245. Jenei V, Sherwood V, Howlin J, Linnskog R, Safholm A, Axelsson L, et al. A t-butyloxycarbonyl-modified Wnt5a-derived hexapeptide functions as a potent antagonist of Wnt5a-dependent melanoma cell invasion. Proceedings of the National Academy of Sciences of the United States of America. 2009;106(46):19473-8.

7 Summary

COPD and IPF are devastating diseases with very limited therapeutic options. Some pathogenetic features are shared between these diseases, such as aberrant fibroblast function and deranged activity of developmental signaling pathways in the lung, e.g. the WNT pathway. We aimed to decipher the role of the non-canonical WNT WNT5A. WNT5A is upregulated in lungs of both COPD and IPF patients and fibroblasts have been described as a source of WNT5A in the lung. However, the background of elevated WNT5A and the consequences on fibroblast function remain poorly studied.

We hypothesized that WNT5A expression in lung fibroblasts is enhanced by stimuli relevant to the pathogenesis of COPD and IPF and that this subsequently leads to aberrant fibroblast behavior.

All following experiments were performed with primary human lung fibroblasts isolated from patients undergoing thoracic surgery. To test our hypothesis, we examined WNT5A expression by immunoblotting and qPCR upon treatment with various cytokines, cigarette smoke extract (CSE) and pharmacological inhibitors. WNT5A function was studied using *in silico* analysis of microarray data, qPCR and functional experiments using both WNT5A stimulation and knockdown.

We showed that the canonical WNT WNT3A, inhibition of GSK-3β and the profibrotic cytokine TGF-β upregulated WNT5A mRNA and protein. The induction of WNT5A expression by TGF-β was dependent on TAK1 and NF-κB signaling. Furthermore, CSE treatment slightly increased WNT5A abundance and potentiated the increase in WNT5A expression induced by TGF-β stimulation. Regarding the autocrine function of WNT5A on fibroblasts, we identified several direct target genes of WNT5A that have been linked to COPD and IPF. Functionally, WNT5A knockdown led to reduced fibroblast proliferation and fibroblast-to-myofibroblast differentiation, WNT5A stimulation resulted in increased fibroblast adhesion.

Our findings support the notion that decreasing WNT5A levels in COPD and IPF lungs might be beneficial regarding deranged fibroblast function. Studying the effect of WNT5A in more complex *in vitro* settings and additional *in vivo* research will be helpful in assessing the impact of WNT5A on the whole lung and the potential of WNT5A as a novel drug target in the therapy of COPD and IPF.

8 Zusammenfassung

COPD und IPF sind schwerwiegende Erkrankungen mit sehr eingeschränkten Therapieoptionen. Manche pathogenetischen Merkmale sind beiden Krankheiten gemein, so zum Beispiel anomale Fibroblastenfunktion und gestörte Aktivität von entwicklungsbiologisch bedeutsamen Signalwegen wie dem WNT-Signalweg. Wir zielten darauf ab, die Rolle des nicht-kanonischen WNTs WNT5A zu ergründen. WNT5A ist sowohl in Lungen von COPD- als auch von IPF-Patienten hochreguliert, als Quelle von WNT5A in der Lunge wurden Fibroblasten beschrieben. Jedoch bleiben der Hintergrund und die Konsequenzen der WNT5A-Erhöhung unzureichend erforscht.

Wir stellten die Hypothese auf, dass die Expression von WNT5A in Lungenfibroblasten durch Faktoren erhöht wird, die in der Pathogenese von COPD und IPF bedeutsam sind und dass dies abweichende Fibroblastenfunktion nach sich zieht.

Alle folgenden Experimente wurden an primären Lungenfibroblasten durchgeführt. Methodisch wurde mit verschiedenen Zytokinen, Zigarettenrauchextrakt, pharmakologischen Inhibitoren und Knockdown-Experimenten gearbeitet. Die Auswertung erfolgte mittels Immunoblotting, qPCR, *in silico*-Analysen von Microarray-Daten und funktionellen Untersuchungen.

Wir zeigten, dass das kanonische WNT WNT3A, Inhibition von GSK-3β und das profibrotische Zytokin TGF-β WNT5A-mRNA und -Protein hochregulierten. Die Induktion durch TGF-β war hierbei von TAK1 und NF-κB abhängig. Weiterhin erhöhte die Behandlung mit Zigarettenrauchextrakt geringfügig die Expression von WNT5A und potenzierte den durch TGF-β-Stimulation verursachten WNT5A-Anstieg. Hinsichtlich der autokrinen Funktion von WNT5A auf Fibroblasten identifizierten wir diverse direkte Zielgene von WNT5A, die bereits mit COPD und IPF in Verbindung gebracht wurden. Funktionell führte der Knockdown von WNT5A zu reduzierter Fibroblastenproliferation und zu reduzierter Differenzierung zu Myofibroblasten, WNT5A-Stimulation hatte erhöhte Fibroblastenadhäsion zur Folge.

Unsere Ergebnisse unterstützen den Eindruck, dass ein Absenken von WNT5A-Spiegeln in COPD- und IPF-Lungen hinsichtlich gestörter Fibroblastenfunktion vorteilhaft sein könnte. Untersuchungen in komplexeren *in vitro*-Versuchsaufbauten und weitere *in vivo*-Forschung werden hilfreich sein, um den Einfluss von WNT5A auf die Lunge in der Gesamtheit zu verstehen und zu beurteilen, ob WNT5A das Potential zu einem Ziel für zukünftige COPD- und IPF-Medikamente hat.

9 Appendix

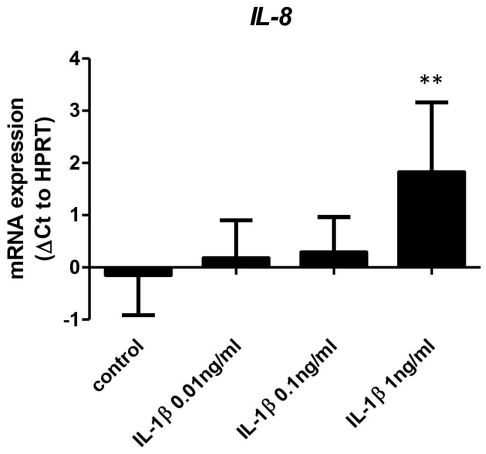

Supplemental Figure 1: IL-1β upregulates IL-8 transcript

Primary human lung fibroblasts were stimulated with different concentrations of IL-1β (0.01 ng/ml, 0.1 ng/ml or 1 ng/ml) and subject to qRT-PCR to determine *IL-8* mRNA levels after 24 h. Statistical analysis was performed using two-tailed paired Student's t-test, **p<0.01 compared to untreated cells. Results are presented as mean + stdev of 3 independent experiments.

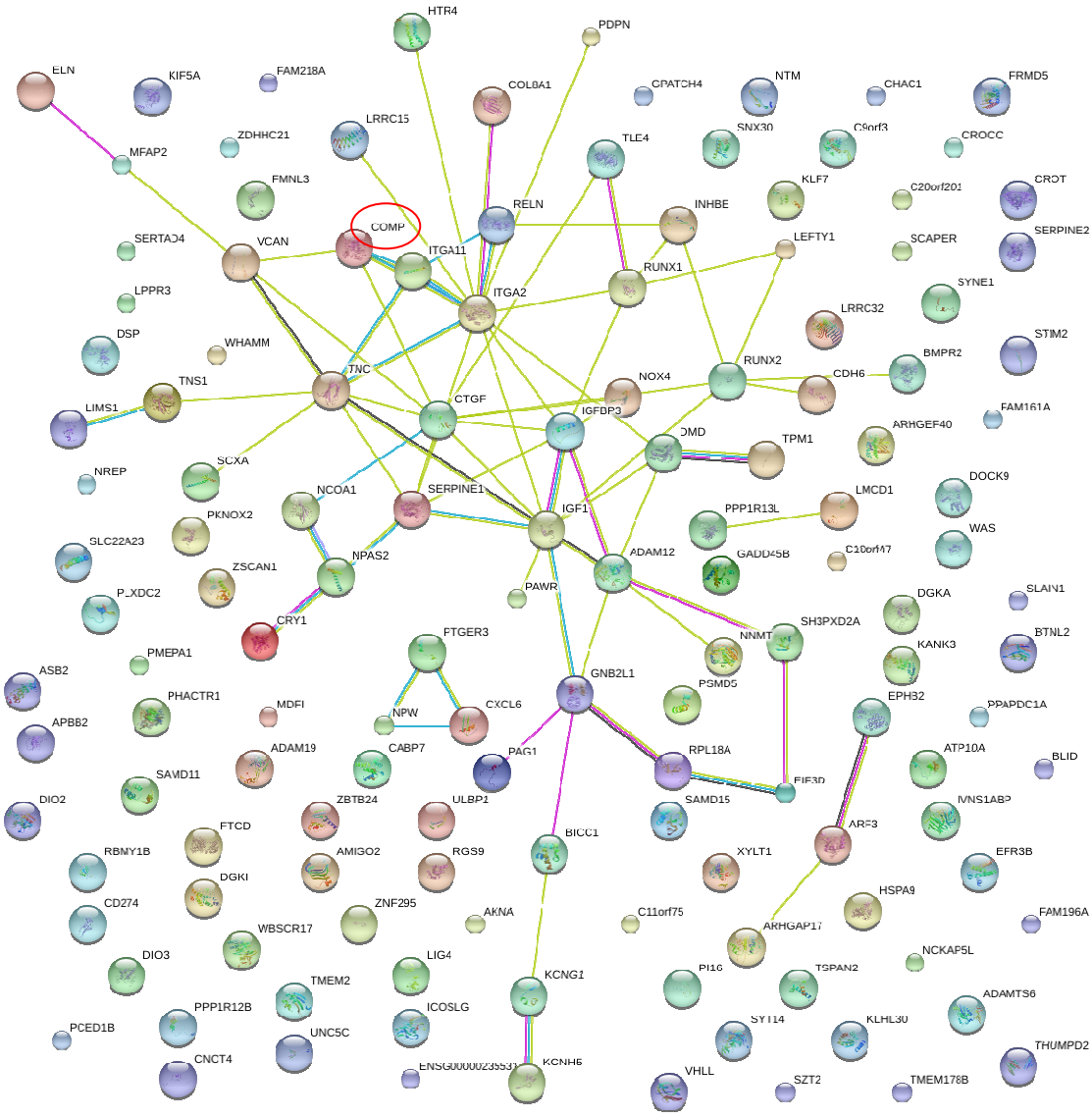

Supplemental Figure 2: Proteins encoded by WNT5A-induced genes interact with each other

STRING analysis uncovering protein-protein interactions was performed with the String database Version 10.0. 139 genes out of the 222 genes significantly upregulated after 6 h of stimulation of primary human lung fibroblasts with WNT5A (100 ng/ml) (compare microarray Fig. 8) encode for a protein listed in the database. COMP is circled in red. Simplified, lines indicate reported or predicted interactions between the connected proteins.

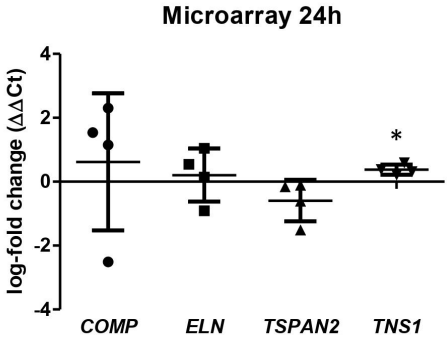

Supplemental Figure 3: WNT5A upregulates TNS1 expression after 24 h

Primary human lung fibroblasts were stimulated WNT5A (100 ng/ml) for 24 h and subject to Agilent microarray analysis. mRNA levels of *COMP*, *ELN*, *TSPAN2* and *TNS1* are presented. Statistical analysis was performed using two-tailed one-sample Student's t-test, *p<0.05. Results are presented as mean log-fold change + stdev of 4 independent experiments.

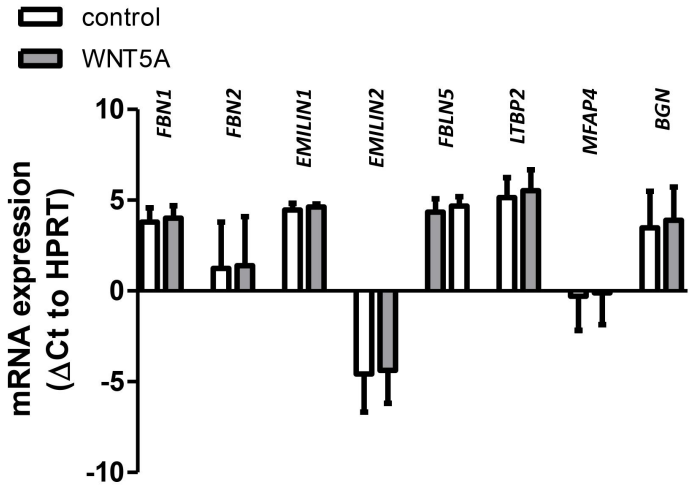

Supplemental Figure 4: WNT5A does not alter expression of elastogenesis-related genes

Primary human lung fibroblasts were stimulated with WNT5A (100 ng/ml) for 6 h and subject to qRT-PCR to determine mRNA levels of elastogenesis-related genes. Statistical analysis was performed using two-tailed paired Student's t-test. Results are shown as mean + stdev of 4-6 independent experiments.

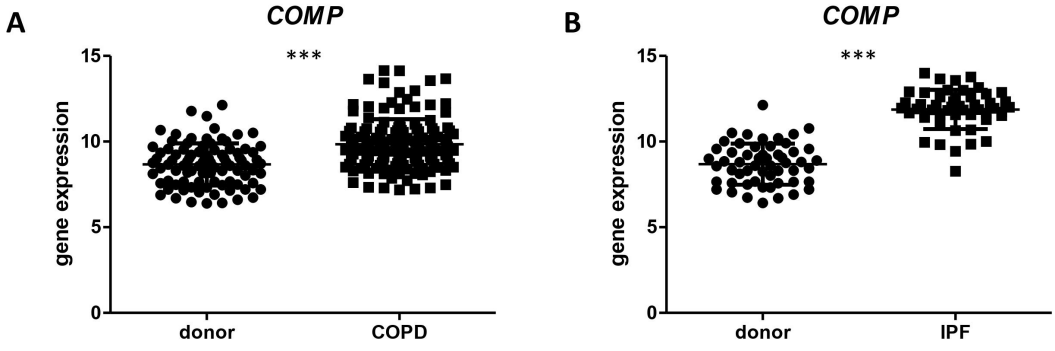

Supplemental Figure 5: COMP transcript is upregulated in COPD and IPF

Data from the published microarray GSE47460 was analyzed. *COMP* mRNA levels of lung homogenate from 144 COPD patients and 91 donors were compared (**A**) as well as COMP mRNA levels in specimen from 50 IPF patients and 55 donors (**B**). Statistical analysis was performed using Mann-Whitney U-test. Results are shown as mean + stdev.

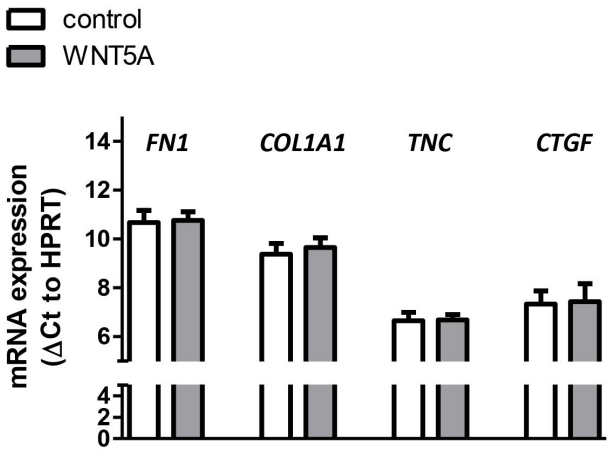

Supplemental Figure 6: WNT5A on ECM

Primary human lung fibroblasts were stimulated with WNT5A (100 ng/ml) for 6 h and subject to qRT-PCR to determine mRNA levels of the ECM components *FN1*, *COL1A1*, *TNC* and *CTGF*. Statistical analysis was performed using two-tailed paired Student's t-test. Results are presented as mean + stdev of 4 independent experiments.

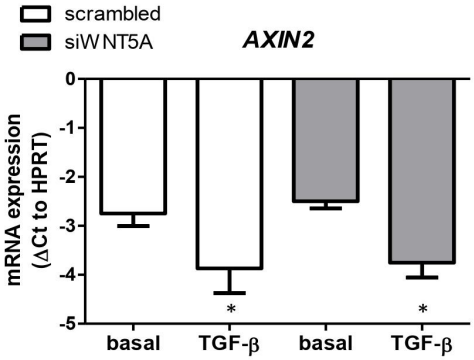

Supplemental Figure 7: Knockdown of WNT5A does not alter *AXIN2* transcript levels

Primary human lung fibroblasts were stimulated with siWNT5A or scr-siRNA in the absence and presence of TGF-β (2 ng/ml). *AXIN2* mRNA levels after 24 h of TGF-β stimulation were determined via qRT-PCR. Statistical analysis was performed using One-Way-ANOVA with repeated measures followed by Newman-Keuls Multiple Comparison Test, *$p<0.05$, compared to basal + scr. Results are presented as mean + stdev of 3 experiments.

10 Publication and presentation

10.1 Publications

HA Baarsma, W Skronska-Wasek, K Mutze, **F Ciolek**, DE Wagner, G John-Schuster, K Heinzelmann, A Günther, KR Bracke, M Dagouassat, J Boczkowski, GG Brusselle, R Smits, O Eickelberg, AÖ Yildirim, M Königshoff. Noncanonical WNT5A signaling impairs endogenous lung repair in COPD. J Exp Med. 2017 Jan;214(1):143-163

Martin-Medina A, Lehmann M, Burgy O, Hermann S, Baarsma HA, Wagner DE, De Santis MM, **Ciolek F**, Hofer TP, Frankenberger M, Aichler M, Lindner M, Gesierich W, Guenther A, Walch A, Coughlan C, Wolters P, Lee JS, Behr J, Königshoff M. Increased Extracellular Vesicles Mediate WNT-5A Signaling in Idiopathic Pulmonary Fibrosis. Am J Respir Crit Care Med. 2018 Jul 25

10.2 Poster presentations

Advancing in IPF Research (AIR) Symposium, Mainz, Germany, February 2016. **F Ciolek**, M Königshoff, J Behr, HA Baarsma. IPF-relevant stimuli induce WNT5A in primary human fibroblasts

Annual conference of the ATS, San Francisco, USA, May 2016. **F Ciolek**, M Königshoff, HA Baarsma. Regulation of Non-Canonical WNT-5A by Primary Human Lung Fibroblasts

Annual conference of the ATS, Washington, USA, May 2017. **F Ciolek**, K Heinzelmann, O Eickelberg, M Konigshoff, H Baarsma. Regulation and Function of Non-Canonical WNT-5A in Human Lung Fibroblasts (presented by Hoeke Baarsma)

11 Eidesstattliche Versicherung

Hiermit erkläre ich, Florian Ciolek, an Eides statt,
dass ich die vorliegende Dissertation mit dem Titel

„Regulation and function of non-canonical WNT signaling in lung fibroblasts in chronic lung diseases"

selbständig verfasst, mich außer der angegebenen keiner weiteren Hilfsmittel bedient und alle Erkenntnisse, die aus dem Schrifttum ganz oder annähernd übernommen sind, als solche kenntlich gemacht und nach ihrer Herkunft unter Bezeichnung der Fundstelle einzeln nachgewiesen habe.
Ich erkläre des Weiteren, dass die hier vorgelegte Dissertation nicht in gleicher oder in ähnlicher Form bei einer anderen Stelle zur Erlangung eines akademischen Grades eingereicht wurde.

Florian Ciolek

Florian Ciolek München, den 26.11.2021

12 Acknowledgements

I would like to thank Melanie Königshoff for the opportunity to be part of a committed international research team, for setting the ideal frame for an experimental thesis and for her constructive and motivating support throughout the whole project. I am also very grateful to my mentor Hoeke Baarsma for his constant help with my daily struggles and his thorough feedback on writing this thesis while being incomparably patient. To Doreen Franke on behalf of all organizers and teachers of the CPC Research School I am thankful for creating a program that made it possible to get to know experimental research in a highly instructive way.

I am endebted to Katharina Heinzelmann on behalf of the CPC Munich bioArchive team for providing the cells I worked with every day and much importantly, to all patients who gave consent to their lungs being analyzed and processed for science. I want to thank Maria Magdalena Stein for her meticulous and kind introduction into the laboratory techniques. I am grateful to Ana van den Berg for her technical support, to Nina Noskovičová and Gerald Burgstaller for their help regarding the adhesion assay, to Korbinian Berschneider for his introduction to the cigarette smoke pump and to Darcy Wagner for her support analyzing the microarray.

Furthermore, I want to thank all people working in the CPC and in particular those from the MK lab who have not yet been mentioned (Aina, Astrid, Carlo, Cedric, Chiharu, Hani, Henrik, Kathrin, John-Poul, Julia, Lara, Mareike, Nadine, Noor, Rabea, Rita, Sarah, Stephan and Wiola) for the great spirit in- and outside the lab.

Lastly, I want to thank my family, my friends and Zarah without whose support all of this would have been impossible.